MOUSE MODELS OF PROSTATE CANCER PROGRESSION AND BONE
METASTASIS

By

Srinivas Rao Nandana

Dissertation

Submitted to the Faculty of the

Graduate School of Vanderbilt University

In partial fulfillment of the requirements

For the degree of

DOCTOR OF PHILOSOPHY

in

Cancer Biology

August, 2010

Nashville, Tennessee

Approved:

Professor Robert J. Matusik

Professor Neil Bhowmick

Professor Vito Quaranta

Professor Chin Chiang

Dedicated to my parents and Bhagavan.

Without your steadfast support and love, this work would not have been possible.

ACKNOWLEDGEMENTS

PREFACE

Prostate cancer is the second leading cause of deaths due to cancer in men in the United States. The American Cancer Society has projected that 192,280 new cases and 27,360 deaths will occur in the year 2009. Mostly, men over the age of 50 are afflicted by the disease and more than 70% of the men diagnosed with prostate cancer are over the age of 65. Most of the patients who suffer from prostate cancer do not die due to the tumor at the primary site but rather due to complications when the tumor has spread to the bone. It is estimated that each year, about 350,000 people die of bone metastasis in the United States. The causative tumor becomes incurable once the bone has been invaded and only 25% of prostate cancer patients are able to live 5 years subsequent to their diagnosis of bone metastasis. The interaction between prostate cancer cells and the bone creates a vicious cycle of bone formation and bone destruction thereby destabilizing the inherently delicate homeostasis within the bone. In prostate cancer, this process leads to metastatic lesions that are predominantly osteoblastic. However within the background of bone formation, several groups have reported that bone resorption is an integral part of prostate cancer bone lesions. Therefore, early detection and treatment before the tumor metastasizes is critical for the survival of the patient.

Creating and characterizing mouse models that better mimic the progression in human prostate cancer is a powerful tool to study and delineate the various steps in tumor progression. Most of the currently available mouse models of prostate cancer successfully recapitulate the early steps of tumor progression in the primary site but fail to metastasize

to other organs especially to the bone. Amongst the existing ones, transgenic models that are created by dysregulating a gene that is widely known to be altered in human prostate cancer are considered to be more reflective of the human disease. This is in contrast to transgenic mouse models that overexpress the small t and large T antigens that despite the phenotype they produce, are considered to have little physiological significance.

This first part of the thesis describes the creation and characterization of the hepsin/myc bigenic model that develops adenocarcinoma in the primary site. The second part of the thesis describes a model that delineates the interactions between prostate cancer cells and the bone microenvironment. This is approached by dysregulating the T-box transcription factor Tbx2 in PC3 human prostate cancer cells and looking at the effect of this dysregulation on the interaction of the cells with the bone microenvironment.

TABLE OF CONTENTS

Chapter

I. INTRODUCTION

II.   MATERIALS AND METHODS

III. HEPSIN COOPERATES WITH MYC IN THE PROGRESSION OF
      ADENOCARCINOMA IN A MOUSE MODEL OF PROSTATE
      CANCER

IV.   BLOCKING ENDOGENOUS TBX2 IN PC3 HUMAN PROSTATE CANCER
      CELLS DECREASES THE OSTEOLYTIC BURDEN WHEN GRAFTED IN
      THE BONE MICROENVIRONMENT

LIST OF TABLES

LIST OF FIGURES

LIST OF ABBREVIATIONS

AR   Androgen Receptor

AP   Anterior Prostate

BMP   Bone Morphogenic Protein

DHT   Dihydrotestosterone

DN   Dominant Negative

DP   Dorsal Prostate

EV   Empty Vector

HGPIN   High Grade Prostatic Intraepithelial Neoplasia

LGPIN   Low Grade Prostatic Intraepithelial Neoplasia

LP   Lateral Prostate

PCa   Prostate Cancer

PB   Probasin

SV40   Simian Virus 40

Tag   Simian Virus 40 Large T antigen

Tbx2   T box 2

TGF β   Transforming Growth Factor β

VP   Ventral Prostate

INTRODUCTION

Prostate:

The prostate is a glandular organ that surrounds the urethra at the neck of the bladder. It contains numerous ducts that produce secretions that contribute to the seminal fluid contents. In rodents, the prostate gland consists of four encapsulated and separate lobes: the anterior prostate (AP), dorsal prostate (DP), ventral prostate (VP) and the lateral prostate (LP). The rodent prostate lobes surround but do not encompass the urethra (Cunha et al., 1987). Anatomically, each prostate lobe is different and produces different secretory proteins. The dorsal and the lateral lobes are often examined collectively as the dorsolateral prostate (DLP) due to their proximity and anatomic size. In human prostate, although the defined zones are not as distinct, McNeal has described three anatomically distinct zones: the peripheral zone, the central zone and the transition zone (McNeal, 1988). The peripheral zone that is considered to be homologous to the rodent dorsolateral prostate is the most common site of prostate cancer in humans (Price, 1963).

Morphologically, the prostate gland consists of the epithelial and stromal cell compartments. The epithelial cells are arranged in two distinct and separate layers. The luminal epithelial cells are columnar cells that produce the prostatic secretions while the basal epithelial cells are flattened by morphology. In addition to these two epithelial cell

types, neuroendocrine cells that are rare are found in the basal cell layer. The stromal cell compartment consists of fibroblasts and smooth muscle cells. The epithelial and stromal cell compartments are thought to be dependent on each other for their survival and are separated by extracellular matrix proteins comprising the basement membrane.

Human Prostate Cancer and its progression:

Prostate cancer is the second leading cause of deaths due to cancer in men in the United States. The American Cancer Society has projected that 192,280 new cases and 27,360 deaths will occur in the year 2009. Mostly, men over the age of 50 are afflicted by the disease and more than 70% of the men diagnosed with prostate cancer are over the age of 65. This high rate of mortality is primarily due to metastasis of the primary tumor. The 5 year survival rate for men diagnosed while the disease is localized is nearly 100% while only 34% of the men diagnosed with metastatic prostate cancer survive beyond 5 years. Therefore, early detection and treatment before the tumor metastasizes is critical for the survival of the patient.

The advancement of prostate cancer in humans is a multi-step process progressing through a number of stages. Typically, following the development of prostatic intraepithelial neoplasia (PIN), the natural course of progression in human prostate cancer involves the development of adenocarcinoma with local invasion, and the final development of distal metastases to sites such as the bone, lung and liver.

Despite the prevalence of the disease, our knowledge of the genetic alterations occurring during prostate cancer is limited. The development of PSA screening in the 1990's resulted in a better diagnosis of PCa and initially the incidence of the disease appeared to increase dramatically. However, it is now recognized that the incidence of the disease has not changed over time. Previously, when PSA screening was not the norm, PCa was diagnosed by clinical syndromes or by Digital Rectal Examination (DRE). However, in the majority of cases, these diagnostic methods were ineffective since the tumor had already metastasized beyond the organ. Today, PSA screening is routinely performed and has clearly revolutionized the clinical management of PCa. Though many cases today are detected by PSA levels in the 2.5-10 ng/ml range, however, using PSA screening for early detection of PCa has its limitations too. Since PSA is specific to the prostate organ rather than PCa, elevation of PSA levels can occur in other benign pathophysiologies of the prostate such as prostatitis, BPH, and Prostatic Intraepithelial Neoplasia (PIN). Therefore, serum PSA levels alone cannot differentiate between adenocarcinoma and other non-malignant diseases of the prostate.

Specific morphologic changes and corresponding changes in gene expression occur during the progression of prostate cancer. The precancerous lesion Prostatic Intraepithelial Neoplasia (PIN) is widely accepted to be the precursor of prostate cancer. PIN is characterized by intra-acinar proliferation and the cells often display nuclear anaplasia. All of the morphologic changes are restricted to the epithelial compartment and the basement membrane is intact. The basal cells though present may have decreased numbers. Notably, chromosomal loss of 8p21 region occurs in 63% of PIN lesions and 90% of prostate cancers (De Marzo et al., 2004). Two of the most notable changes during

this stage of the disease are the marked up-regulation of the cell-surface protease hepsin (Chen et al., 2003; Dhanasekaran et al., 2001; Ernst et al., 2002; Luo et al., 2001; Magee et al., 2001; Stamey et al., 2001; Stephan et al., 2004; Welsh et al., 2001) and loss of expression of the prostate-specific homeobox protein Nkx3.1 (Bowen et al., 2000).

PIN progresses to adenocarcinoma and this transition is characterized by cytologic atypia including enlargement of nuclei and nucleoli. In addition, the basal cells are lost. Notably, the basement membrane is disrupted and the tumor displays local invasion. The organization of epithelial cells is lost progressively and the tumor changes from well differentiated (Gleason score 2-4), to moderately differentiated (Gleason score 5-6) to poorly differentiated (Gleason score 8-10). A number of genetic alterations are linked with the transition to prostate adenocarcinoma, most notable of which are the inactivation of the transcription factor KLF6 (55% of primary tumors) (Narla et al., 2001) and loss of PTEN (10-15% of primary tumors) (Wang et al., 1998). In addition, amplification of the c-myc locus (8%) (Jenkins et al., 1997) and loss of the cell cycle regulator protein Rb (19%)(Bookstein et al., 1990; Jarrard et al., 2002) have been reported. Poorly differentiated prostate adenocarcinomas that have advanced to Gleason score 7-10 often show loss of expression of cell adhesion proteins such as E-cadherin, alpha catenin, KAI1, B4 integrin and basement membrane proteins laminin-332 and collagen VII (Dong et al., 1995; Gao et al., 1997; Nagle et al., 1995; Umbas et al., 1994). The roles of Myc overexpression, and inactivation of PTEN, p27 and Rb in prostate cancer have been demonstrated using mouse model systems (Ellwood-Yen et al., 2003; Maddison et al., 2004; Trotman et al., 2003).

The next critical step of PCa progression is the ability of the tumor cells to spread to distant organs through the blood and lymphatic circulation systems. This step represents an important hallmark of cancer progression because the primary tumor that is localized to the organ is curable while the tumor that has metastasized to distant organs is lethal. This stage is morphologically characterized by the presence of metastatic foci in the lymph nodes. Several genes that are thought to be associated with metastasis have been reported. Notably, of the tumors that have metastasized, PTEN is lost in 30-43% (Cairns et al., 1997) and myc is amplified in up to 21% (Jenkins et al., 1997) of the tumors. Additionally, over-expression of the transcription repressor EZH2 (Varambally et al., 2002) and constitutive upregulation of the hedgehog signaling pathway (Karhadkar et al., 2004) have been reported in metastatic prostate cancer.

Androgen Receptor and prostate cancer progression:

The androgens together with the androgen receptor (AR) play an important role in normal prostate differentiation and prostate cancer progression (Beato, 1989; Cunha, 1994; Cunha et al., 1987; Evans, 1988). The AR is expressed throughout the initiation and progression of PCa. Normal prostate epithelial cells and the majority of prostate adenocarcinomas require androgens for their survival. Androgen ablation remains the gold standard for the treatment of prostate cancer. Although the tumor initially regresses in response to androgen ablation, it eventually becomes hormone refractory and continues to grow in androgen-ablated conditions. It is believed that this hormone refractoriness is due to the clonal expansion of androgen insensitive cells. There is no effective treatment

for hormone-refractory metastatic prostate cancer which is lethal. The molecular mechanisms by which prostate cancer progresses from androgen dependent to androgen refractory state are not yet fully known.

Mouse Models of prostate cancer:

Transgenic mouse models have been long exploited and provide an excellent opportunity to identify genes that contribute to the development of prostate adenocarcinoma, with the eventual goal of to elucidating the molecular basis of targeted drug therapy for human prostate cancer. Developing mouse models to delineate the mechanisms that control tumor progression and metastasis presents a formidable challenge since no single model appears to reflect all the changes that occur in human prostate cancer. Recently, several advances have been made in the area of mouse engineering techniques and hence the effort is to generate a mouse model that mimics human cancer in as many molecular features as possible. It appears that the development of tumor pathology in genetically engineered mouse models for prostatic adenocarcinoma falls into several categories. In a few mouse models, the transgene induces epithelial hyperplasia combined with stromal proliferation, thereby reflecting the pathophysiology of benign prostatic hyperplasia (BPH). In some models, the transgene induces abnormal proliferation of the epithelial cells with the result of producing a few layers of epithelial cells known as LGPIN, similar to what is found in humans. Other models mimic human HGPIN in which the epithelial cells proliferate further to occupy the glandular lumen and display large pleiomorphic nuclei with prominent nucleoli. Only a very limited number

of models develop metastasis to distant sites. Examples of metastasis models include those expressing both SV40 Large-T/small-t antigen genes and bigenic mouse models whereby two transgenic lines have been crossbred. Therefore, mouse models showing metastasis have been the most difficult to create. The two most important factors in the creation of transgenic models are the choice of promoter to target the prostate and the transgene to induce the development and progression of prostate cancer.

Selection of the promoter:

Of critical importance is the choice of promoter to target the transgene to the tissue of interest. It was found that two different androgen receptor (AR) binding sites, ARBS-1 (located at position -236 to -223) and ARBS-2 (at position -140 to -117) in the probasin (PB) promoter were required for maximal induction of CAT gene expression in response to androgens (Rennie et al., 1993). The region spanning both elements (-244 to -96) was termed as androgen responsive region (ARR) (Kasper et al., 1994). Later, (Yan et al., 1997) isolated a 12 kb fragment of the PB promoter (termed LPB) that produced considerably higher levels of CAT gene expression in the prostate of transgenic mice. The advantage of this LPB promoter was that it remained specific to the luminal cells as was the smaller -426/+28 bp PB promoter fragment but it targeted high levels of transgene expression. Subsequently, the ARR_2PB promoter was developed by linking two ARRs to the PB promoter and was consistently efficient in driving high levels of transgene expression in transgenic mice (Ellwood-Yen et al., 2003; Zhang et al., 2000). The shorter probasin promoter (-426/+28) also specific to the prostate, drives a lower

level of transgene expression. The C3(1)-c-myc transgenic mouse model that is driven by the C3(1) promoter element primarily develops hyperplasia with dysplasia. In contrast, the Lo-Myc model and the Hi-Myc models driven by the PB and ARR$_2$PB promoters, respectively, develop locally invasive adenocarcinoma, except that progression in the Hi-Myc model takes half the time as compared to Lo-Myc mice (Ellwood-Yen et al., 2003). Therefore, promoter selection is important for driving high levels of expression that is sufficient to display a phenotype in the prostate.

Bigenic models:

Several mouse models demonstrate that single gene disruptions lead in most cases, to LGPIN and HGPIN and not adenocarcinoma nor metastatic disease. Therefore, a number of bigenic mouse models have been created in an effort to determine if two genetic hits promote the disease, leading to metastasis. If the phenotype of a single gene model is limited, crossbreeding with another mouse model to generate a bigenic model often displays greater phenotypic changes. For instance, the phenotype of p27Kip1 -/- and PTEN -/- mice range from mild hyperplasia to dysplasia, respectively. However, the bigenic model in which these two lines were crossbred (PTEN +/- x Cdkn1b -/- model) displays locally invasive tumors in 25% of the mice. Similarly, although the mouse model in which Nkx3.1 is lost displays hyperplasia and dysplasia, the bigenic model resulting in cross between loss of Nkx3.1 in combination with PTEN haploinsifficiency in PTEN +/- x Nkx3.1 -/- prostates displayed HGPIN and early carcinoma lesions (Kim et al., 2002). Further, mice with PTEN +/- x Nkx 3.1 -/- prostates showed increased

HGPIN/early carcinoma as compared to PTEN+/- X Nkx 3.1+/- prostates showing that the transformation rate was dependent on the number of alleles lost (Kim et al., 2002). Therefore bigenic models with two or three genetic hits have clearly shown that progression of disease in mouse models requires more than perturbation of a single gene.

Prostate cancer mouse models carrying the small t and large T antigen transgenes:

Several prostate cancer mouse models have been generated using the SV 40 Large-T and small-t antigens. The SV40 large-T antigen acts by binding p53 (Pipas and Levine, 2001) and Rb (DeCaprio et al., 1988). In contrast, the small-t antigen facilitates cellular transformation by providing essential mitogenic signals (Asamoto et al., 2002). The Lady transgenic model was generated by driving the Large-T antigen (Tag) under the influence of the long PB promoter (LPB-Tag) to the mouse prostate (Kasper et al., 1998; Masumori et al., 2001). The 12T-7 line is one of the several lines obtained from this transgenic mouse and is the most extensively studied among the LPB-Tag transgenic lines. The 12T-7 line develops multifocal lesions that display groups of cells with eleongated hyperchromatic nuclei interspersed among normal epithelial cells. These lesions further progress from LGPIN to HGPIN with localized intraprostatic invasion (Kasper et al, 1998). These tumors were androgen dependent since the tumors regressed after castration and subsequent administration of androgens restored the pre-castration phenotype. One of the other LPB-Tag lines, the 12T-10 model displayed PIN lesions that progressed to neuroendocrine (NE) prostate cancer with metastases to lymph nodes, liver, lung spleen, kidney and occasionally to bone (Masumori et al., 2001). The occurrence of

bone metastases in this model was 3/21 or 14% of mice. Other models including the TRAMP model (Gingrich et al., 1996; Greenberg et al., 1995; Kaplan-Lefko et al., 2003), C3(1)-SV40 Large-T/small-t (Shibata et al., 1996a; Shibata et al., 1996b), cryptidin 2-SV40 Large-T/small-t (Perez-Stable et al., 1996), gp91-phox-SV40 Large-T/small-t (Skalnik et al., 1991), PSP94-SV40 Large-T/small-t (Gabril et al., 2002) and the (-426) PB-Large-T/small-t transgenic rat model (Asamoto et al., 2002; Cho et al., 2003) were generated with the SV40 early gene coding region expressing both Large-T as well as small-t antigens. All these models, displayed prostate tumorigenesis and progression to HGPIN. Further, all the models carrying the Large-T and small-t antigen transgenes developed NE differentiation and NE metastases. Furthermore, another important feature common to models harboring the Large-T and small-t antigen is that upon castration, the primary tumors regress initially, however continued androgen deprivation causes the tumors to grow in an androgen independent manner. In human prostate cancer, primary tumors that are NE in nature are very rare, however, NE differentiation is observed in a few foci in some prostate adenocarcinomas (di Sant'Agnese and Cockett, 1996).

Extracellular matrix molecules and prostate cancer progression:

Extracellular and cell surface proteases are believed to play an important role in final stages of progression of the primary tumor i.e. invasion and metastasis. It is believed that these proteases are involved in the cleavage of extracellular matrix proteins in turn facilitating tumor cells to invade the connective tissues, blood and lymph vessels and in the final step metastasize to distant sites (Noel et al., 1997; Quaranta and Giannelli, 2003;

Woodward et al., 2007). These steps are brought about by various proteases and previous reports have implicated matrix metalloproteases (MMPs) (Giannelli et al., 1997; Koshikawa et al., 2004; Pirila et al., 2003). Apart from MMPs, serine proteases have been reported to be involved in degrading the extracellular matrix proteins of which the type II transmembrane serine proteases are a special subset. While the N-terminal cytoplasmic domain of serine proteases associates with intracellular molecules and participates in signaling, the C-terminal domain is located at the cell surface and interacts with extracellular matrix components. Several studies have shown that hepsin, a type II transmembrane serine protease (TTSP), is upregulated at both the mRNA and protein levels in more than 90% of human prostate cancers. For example, one study reported that hepsin is up-regulated by 34 fold in Gleason grades 4 and 5 (Landers et al., 2005; Stephan et al., 2004). Hepsin levels have been correlated positively with disease aggressiveness with highest hepsin expression levels present in tumors of Gleason grade 4/5 (Xuan et al., 2006). This suggests a role for hepsin in aggressive prostate cancers.

The PB-Hepsin transgenic mice:

The construct utilized for making the PB-hepsin transgenic mice contained the modified probasin promoter ARR_2PB, the b globin intron, full length mouse hepsin Cdna, internal ribosome entrance site (IRES) and humanized renilla GFP (hrGFP) cDNA sequence. This configuration of the transgene drives the expression of hepsin and hrGFP from the same transcript and thus specificity of transcription can be monitored by expression of GFP. Histologically, the 3-4 month old PB-hepsin mice did not show any

obvious abnormalities of the prostate gland, but in contrast the one year old mice displayed separation between the layers of epithelial cells and stromal cells. It was observed that these areas of separation corresponded with epithelial cells that expressed the greatest levels of hepsin. Since the basement membrane separates the epithelial and stromal layers in the prostate, the authors analyzed two basement membrane markers, Laminin-332 and Collagen IV. While Laminin-332 staining appeared as a continuous line in the wild type mice separating the epithelial and stromal cell layers, in contrast, Laminin-332 staining appeared weak or completely absent in the PB-Hepsin mice. Further, Collagen IV staining revealed a diffused localization in the PB-hepsin mice. In addition, the staining of α6β4 integrin, a major basement membrane receptor that is lost in human prostate cancers (Bonkhoff, 1998; Davis et al., 2001), was observed as a discontinuous line in the PB-hepsin mice in contrast to a continuous line in the wild type littermates. In summary, staining with markers for the basement membrane and structures of cell-substratum adhesion proteins indicated that the basement membrane structure is severely compromised in the PB-hepsin transgenic mice. Further investigation of the PB-hepsin transgenic mice revealed that the prostate undergoes normal differentiation, proliferation and apoptosis.

The PB-hepsin-12T-7f bigenic mouse model of prostate cancer:

The hepsin mediated disruption of the basement membrane in the PB-hepsin transgenic mice is of interest since in human prostate cancer progression, the basement membrane gets disrupted during the progression from localized primary tumor to

invasive metastasizing cancer (Abate-Shen and Shen, 2000). To investigate the role played by hepsin expression in prostate cancer, the hepsin transgenic mice were crossed with the LPB-Tag line12-T7f. The prostates of the 12T-7f transgenic line display massive enlargement of the prostate, develop high grade PIN and limited foci of adenocarcinoma by 20 weeks, but do not display any metastases. Examination of the PB-hepsin-12T-7f bigenic mice at 21 weeks displayed adenocarcinoma with half of the mice showing histological features of rosette formation indicating neuroendocrine differentiation. Immunohistochemical staining with the proliferation marker Ki67 showed no differences in cell proliferation between the LPB-Tag and the LPB-Tag/PB-Hepsin mice. However, the bigenic mice displayed increased apoptosis as indicated by TUNEL staining. Interestingly, immunofluorescent staining with antibodies that recognize extracellular matrix proteins revealed that that collagen IV staining was severely reduced in the LPB-Tag/PB-Hepsin mice, also beta4 integrin revealed disorganized basement membrane in the double transgenic animals. These changes in the staining pattern of basement membrane proteins in the bigenic mice indicate hepsin mediated disruption of the basement membrane. More importantly, by 21 weeks of age, 24% of the bigenic LPB-Tag/PB-hepsin mice developed metastases to liver, lung and bone. Notably, these numbers could be an underestimation since only the femur bones which represent only a small fraction of total bone mass was analyzed in the study. These metastatic lesions contained tightly packed cells that show morphologic features of NE differentiation of nuclear molding and high nuclear/cytoplasmic ratio. Further, these lesions, akin to metastatic lesions in other SV40 T antigen driven mouse models including TRAMP, CR2-T-Ag and LPB-Tag line 12-T10 stained positively for synaptophysin confirming

their NE phenotype. It is possible that these metastatic lesions are either NE in origin or that they undergo transdifferentiation from epithelial to NE cell type during the process of metastasis. Although the metastatic lesions in the hepsin bigenic mice are NE in nature, it still is one of the very few models that develop bone metastasis. Bone metastasis is a very important feature in prostate cancer mouse models since human prostate cancer preferentially metastasizes to bone and the mechanisms responsible for bone metastasis are largely unknown. Interestingly, while the bone metastases in human prostate cancer are predominantly osteoblastic, in the bone lesions in LPB-Tag/PB-Hepsin mice no obvious osteoblastic or osteolytic characteristics were detected.

The PB-Myc model:

Multiple studies in human prostate cancer have shown increased Myc gene copy number in up to 30% of tumors including PIN lesions (Fleming et al., 1986; Jenkins et al., 1997; Nesbit et al., 1999; Qian et al., 1997; Sato et al., 1999). However, this observation is not conclusive since Myc is one of the many genes located in the 8q24 amplicon (Elo and Visakorpi, 2001). Several studies have shown that the mechanism by which Myc induces cancer is due to its effect of increased cell proliferation thus contributing to tumorigenesis. In contrast, several studies have also documented the pro-apoptotic activity of Myc, particularly in conditions of limiting survival factors or low serum. (Ahmed et al., 1997; Pelengaris et al., 2002b; Prendergast, 1999). Further, these findings are in agreement with several transgenic mouse models expressing Myc that have demonstrated that the response to Myc expression is critically dependent on the

14

associated survival signals (Pelengaris et al., 2002a; Pelengaris et al., 2002b). To study the effect of increased Myc expression in mouse prostate, human c-Myc was expressed from two different strength prostate-specific probasin promoters, (-426/+28) probasin-Myc and ARR$_2$/probasin-Myc and the transgenic Myc mice were termed as Lo-Myc and Hi-Myc mice respectively. The probasin gene starts to express at a low level in the mouse prostate at 1-2 weeks of age and expression increases as androgen levels increase between 4 and 8 weeks of age. The ARR$_2$PB probasin is the stronger promoter since it contains two additional androgen response elements thus increasing the androgen dependent expression (Wu et al., 2001b; Zhang et al., 2000). While the Lo-Myc mice developed PIN lesions at 4 weeks, the Hi-Myc mice displayed PIN lesions at 2 weeks. Transition from PIN to invasive cancer was evident in Lo-Myc mice after 1 year while the Hi-Myc mice displayed faster progression with invasive adenocarcinoma after 6 months. This suggested that the dosage of Myc is directly related to the rate of cancer progression. Ki67 and TUNEL staining showed an increase in both proliferation and apoptosis as the tumor progressed from PIN to invasive cancer. The PIN lesions and adenocarcinoma lesions in both Lo-Myc and Hi-Myc mice did not display morphologic features of neuroendocrine differentiation and were negative for synaptophysin staining.

Laminin-332, a component of the basement membrane (BM) is a substrate of hepsin:

Laminin-332 (previously known as Laminin-5) is an Extracellular Matrix (ECM) molecule and is an important component of the basement membrane that separates the

epithelial and stromal compartments (Rousselle et al., 1991). It is a glycoprotein consisting of three polypeptide chains α3, β3 and γ2 that are linked by disulfide bonds (Aumailley et al., 2005). Laminin-332 has been reported to play critical roles in development, wound healing and tumorigenesis (Ryan et al., 1996). Although Laminin-332 is over-expressed in several tumor types including oral, cutaneous, esophageal, colon, laryngeal, tracheal and cervical cancers (Marinkovich, 2007), interestingly it has been reported to be lost in prostate cancer (Calaluce et al., 2001; Davis et al., 2001; Hao et al., 2001). It has been reported that Laminin-332 is cleaved by several matrix metalloproteases (MMPs) that resulted in increased cell migration(Giannelli et al., 1997; Koshikawa et al., 2004). Interestingly, the hepsin transgenic model demonstrated disorganized basement membrane; however, the mechanism involved in this disorganization was not revealed. It was reported that the hepsin transgenic mice exhibited weaker immunohistochemical staining of Laminin-332 as compared to wild type mice. In a recent study, it was reported that hepsin directly cleaves the b3 chain of Laminin-332 (Tripathi et al., 2008). The authors also reported that hepsin-cleaved Laminin-332 enhanced the motility of DU145 prostate cancer cells, thus postulating that direct cleavage of Laminin-332 may be one mechanism by which hepsin promotes prostate tumor progression and metastasis, possibly by up-regulating prostate cancer cell motility (Tripathi et al., 2008).

Bone metastasis in prostate cancer:

The incidence of prostate cancer has consistently risen in the recent years and the disease is the cause of more gender-specific deaths due to cancer than any other cancer. About 1 in 5 men will be diagnosed with prostate cancer during the lifetime, and 1 in 33 will die of the disease. The morbidity and mortality in prostate cancer patients can almost universally be attributed due to metastasis to distant sites, predominantly the bone. The disease is curable when it is confined to the prostate gland but so far, efforts at treatment and cure of metastatic disease have met with limited success. About 80% of patients who have succumbed to advanced hormone refractory prostate cancer have clinical evidence of metastases to the bone and histologically, 100% have bone involvement (Bubendorf et al., 2000; Roudier et al., 2003; Saitoh et al., 1984). It has been reported that bone is the predominant site of metastases for prostate cancer followed by breast cancer.

As with all cancers, in order to form metastases in bone, prostate cancer cells must first detach from the epithelial tissue by and invade surrounding tissue producing proteolytic enzymes. The epithelial cells must invade the adjacent stromal compartment, penetrate the basement membrane and endothelial cell layer and enter the blood circulation (Liotta and Kohn, 2001). The cells then travel to distant organ sites, most notably bone in the case of prostate cancer. This series of initial events has been described as inefficient and therefore many cancer cells do not survive and get past the protective host-surveillance mechanisms (Fidler, 1978; Liotta and Kohn, 1990; Zetter, 1990). The prostate cancer cells that have survived enter the wide-chanelled sinusoids of

the bone marrow cavity, adhere to the extracellular matrix, proliferate and form new blood vessels.

Although the mechanisms of the metastatic process to the bone are poorly understood, the widely believed mechanism is the seed and soil hypothesis first proposed by Steven Paget more than 100 years ago. Paget's theory of metastasis proposes that the tumor cells (seed) find a suitable environment (soil) and so the migration of tumor cells to bone may be a result of the adhesion and growth properties of the tumor cells. (Fidler, 2003). Another theory proposed by Jacob *et al* suggests that specific homing factors in the bone facilitate the migration of cancer cells to the bone (Jacob et al., 1999). Several studies have shown that specific growth factors in bone can support and facilitate the growth of prostate cancer cells (Chackal-Roy et al., 1989; Gleave et al., 1991). Bone marrow, the site where cancer cells invade is a rich bed of growth factors and cytokines that promote the growth of tumor cells. Additionally, the bone is rich in transforming growth factor-β (TGFβ) and Insulin-like growth factor (IGF)-1 that stimulate the invading tumor cells.
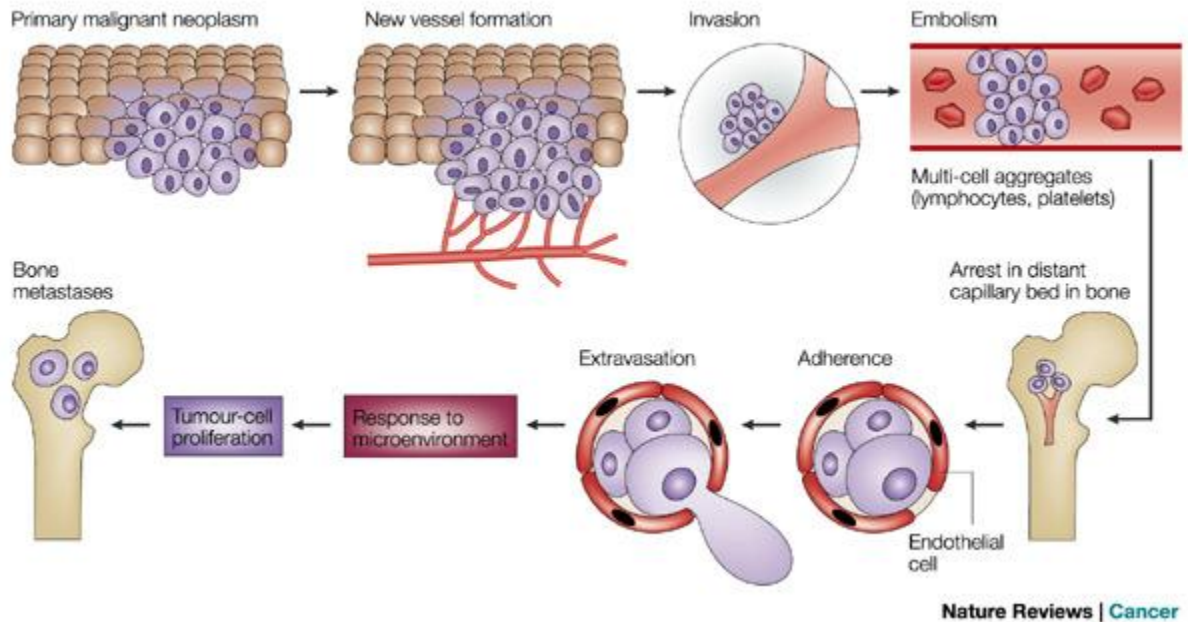
Figure 1: Steps involved in the metastasis of tumor cells from the primary tumor to the bone. *(From Mundy GR, Nature Reviews Cancer, 2002, 2: 584-593)*

Prostate cancer metastases are predominantly osteoblastic in nature:

Traditionally, bone metastases have been classified as either osteolytic or osteoblastic. It is believed that osteolytic lesions are a result of osteoclast-activating factors. These factors are released by the tumor cells in the bone microenvironment and parathyroid-hormone-related peptide (PTHrP) is the most notable of these factors. Conversely, osteoblastic lesions are thought to be caused by cancer cells that activate osteoblast proliferation and differentiation with resulting bone formation. It has now been realized in the field of bone biology that these two lesion types are the two extremes – morphological analyses of bone metastatic lesions in patients has shown that bone lesions are composed of both osteoblastic and osteolytic components.

The metastatic lesions in prostate cancer are caused due to a complex interaction between the tumor cells themselves and the bone microenvironment, resulting in the induction of a mixture of osteolytic and osteoblastic lesions, but predominantly the lesions are osteoblastic in nature. Human prostatic adenocarcinoma resulted in osteoblastic lesions in the bone in approximately 90% of cases (Autzen et al., 1998). The evidence for increased bone formation in human prostate cancer metastases arises from a number of sources. Firstly, nuclear bone scans in addition to X-rays have frequently displayed extensive osteoblastic activity and this has been confirmed quantitatively by bone histomorphometry. Bone biopsies in several prostate cancer patients having advanced disease have thus shown increases in osteoid surface and in osteoid volume, whereas this has not been observed in biopsies from prostate carcinoma patients having localized tumors (Clarke et al., 1993).   This new formation of bone was associated with an increase in the mineral apposition rate therefore implying the formation of mineralized new bone. Further, histologic observations have shown an increase in woven bone that is associated with metastatic prostate carcinoma showing the presence of multiple osteoblast cells adjacent to the tumor tissue-bone interface. Osteoblastic metastases can potentially cause hypocalcemia and cause pathologic fractures as the newly woven bone is intrinsically of low strength (Szentirmai et al., 1995). The osteoblastic metastases lack a suitable mouse model and information about these lesions is limited to studies of human prostate cancer patient specimens. The pathophysiology of osteoblastic and osteolytic lesions of bone metastases involves interactions between tumor cells, osteoblasts, osteoclasts, endothelial cells, fibroblasts, bone marrow precursor cells and cells of the immune system.
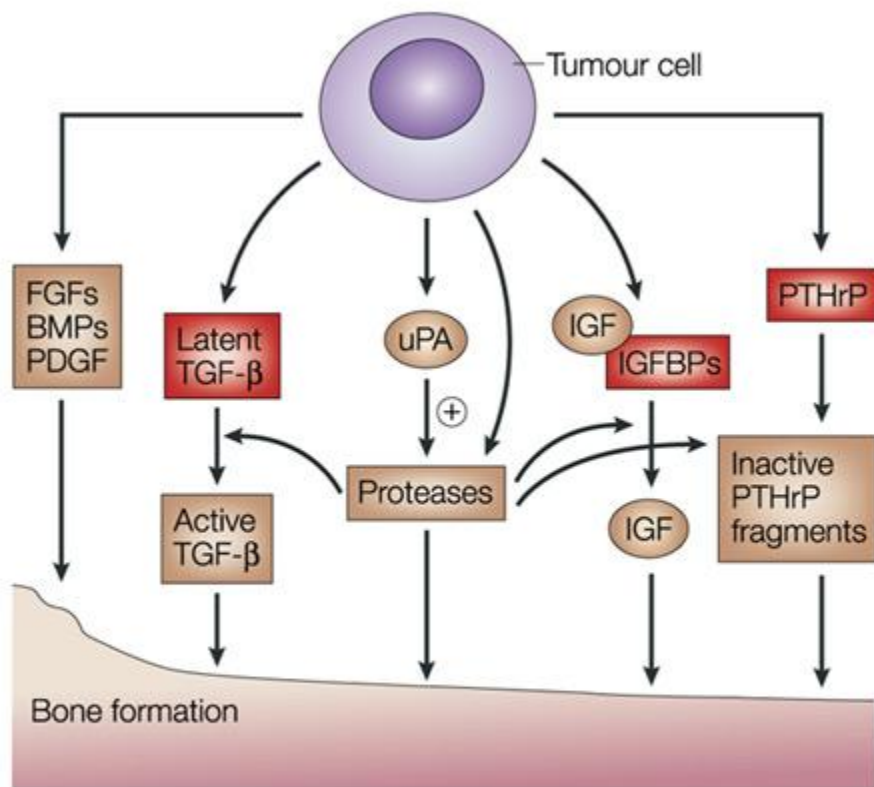
Figure 2: Mechanistic model of osteoblastic metastases and bone formation in human prostate cancer. *(From Mundy GR, Nature Reviews Cancer, 2002, 2: 584-593)*

Mechanisms of osteoblastic metastasis:

There is now evidence that multiple factors stimulate bone formation that is associated with osteoblastic lesions. Among them, endothelin-1, a ubiquitous growth factor has been reported to activate osteoblast proliferation and bone formation in bone

organ cultures. Patients with advanced hormone refractory prostate cancer with metastatic lesions were found to have significantly higher plasma concentrations of endothelin-1 as compared to patients without metastases or normal controls. Further, expression of endothelin-1 is increased in breast cancer cell lines that produce osteoblastic metastases (Nelson et al., 1995). Endothelin-A-receptor antagonists have been shown to inhibit both osteoblast proliferation and bone metastases (Yin et al., 2003). The following are the factors thought to play a role as mediators of osteoblastic metastases in prostate cancer

The transforming growth factor-β family: Several members of the transforming growth factor-β family have been reported to stimulate the proliferation of osteoblasts in vitro and new bone formation *in vivo* (Marcelli et al., 1990). TGF-β is highly expressed by differentiated osteoclasts and osteoblasts, presnt in the bone matrix and is released in its active form in bone resorption as a result of osteoclasts. Although TGF-β has been reported to play a role in osteoblastic metastases, it could also mediate osteolytic metastases under certain circumstances. It has been reported that TGF-β induces PTHrP activity (Guise, 2000). PC3 human prostate cancer cells express high levels of TGF-β2 which is known to support bone formation *in vivo.* Several bone morphogenic proteins (BMPs) that belong to the TGF-β superfamily are expressed in both normal and neoplastic human prostate tissue − namely, BMP2, BMP3, BMP4 and BMP6 (Harris et al., 1994a).

Proteases: It is known that proteases that activate growth factors like TGF-β play important roles in the bone (Dallas et al., 1995; Dallas et al., 1994). Urokinase or urinary

plasminogen activator (uPA) is a protease that has been implicated in processes such as embryo implantation, wound healing and extracellular matrix breakdown thus facilitating invasion of the tumor. It has been shown that overexpression of uPA in rat prostate cancer cells results in the induction of bone metastases *in vivo* (Achbarou et al., 1994). It was reported that the amino-terminal fragment of uPA has mitotic activity for osteoblasts and that its carboxy-terminal domain that has the proteolytic activity may mediate invasiveness of the tumor or the activation of growth factors (Rabbani et al., 1992). It is possible that uPA acts by cleaving plasmin, the latent TGF-β binding protein that masks TGF-β activity and thereby prevents the sequestration of TGF-β. Another potential mechanism of metastasis of prostate cancer cells is related to a serine protease, prostate specific antigen (PSA) that is produced in excess by prostate cancer cells and is widely used as a marker of tumor burden. It has been reported that PSA cleaves PTHrP at the amino terminus and has the potential to activate other growth factors produced by prostate cancer cells (Cramer et al., 1996; Iwamura et al., 1996). Though not known, a possible mechanism is that PSA cleaves osteoclast-stimulating growth factors such as insulin-growth factor-1 (IGF-1) and TGF-β and thereby activating them.

Growth Factors: Prostate cancer cells have been reported to express fibroblast growth factors (FGFs) that are thought to mediate the proliferation of osteoblasts in prostate cancer patients (Canalis et al., 1988; Canalis et al., 1987; Dunstan et al., 1999; Izbicka et al., 1996; Mansson et al., 1989; Matuo et al., 1987; Mayahara et al., 1993). PDGF-BB has also been shown to as a potential mediator of osteoblastic response (Yi et al., 2002). In addition, data has shown that prostate cancer cells produce bone morphogenic proteins

(BMPs) and also express BMP receptors, thus indicating a potential autocrine role (Bentley et al., 1992; Harris et al., 1994b; Ide et al., 1997).

Therapeutic approaches to minimize or reverse the osteoblastic response:

The bone morphogenic proteins are members of the transforming growth factor-β superfamily that are known to be important for skeletal development and have been reported to induce osteogenesis (Hogan, 1996; Reddi, 1998). It is believed that BMPs play a major role in the osteoblastic response of prostate cancer cells. This is because prostate cancer cells express BMPs and their receptors, which on binding to the ligand promote SMAD1 signaling and over-express osteoprotegerin, an inhibitor for the production of osteoclasts (Brubaker et al., 2004). Further, there have been recent reports that BMP2 and BMP6 stimulate the invasive potential of prostate cancer cells (Dai et al., 2005). It is therefore thought that one therapeutic approach to inhibit osteogenesis is through the use of BMP inhibitors. Interestingly, noggin which acts as a BMP inhibitor has been shown diminish the growth of prostate cancer cells in the bone (Feeley et al., 2006). In addition, noggin has been shown to inhibit the effects of BMP6 in vitro on human prostate cancer cells (Haudenschild et al., 2004). These reports lend support to the hypothesis that one approach towards the management of prostate cancer bone metastases would be through the use of BMP inhibitors.

The Wnts are a large family of proteins that are produces by prostate cancer cells and play a role in bone formation. The canonical Wnt pathway that acts through two

interacting receptors, frizzled and LRP5/6, results in the nuclear localization of β-catenin which in turn regulates a largely unknown set of genes that mediate bone formation (Westendorf et al., 2004). Dickkopf-1 has been reported to inhibit Wnt activity (Kawano and Kypta, 2003). In a recent report, it was shown that Wnt signaling is important in inducing bone formation (Hall et al., 2005). They showed that the inhibition of dickkopf-1 changed the normally highly osteolytic PC3 cells to an osteoblastic cell line. Further, they showed that by over-expressing dickkopf-1 in the C4-2B cells, which normally produce a mixed osteolytic-osteoblastic lesions when injected into mouse tibia, turned C4-2B cells into osteolytic lesions. This report is the first direct *in vivo* study showing the role played by Wnt in prostate cancer bone metastasis. It is speculated that in the future, inhibitors of Wnt signaling will be used in prostate cancer models of bone metastasis.

The first clinical trial to specifically target osteoblasts in prostate cancer patients who have bone metastases are based on antagonists to endothelin-A receptor. Endothelin-1 is a powerful vasoconstrictor, levels of which are elevated in patients with advanced prostate cancer (Nelson et al., 1995). Further, endothelin-1 has been reported to play a role in stimulating osteoblasts (Takuwa et al., 1989; Yanagisawa et al., 1988). The administration of endothelin-A receptor antagonists (ABT-627) in preclinical animal models reduced the number of metastatic lesions caused by endothelin-1 over-expressing xenografts of breast cancer (Nelson et al., 1995; Yin et al., 2003). In addition, several other studies have validated the important role played by endothelin axis in the induction of osteoblastic response (Fizazi et al., 2003; Guise and Mohammad, 2004). Atrasentan (trade name for ABT-627) is being used in clinical trials and has been reported to be well tolerated and to delay the progression of hormone refractory prostate cancer in some men

(Carducci et al., 2002; Carducci et al., 2003; Zonnenberg et al., 2003). Further, Atrasentan has been reported to significantly attenuate the blood levels of PSA as well as alkaline phosphatase, a marker of bone formation, suggesting that it effects both tumor cells and osteoblasts (Nelson et al., 2003).

Therapeutic approaches to minimize or reverse the osteolytic response:

The fact that bone metastases in prostate cancer have an osteolytic as well as osteoblastic component has been appreciated only in the recent years. There have been several reports of increased biochemical markers of osteolysis that depict bone resorption in prostate cancer patients (Berruti et al., 2005; Brown et al., 2005; Fukumitsu et al., 2003; Lipton et al., 2001; Noguchi et al., 2003; Petrioli et al., 2004). These markers include the N-telopeptide of type 1 collagen, the pyridinoline-cross peptides and deoxypyridinoline-cross lined peptides. However, there have been mixed reports as to the efficacy of these markers in comparison to PSA in the detection of osteoblastic metastases and in the monitoring the progression of the tumor (Fukumitsu et al., 2003; Noguchi et al., 2003).

It is thought that prostate cancer patients with bone metastases suffer from three processes or insults that result in decreased bone density. First, older men have decreased hormone levels that is thought to be critical in maintaining the bone remodeling system in a balanced state (Riggs et al., 1998; Stege, 2000). Though this process of bone resorption is slower than experienced by menopausal women, however, it is apparent clinically.

Secondly, androgen deprivation therapy results in additional loss of bone in prostate cancer patients and can exceed the bone loss encountered in early-stage menopausal women (Eastell, 1998; Higano et al., 2004; Smith et al., 2003). The third insult is as a result of factors produced by prostate cancer cells within the bone microenvironment that promote osteolysis. These factors include interleulin-1, interleukin-6, interleukin-11, parathyroid hormone related protein and RANKL (Keller and Brown, 2004; Roodman, 2004). Apart from the morbidity experienced by prostate cancer patients due to these osteolytic events, bone lysis in turn releases a slew of growth factors that are present in the bone matrix. These factors are known to stimulate the growth of prostate cancer cells and thus constitute a vicious cycle of bone remodeling (Clines and Guise, 2005). Therefore, to reduce the osteolytic onslaught, two approaches that are complimentary to each other have been used. The first involves bisphosphonates that reduce the degradation of bone and the other approach makes use of the inhibition of the OPG/RANK/RANKL system.

Bisphosphonates: Bisphosphonates are pyrophosphate analogues that have been reported to affect osteoclasts by several mechanisms (Rogers et al., 1997). Further, multiple investigations have reported that bisphosphonates have anti-tumor effects (Aparicio et al., 1998; Hiraga et al., 2001; Shipman et al., 1998; Tassone et al., 2003) and that administration of zoledronic acid, a new generation bisphosphonate, effects prostate cancer (Lee et al., 2001; Oades et al., 2003). In a recent report, it was found that zoledronic acid inhibited the growth of prostate cancer xenografts when implanted in the tibia of severe combined immunodeficient mice (Corey et al., 2003). The study revealed that zoledronic acid prevented the growth of these tumors if administered in either way –

as a preventative or as a method of treatment after the tumor had established growth. It was further especially noted in the study that bisphosphonate significantly affected the growth of prostate cancer xenografts that were osteoblastic in nature.

A number of clinical trials on hormone refractory prostate cancer patients with metastases have been performed (Ernst et al., 2003; Saad et al., 2002; Small et al., 2003). Several investigators have recently reviewed the use of bisphosphonates in prostate cancer patients (Brown et al., 2004; Green, 2005; Higano, 2003; Pinski and Dorff, 2005; Smith and Nelson, 2005). Of all the clinical trials, the Zometa 039 study is the only trial that showed promising results of reducing the skeletal metastases including morbidity from pain. However, overall, it is thought that bisphosphonates have undoubtedly benefited in reducing the loss of bone density in aging men and that it will have a significant role in the treatment of prostate cancer metastases. Another approach that investigators are pursuing in pre-clinical models of prostate cancer is combinational therapy whereby both the bone as well as tumor microenvironments are being targeted (Bertelli et al., 2006; Efstathiou et al., 2005; Vordos et al., 2004; Witters et al., 2003).

Fc-OPG: OPG acts as a soluble decoy receptor for RANKL and represses the differentiation of osteoclasts through the mechanism of RANK/RANKL interaction. It has therefore been surmised that in theory, OPG could be a treatment option for osteolytic bone lesions. Reports of preclinical studies have shown that OPG has an effect on prostate cancer cells growing in the bone microenvironment (Corey et al., 2005; Kiefer et al., 2004; Quinn et al., 2005; Yonou et al., 2003; Zhang et al., 2001). These

studies have revealed that OPG has its effect on the growth of prostate cancer cells in the bone microenvironment through the suppression of osteolysis.

Monoclonal antibodies to RANKL and soluble RANK Fc: One of the potential disadvantages of using OPG to effect prostate cancer bone metastases is that OPG acts as a survival factor by binding to the tumor necrosis factor-related apoptosis inducing ligand (Corey et al., 2005; Holen et al., 2002; Shipman and Croucher, 2003). Therefore to avoid this drawback, investigators have been using soluble RANK-Fc and monoclonal antibodies to RANKL in order to block RANK-RANKL interaction (Bekker et al., 2004; Sordillo and Pearse, 2003). In a report using a preclinical prostate cancer model, Zhang et al showed that soluble RANK-Fc reduced the tumor-induced osteoblastic lesions along with a reduction in the markers of bone resorption and serum PSA. (Zhang et al., 2003). Another report showed that administration of AMG-162, a human monoclonal antibody to RANKL resulted in a significant decrease in markers of osteolysis (Bekker et al., 2004).

Targeting senescence pathways in cancer:

Senescence or irreversible proliferation arrest has recently been recognized as a drug responsive strategy that has the potential to influence the outcome of cancer therapy. Chemotherapy has been used to treat cancer for decades. However, treatment strategies that use high drug doses are often associated with toxic side effects. Similarly low doses of drugs are not very effective due to patient relapse and drug resistance. It has been

shown that low doses of drugs can induce senescence as opposed to high concentration of drugs that are required for apoptotic cell death. Hence a better approach for treatment would be to force cells to undergo senescence since much less concentration of drug is required for induction of proliferation arrest (Chang et al., 2002; Schmitt, 2003; Zheng et al., 2004). A good understanding of the strategies by which cancer cells can be forced into senescence can prove to be very useful for cancer therapy particularly due to the drug resistance issue.

The T-box gene family:

The T-box family genes comprises of a family of DNA binding transcription factors that are evolutionarily and molecularly linked by the presence of a conserved DNA-binding motif known as the T-box (Papaioannou, 2001)The T-box genes have been found in all metazoans, ranging from hydra to humans and are conspicuous for the key roles they play during embryonic development (Adell et al., 2003; Papaioannou, 2001; Showell et al., 2004) Several observations suggest that T-box genes perform important developmental functions. First, the expression of most of T-box genes is specific during the window of embryonic development. Secondly, genetic developmental diseases in humans are known to be caused by mutations in several T-box genes. Thirdly, studies in mice achieved by targeting mutations in T-box genes have found severe developmental phenotypes that mimic human disorders (Chapman and Papaioannou, 1998; Naiche and Papaioannou, 2003). The vertebrate genome has at least 18 different T-box genes with diverse functions. The T-box genes comprise of a number of subfamilies that are

arranged based on studies of phylogeny and expression. The Tbx2 subfamily consists of two pairs of linked genes which are thought to be a product of two-gene clusters (Agulnik et al., 1996). As a result, in humans, Tbx2 and Tbx4 cluster on chromosome 17q23 and Tbx3 and Tbx5 cluster on chromosome 12q24 (Agulnik et al., 1996). However, Tbx2 on 17q23 has more homology to Tbx3 whereas Tbx4 has greatly related to Tbx5. The T-box proteins interact as monomers or dimmers and bind to the brachyury response element (TTT(G/C)ACACCTAGGTGTGAAA) (Kispert and Herrmann, 1993). Of all the T-box genes, Tbx2 and Tbx3 are the only T-box factors that are known to function as transcriptional repressors (Carreira et al., 1998; He et al., 1999). This activity is known to be performed by both the N- and C-terminal repression domains in Tbx2 (Paxton et al., 2002).

Tbx2 can suppress p19(Arf) and p21 to promote immortalization:

The Arf/Mdm2/p53 pathway is one of the best known mechanisms in the cell for senescence downregulation (Lowe and Sherr, 2003). A number of oncogenes or mitotic signals can enhance the expression of alternate reading frame (Arf) that causes the binding of Mdm2, p53 stabilization, and the resulting expression of p53 target genes. This pathway can act as a precursor of oncogenic transformation in primary cells with the resultant induction of p53–dependent senescence or apoptosis. Alternatively, cell cycle arrest can be p53 independent too. On the other hand, silencing or inhibition of Arf can also lead to the same result i.e. bypass of senescence, proliferation, failure to cause apoptosis and immortalization of cells. Jacobs *et al.* reported on a genetic screen to

identify genes that are responsible for inhibiting senescence which showed that Tbx2 promoted the bypass of senescence through the inhibition of p19(Arf) (Jacobs et al., 2000). They found that this inhibition was at the transcriptional level. Further, Tbx2 could promote the bypass of senescence in mouse embryonic fibroblasts (MEFs) that were predisposed to senescence. In the same study, over-expression of endogenous p19(Arf) in MEFs expressing Tbx2 resulted in senescence. This showed that p19(Arf) acts downstream of Tbx2 and that Tbx2 can control the bypass of senescence by negatively regulating p19(Arf). It has been shown that in primary cells, overexpression of oncogenes such as c-myc or activated Ras can promote senescence by activating p19(Arf) expression. The cells use this strategy to sense uncontrolled activation of mitogenic signaling pathways thereby promoting p53-dependent cell cycle arrest. Enhanced expression of Tbx2 can help promote the transformation event by downregulating the p19(Arf)-dependent pathway that would otherwise prevent abnormal myc or Ras expression from promoting transformation (Jacobs et al., 2000). Similar to p19(Arf), the p21(Waf1) cyclin-dependent kinase inhibitor plays a key role in senescence and in cell cycle arrest after DNA damage (Bendjennat et al., 2003; Gartel et al., 1996). The most described signaling pathway for chemotherapeutic agent-induced induction of proliferative arrests is initiated by DNA damage. In response to DNA damage, cell cycle is arrested and this effect is mediated through checkpoints which allow repair before the start of the next cell cycle. The stabilization of p53 leading to enhanced transcription of p21(Waf1) is the most important event for drug induced G1-S checkpoint leading to senescence. Approaches leading to both suppression and over-expression of p21 have resulted in increased sensitivity of cancer cells to genotypic stress leading to senescence.

Expression of p21 is regulated by both p53 dependent (el-Deiry et al., 1994) and independent pathways (Roninson, 2002). But the ability of p21 to enhance cellular response to drugs is usually independent of p53 status. It has been shown that ectopic expression of p21(Waf1) sensitized hepatoma cell line Hep 3B (p53 null cell line) to cisplatin (Qin and Ng, 2001).

In another study, p21(Waf1) sensitized human non small cell carcinoma H1299 (p53 null) and colon carcinoma DLD-1 (p53 mutant) cell lines to all transretinoic acid (Teraishi et al., 2003). p21(Waf1) also facilitated drug induced cell death in cells with functional p53 (De Schepper et al., 2003). In light of p21's role in the mediation of drug-induced senescence, one possible strategy to induce senescence is through the inhibition of genes that negatively regulate p21. It has been shown that Tbx2 can bind and repress the p21 promoter *in vitro* and *in vivo*. Small interfering RNA-mediated down-regulation of Tbx2 expression resulted in a robust activation of p21 expression (Prince et al., 2004).

Tbx2 and cancer:

It is now known that genes and signaling pathways that play important roles during development are dysregulated in cancer and may cause tumor initiation or progression. Amongst the mechanisms that can contribute to deregulation of these factors is the process of gene amplification that results in the overexpression of the amplified gene. Tbx2 is one such gene within the 17q23 amplicon (Barlund et al., 2000; Sinclair et al., 2002; Wu et al., 2001a). In prostate cancer, it has been reported that this region is

frequently amplified in 46% of late stage hormone refractory adenocarcinomas and in 31% of metastases (Andersen et al., 2002). In a study of breast cancer cell lines using Southern blot and fluorescence *in situ* hybridization (FISH), Tbx2 was shown to be amplified three of six cell lines and the MCF7 cell line had 50 copies of the gene (Barlund et al., 2000; Sinclair et al., 2002; Wu et al., 2001a). Using microarray techniques, similar results were observed (Barlund et al., 2000). Tbx2 overexpression was confirmed by RT-PCR in each of the cell lines that had the amplification. In the study, Tbx2 was amplified in 8.6% of the cases in 372 primary breast tumors. In another study of breast tumors, Tbx2 was observed to be amplified 200-fold for one breast tumor (Rouillard et al., 2001). RT-PCR analysis was used to confirm over-expression of Tbx2. Further, Tbx2 was also found to be amplified in 19 of 27 BRCA1 and BRCA2 tumors as compared with 8 of 27 sporadic controls, thus showing that Tbx2 is preferentially over-expressed in BRCA1 and BRCA2 associated tumors (Rouillard et al., 2001). In another study, Tbx2 was reported to be overexpressed in melanoma cell lines and shown to target histone deacetylase 1 to the p21Cip1 (CDKN1A) initiator. Expression of dominant negative Tbx2 resulted in up-regulation of p21cip1 and induced senescence in p21 null B16 melanoma cells. These results indicate that endogenous Tbx2 is critically required to enhance proliferation and suppress senescence in melanomas (Prince et al., 2004).

Tbx2 and Sonic Hedgehog signaling:

Sonic hedgehog (Shh) signaling has been reported to be upregulated in prostate tumors (Fan et al., 2004). Tbx2 and Sonic hedgehog regulate each other in a feedback and

feed forward mechanism. It has been shown that Tbx2 can activate the expression of Shh during the development of chick limb. Conversely, Shh signaling also regulates Tbx2 (Rowley et al., 2004). Shh activates Tbx2 in the posterior mesenchyme in chick limb development (Suzuki et al., 2004; Tumpel et al., 2002). In another study looking at the role of Shh in mouse lung development, Tbx2 was found to be significantly repressed in Shh (-/-) mouse (Li et al., 2004). This tight feedback and feed forward mechanism of regulation between Tbx2 and Shh is essential for digit identity and proper lung development.

BMP signaling, prostate cancer and Tbx2:

Several reports have shown that BMPs can promote the development and progression of osteoblastic lesions in prostate cancer (Autzen et al., 1998; Bobinac et al., 2005; Feeley et al., 2005; Thomas and Hamdy, 2000) Expression of BMP receptors correlate with the tumor grade in prostate cancers (Kim et al., 2000). In a study, BMP2 stimulated cellular migration and invasion of prostate cancer cells in a dose dependent fashion (Feeley et al., 2005). Data from several experimental systems show that BMP (bone morphogenic protein) 2/4 signaling can activate Tbx2 expression. Conditional inactivation of BMP2 in mouse myocardium caused loss of Tbx2 expression (Ma et al., 2005). Misexpression of Tbx2 in chick digit development caused misexpression of BMP2. Further, Tbx2 rescued noggin inhibited BMP signaling (Suzuki et al., 2004).

These data suggest a tight feed forward and feedback control of expression between Tbx2 and BMP signaling.
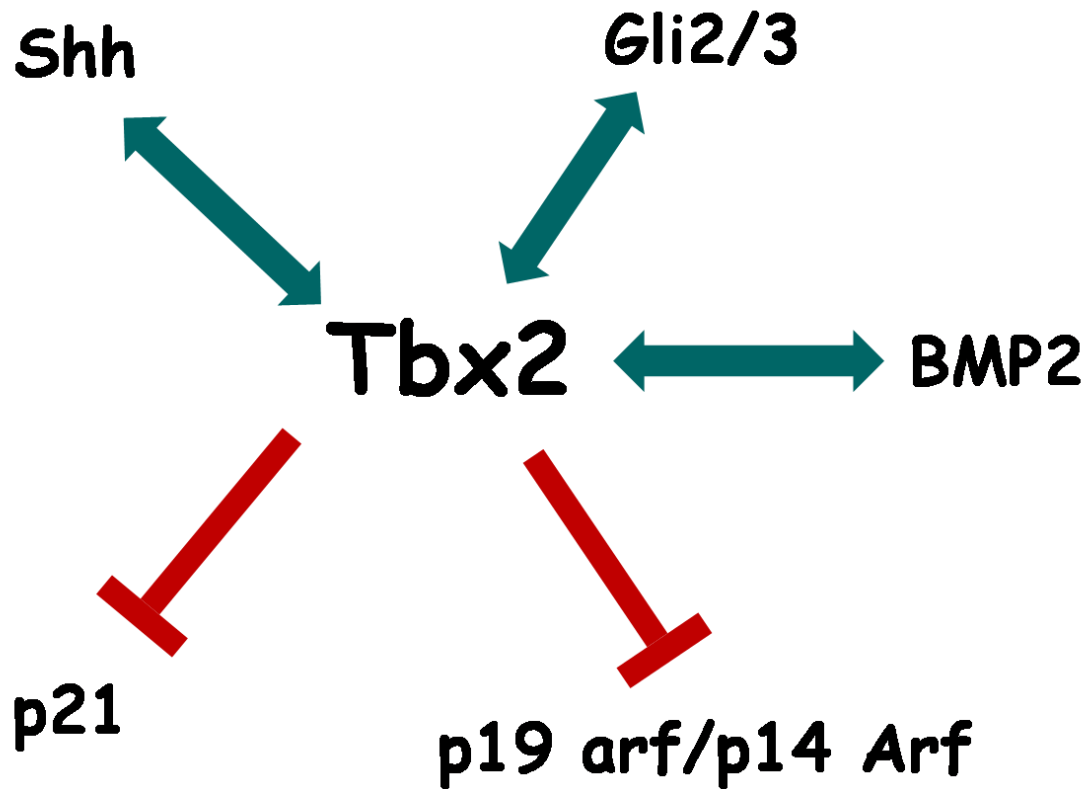
Figure 3: Tbx2 and its signaling pathways. Tbx2 represses p21 and p19arf / p14 arf at the transcriptional level. Also, Tbx2 has a feedforward - feedbackward regulation with Shh and BMP2.

CHAPTER II

MATERIALS AND METHODS

Generation of hepsin/myc mice:

Mice were housed in the animal care facility at Vanderbilt University Medical Center in accordance with the National Institutes of Health (NIH) and institutional guidelines for laboratory animals. The PB-Hi-myc and PB-hepsin mouse models have been described elsewhere (Ellwood-Yen et al., 2003; Klezovitch et al., 2004). These models were generated by utilizing the probasin promoter (ARR_2PB) to target the myc and hepsin genes, respectively, to the mouse prostate. The ARR_2PB sequence consists of the original probasin sequence PB (-286/ +28) combined with an additional androgen response region (Zhang et al., 2000)(Zhang et al., 2000)(Zhang et al., 2000)(Zhang et al., 2000)(Zhang et al., 2000)(Zhang et al., 2000)(Zhang et al., 2000). PB-hepsin and PB-Hi-myc mice were maintained in CF7BL/6J and FVB backgrounds respectively. All the mice were F1 offspring so the PB-Hi-myc mice were age matched and genetically matched to the hepsin/myc mice, therefore the Pb-Hi-myc and hepsin/myc bigenic mice were 50% C57BL/6J and 50% FVB. Mice were analyzed starting at 3 months of age.

Tail Digestion and DNA isolation:

A piece of mouse tail approx 2 cm was cut with the help of a sterile scissors and put in a tube on dry ice. 100 ml of the digestion buffer was made with 5 ml of 1M Tris-Hcl Ph 8.0, 20ml of 0.5 M EDTA, 10 ml of 10% SDS, 2 ml of 5.0 M NaCl & 63 ml of DNA RNAse free water. The tube was incubated at 55 deg C with vigorous shaking overnight. The supernatant (500µl) was transferred at room temperature to 1 ml of 100% ethanol. The tube was then gently inverted so that the DNA strands would precipitate. With the help of a glass micro-capillary tube (Kimax-51 34505), the DNA strands were hooked out and transferred to a tube containing 1 ml of DNA RNA ase free water. The tube was then vortexed vigorously placed at 4 deg C so that the DNA would dissolve in the water.

Whole dissection of the mice:

Mice were sacrificed by cervical dislocation method following the inhalation of an anesthetic agent in accordance with the policy of the Vanderbilt University Animal Care Committee. The organs removed were as follows: prostate, seminal vesicle, testes, vas deferens, bladder, periurethral glands, bulbourethral glands, para-aortic lymph nodes, liver, spleen, kidney, and lung. Part of the tissue was fixed in 10% formalin for histology examination and the rest was frozen on dry ice and stored at -80° C for RNA and protein extraction. As every prostate lobe exists as a pair, one of the pair was frozen while the other was fixed.

First, the genitourinary organs were removed. The mouse was anesthetized with isoflurane and sacrificed following cervical dislocation method. The abdominal area was sprayed with 95% ethanol and incisions were made longitudinally and horizontally to expose the abdominal cavity. The bladder was pulled with the aid of forceps and the prostate, seminal vesicles and urethra were identified. The urethra was cut below the prostate while the bladder was held with the foreceps. The bladder along with the attached genitourinary system was removed and was separated into the different lobes of the prostate (anterior, dorsal, ventral, lateral), seminal vesicle, bladder and urethra. Anatomically, all the prostate lobes are directly attached to the urethra. The anterior lobes run along the seminal vesicles, the ventral lobes rest on top of the bladder surrounded by the urethra while the dorsal lobes surround the urethra.

Next, the remaining organs of the abdomen were removed. The para-aortic lymph nodes that are located on both sides of the abdominal aorta were removed. The testis and epididymi were removed and separated. The bulbourethral glands that are located on both sides of the urethra were removed. The kidneys, liver and spleen were removed.

Finally, the organs of the chest cavity were removed. The chest area was sprayed with 95% ethanol and ribs and the chest cavity was exposed by cutting the ribs and sternum. The heart along with the entire lung was pulled out and the lung was separated from the heart. The neck was sprayed with ethanol and cut with longitudinal and horizontal incisions. The neck lymph nodes and the submandibular gland were removed.

Microtomy:

Even though the rate of formalin fixation of tissue is 1 mm/hr, the tissue was fixed for 1 day for optimum histology. Following formalin fixation, the tissue was stored in 50% ethanol at 4° C until processing was performed. For fixing bone, decalcification was performed following formalin fixation by soaking in 5% formic acid at 4° C overnight, rinsed in tap water for 30 min, and then placed in 50% ethanol prior to processing. The paraffin embedded tissue block was placed on ice for atleast 30 minutes prior to microtomy. The Millipore waterbath was set at 42° C and the microtome was adjusted to cut 5 µm thick sections. If the blades were new, the blades were run through Styrofoam three times prior to use to remove the Teflon coating which could cause a smear on the section. The blade was then placed deep in the microtome holder, such that the blade edge just stuck out of the holder, this was to minimize any vibration during cutting that could cause the tissue section to have "vertical blinds". The angle of the blade was adjusted to 5 degrees. The piston holding the block was extended from the body of the microtome at the least possible distance to minimize vibration during cutting. The leading edge of the tissue chain was held with forceps and the blocks were cut quickly. With the help of a brush, the lagging end of the tissue chain was broken and the tissue chain was laid on the water bath. The brush was used to pull flat any creases that were created. Individual sections in the chain were separated by piercing holes at the border between sections with a skewer and the sections were pulled apart with a brush. The skewer was occasionally dipped in a 1:1 mixture of xylene and 100% ethanol to dissolve the borders. With the aid of a brush, the individual sections were moved across the water surface and placed on a partially immersed Superfrost Plus AAS coated slide (VWR Scientific) The

first two sections of any tissue chain were discarded since the thickness was not accurate due to expansion caused by the block warming up. The slides were allowed to dry by resting in an upright position after any extra moisture was removed by blotting away. The slides were then placed in an oven at 65° C for 30 min so that the paraffin would melt away, thus ensuring that the tissue sections would not fall off during the experimental protocol.

RNA Isolation:

The protocol and reagents used were from the RNeasy Midi kit (Qiagen 75144). All the tools used were either sterilized or dipped in 3% HCl in 100% ethanol. A rotor-stator homogenizer at setting 4 for 20 sec on ice was used to homogenize the tissue. In between samples, the homogenizor probe was washed with Millipore, DEPC water, and wiped clean with a Kimwipe tissue. RNA kit was then used to extract RNA from the homogenized tissue samples. The RNA samples were then diluted in 50mM NaOH or DEPC water to read the optical density at 260 nm (OD_{260}) on a spectrophotometer. The concentration of the RNA was calculated by the following formula: $\mu g/\mu l = OD_{260}$ X 40 (as RNA constant) x dilution factor x 1/1000 (unit conversion). For DNA, the constant used was 50.

Concentration of RNA or DNA by ethanol precipitation:

For RNA, 1/10th the sample volume of 3M sodium acetate and 2.5X the sample volume of 100% ethanol was added to the sample. For DNA, 1/0th the sample volume of 3M sodium acetate and 2X volume of 100% ethanol was added to the sample. The samples were then placed at -80° C for 1 hour and centrifuged at 15,000 rpm at 4° C for 30 minutes. The supernatant was discarded and the pellet was washed with 0.5 ml of cold (4° C) 70% ethanol and centrifuged for 5 min at 15,000 rpm. After the ethanol was aspirated off, the pellet was resuspended in nuclease free water and the concentration was determined with the help of a spectrophotometer.

Quantitative real-time reverse transcriptase polymerase chain reaction (q RT-PCR):

RNA was extracted from tissue samples fixed in RNA later using the RNeasy mini kit (Qiagen, Valencia, CA, USA) according to the manufacturer's protocol including treatment with DNase. RNA concentration was measured using a spectrophotometer and RNA quality was assessed by agarose gel electrophoresis. Hepsin copy numbers were determined using a Lightcycler fluorescent temperature rapid-air cycler (Roche Molecular Biochemicals, Indianapolis, IN) with cDNA standard curves and the double-stranded DNA-binding fluorescent probe SYBR green (Biorad, Hercules, CA, USA) The forward hepsin primer (5' CTCTAGCTCCCTGCCTCTCA 3') and reverse hepsin primer (3' CGTTGCTTATGATGGGAACC 5') generated a 170 bp amplimer. Melting curve

analysis that compared the melting curves from the samples, standards and negative controls confirmed the specificity of the amplimer in each reaction. Copy numbers of mRNA were calculated, using the Lightcycler software (version 3.5), from serially diluted (1:10) standard curves (10^9-10^3 copies). The standards that were serially diluted were simultaneously amplified along with the unknown samples to generate a linear standard curve using the fit points analysis method. Also, real-time RT-PCR was performed for 18S as a loading control using a cDNA template, the forward 18S primer (5' CAAGAACGAAAGTCGGAGGTTC), and the reverse 18S primer (5' GGACATCTAAGGGCATCACAG).

One step RT-PCR was performed in a Lightcycler machine with 200 ng of RNA, 1 mM of MgCl2, 1.25 µM each primer. Reverse transcription was performed at $55\,^o$ C for 15 min followed by denaturation at $95\,^o$ C for 30 sec. Amplification was performed with 45 cycles of 95° C for 1 sec, 50° C for 5 sec, 72° C for 10 sec, and 82° C at 5° C / sec. for 2 sec for single acquisition to quantiate the product. Melting was performed with 95° C for 0 sec, 65° C for 20 sec, and 95° C at $0.1\,^o$ C / sec for 0 sec for continuous acquisition to determine specificity.

General Immunohistochemistry Protocol:

Tissue sections that were 5 µm in thickness were deparaffinated and rehydrated by sequential washings in 100% xylene, 100% ethanol, 100% ethanol, 70% ethanol, and 50% ethanol for 3 minutes each. The slide rack was then dipped in Millipore water. 10X

PBS buffer was made by mixing 160.0 g of NaCl, 4.0 g of KCl, 28.8 g of Na2HPO$_4$, and 4.8 g of KH2PO$_4$ then make up the volume to 2 liters while adjusting the pH to 7.4. For optimization of signal, antigen retrieval was performed with 0.01 M citrate, 1 M urea, or proteinase K (DAKO S3020) digestion. The citrate solution was prepared by combining 10.8 ml of 0.1 M anhydrous citric acid (Fisher A940-500; 1.91 G/100 ml), 49.2 ml of 0.1 M tri-sodium citrate acid (Sigma C-8542; 14.705 g/500 ml), and 540 ml of H$_2$O. The urea solution was prepared by dissolving 36.0 g of urea (Fisher BP 169-212) in 600 ml of millipore water. To perform antigen retrieval with citrate or urea solution, the slide rack was placed in the solution, the solution was heated (5 min 30 sec) to bring to boiling by microwaving at full power, then the solution was microwaved at 30% power for 20 minutes, and cooled at room temperature for 1 hr. For antigen retrieval with proteinase K, the sections were incubated with the solution for 15 min at room temperature.

Following antigen retrieval the slides were washed thrice in 1X PBS. The tissue sections on the slides were encircled with the help of a PAP pen. The slides were treated with Peroxidase Blocking Reagent (DAKO S2001) to block endogenous peroxidase activity. The slides were washed thrice in 1X PBS. Next, the slides were blocked with blocking buffer for 30 min at room temperature. The blocking buffer was either 1% DIG in Tris-NaCl pH 7.5 or 10% normal serum in 1X PBS. The 1% DIG in Tris-NaCl was prepared by combining 50 ml of 1M Tris-HCl pH 7.5, 15 ml of 5 M NaCl, 435 ml of H$_2$O, and 5 g of DIG blocking reagent (Roche 1096176) then stirring until dissolved (about 1 hr). Normal serum was of the same animal origin as that of the secondary antibody. After blocking, the excess buffer was blotted off but the slides were not washed. Negative control solution (100 µl) was added to one section and the primary

antibody solution (about 100 µl) was added on top of the adjacent tissue section of the same slide, carefully making sure that each solution remained within the boundary of the encircled PAP pen. The negative control solution was normal IgG of the same animal origin and at the same concentration as the primary antibody in PBS, a 1:5 mixture of primary antibody and blocking peptide in PBS, or PBS alone. The primary antibody and negative control solutions were made with either 1X PBS or 2% filtered bovine serum albumin in 1X PBS. The slides were the placed in a covered, humidified slide box with wet paper towels at the bottom at 4° C overnight.

After the incubation with the primary antibody, the slides were removed from the humid chamber and washed thrice with 1XPBS for 5 minutes each time. Secondary antibody solution (about 100 µl) was added to each tissue section and the slides were incubated in a covered humid box for 2 hrs at room temperature. The secondary antibody was made either with 1X PBS or 2% bovine albumin serum and 5% normal serum in 1X PBS. The secondary antibody was aspirated off and the slides were washed with 1X PBS three times, 5 min each. Next, the tertiary antibody conjugated to horseradish peroxidase was added to the sections and the slides were incubated at room temperature for 1 hr. The tertiary antibody was blotted off and the slides were washed three times in 1X PBS for 5 min each time. Slides were then immersed in 50 mM Tris-Hcl at pH 7.4 for a few minutes. DAB solution (3,3' diaminobenzidine tetrachloride) was prepared using the Liquid DAB Substrate-Chromogen System (DAKO K3466). DAB solution (100 µl) was added to each slide individually and the sections were observed under a microscope for color development. The reaction was stopped by blotting off the excess DAB solution and the slides were immediately placed in H_2O.

The slides were counterstained with hematoxylin for nuclear visualization. Hematoxylin was filtered prior to each use. The slides were dipped twice in hematoxylin, twice in tap water, and placed under running tap water for 1 minute. Then the slides were dipped ten times in ammonium water, twice in tap water, and washed under running tap water for 1 minute. The slides were dipped in 95% ethanol for 20 times. The slides were dehydrated by dipping them sequentially in 100% ethanol, 100% ethanol, xylene, and xylene for 3 minutes each. The slides were transferred to a third container of xylene before being cover slipped with cytoseal 60 (Richard-Allan Scientific 83104). Any bubbles were pushed away from the tissue section by gently pressing with a forceps.

The following primary antibodies were used (with the indicated dilutions in PBS): AR N-20 Santa Cruz Biotechnology Inc., sc-816 (1:1000); Foxa1 C-20 sc-6553 (1:1000), Hepsin Cayman Chemical cat# 100022 (1 µg/ml) and Myc N terminal antibody Epitomics cat #1472-1 (Gurel et al., 2008)(Gurel et al., 2008)(Gurel et al., 2008)(Gurel et al., 2008)(Gurel et al., 2008)(Gurel et al., 2008)(Gurel et al., 2008) (dilution 1:1000). Staining was visualized using Vectastain ABC kit (Vector Laboratories Inc, Burlingame, CA, USA) and 3,3'-diaminobenzidine tetrahydrochloride (Dako).

Western Blot:

The lysis buffer for protein extraction was prepared by mixing 10 ml of RIPA buffer (PBS at pH 7.4, 1% NP-40, 0.5% sodium deoxycholate, 0.1% SDS), 100 µl of 100 mM PMSF, and one tablet of Complete Mini protease inhibitor cocktail (Roche

1836153). Lysis buffer (6 to 10 times of tissue volume) was added to the frozen tissue. The tissue in lysis buffer was subjected to sonication at setting 5 for 20 sec. This was repeated 3 times until the tissue was homogenized. Between samples, the probe was washed with distilled water and 95% ethanol then wiped with a Kimwipe. The homogenized tissue was centrifuged for 10 min at 14,000 at 4° C. The supernatant that was proteinaceous was transferred to a new tube. Protein estimation of the samples was performed using the Bio-Rad Protein Assay (Bio-Rad Laboratories 500-0006) and a BSA standard curve measured at OD_{595} was carried out. The protein extract was stored at -80° C.

Protein electrophoresis was done utilizing the XCell SureLock Mini-Cell (Invitrogen E10001), 7% Tris-Acetate gels (Invitrogen EA035A), AND Tris-Acetate SDS Running Buffer (Invitrogen LA0041). Protein lysates were mixed with LDS sample buffer (Invitrogen NP0007) and β-mercaptoethanol then heated for 10 minutes at 70° C. The gel was securely placed the cell and the wells were flushed with the buffer with a pipette. The samples were centrifuges briefly, loaded onto the gel along with a protein ladder, and electrophoresed for about 1 hour at 150 volts.

The proteins were transferred using the Mini Trans-Blot cell (Bio-Rad) and PVDF filter paper sandwich (Invitrogen LC2005). The 10X transfer buffer was prepared by combining 19.3 g of Tris base and 90 g of glycine, then making up the volume to 1 liter with water. The protein was run such that it migrated towards the red (positive) wall. Four filter papers were immersed in 1X transfer buffer. Two filter papers were placed on the black side of the sandwich case. The Tris-Acetate gel was then placed on top of the

filter papers. The membrane was placed on top of the gel. The remaining two filter papers were placed on top of the membrane. A falcon tube was rolled on top of the sandwich to remove any bubbles. The sandwich was closed and inserted into the cell with the clear side facing the red wall. A stir bar was placed at the bottom of the cell. The cell was filled with the transfer buffer and run at 30 volts while stirring for overnight at 4° C.

The membrane was removed from the cell and gently washed in distilled water with the protein side facing up. The membrane was stained with Ponceau S solution (Sigma P7170) to visualize the bands inorder to ensure that proper transfer occurred without air bubbles. The membrane was rinsed with distilled water 3 times remove excess Ponceau S. Next, the membrane was blocked by incubating with blocking buffer containing 5% skimmed milk dissolved in TBS-T buffer (200 mM Tris, 1.37 M NaCl, 0.1% Tween-20). 10X TBS was prepared by combining 24.2 g of Tris and 80.0 g of NaCl then making up the volume to 1 liter with water while adjusting the pH to 7.6. 1 ml of Tween-20 was mixed to 1 liter of 1X TBS to make the TBS-T buffer. The membrane was blocked at room temperature for 1 hour while shaking gently.

The membrane was washed three times with 1X TBT-T for 15 min each. For Laminin-332 detection, the membrane was incubated with primary polyclonal antibody to C-terminus of Ln-332 β3 chain (1:500 sc-20775; H-300; Santa Cruz Biotechnology, Inc). The membrane was washed three times with 1X TBS-T for 15 min each. Next, the membrane was incubated with horseradish peroxidase linked anti-rabbit Ig (Amersham NA9340) at 1:2000 dilution in blocing buffer for 2 hr at room temperature. The membrane was washed thrice with 1X TBS-T for 10 min each.

Protein bands were visualized using the ECL plus (Amersham RPN2132) and BioMax MR Film (Kodak 870-1302). Development of the film was performed in the dark room with red safety lighting. The ECL Plus reagents were mixed in a falcon tube. The membrane was dipped for one minute in the ECL Plus mixture and then blotted on paper to remove excess reagent. The coated membrane was wrapped in a plastic wrap, placed in a cassette and taped down. A piece of BioMax film was placed on top of the membrane, then the cassette was closed for the desired exposure time. The film was then run through the developer to produce the bands. The bands in the protein ladder were marked and used to determine the size of bands in the lanes.

For β-actin visualization, the Laminin-332 Western membrane was stripped by incubation with the stripping solution (2% SDS, 62.5 mM Tris-HCl (pH 7.4), 100 mM β-mercaptoethanol) for 30 minutes at 55° C. The membrane was then blocked and probed with monoclonal anti-β-actin antibody (Sigma A5411) at 1:10,000 in blocking buffer followed by horseradish peroxidase linked anti-mouse Ig (Amersham NA931V) at 1:2000 dilution in blocking buffer. Bands were visualized with ECL plus and Biomax MR Film.

In situ hybridization:

Freshly dissected prostates were rinsed twice in PBS and fixed in 4% paraformaldehyde – PBS fixative for 15 minutes to overnight depending on the size of the tissue mass with gentle rocking (in glass scintillation vials). Fixed tissue was then placed in cassettes and

dehydrated by washing at 4° C with cold PBS followed washing with 50% ethanol, 70% ethanol, 90% ethanol and 100% ethanol for 30 minutes each.

Fixation of the tissue was followed by embedding in paraplast. The tissue cassettes were then washed for 30 minutes each, in ethanol, mixture of ethanol and xylene, xylene, mixture of xylene and wax, and finally three times in wax. At the end of the third wax wash, tissues were oriented in the mold with a warmed foreceps and embedded blocks were stored at 4° C before sectioning. The blocks were sectioned on slides previously washed in DEPC water and dried. The tissue sections were cut and placed on DEPC water before placing them on the slides. The slides were stored at 4° C.

The probe was prepared by adding 10 µl of DEPC H_2O, 3 µl of 100 mM DTT, 3 µL of 10x transcription buffer, 1 µl of 10mM rATP, 1 µl of 10mM rCTP, 1 µl of 10 mM rGTP, 1 µl of template DNA, 1 µl of RNase inhibitor, 10 µl of ^{35} – thio UTP and 1 µl of enzyme (T7/T3/SP6). The probe was then incubated for 3 hours at 30° C. The DNA template was digested by adding 1 µl DNase I and incubated at 37° C for 15-30 minutes, and the DNase was topped by adding 3 µl of 200 mM EDTA. The reaction volume was made up to 50 µl with DEPC-H_2O and purified using Kodak NuClean R50 Disposable Spun Column. 10 µl of 10 mg/ml yeast tRNA was added and the reaction volume was made upto 100 µl by adding DEPC – H_2O. 50 µl of 4M NH_4-OAc and 200 µl of Et-OH was added, left at room temperature for 10 minutes and centrifuged at 15,000 rpm for 15 minutes. The pellet was rinsed in 500 µl of 70% EtOH and resuspended in 100µl 10mM DTT and 1µl of RNase inhibitor was added. 2 µl of probe solution was taken and specific activity was counted by a scintillation counter. The probe was diluted with 10 mM DTT

so that the final activity was 1×10^{6} cpm/µl and the probe stock solution was stored at $-70\,^{\circ}$ C until use.

The sections were pretreated for hybridization in the following manner:

The tissue on the slides was prepared for hybridization by the removal of wax, leaving the sections intact on the slide. This was followed by a deproteinization step to make the tissue more porous to the probe.

The slides were placed in a glass rack and transferred from one solution to the other in glass staining jars, tapping occasionally at each step. The sections were dewaxed through a series of washes at room temperature:

Xylenes	3 times, 5 minutes each
100% ethanol	3 times, 2 minutes each
95% ethanol	1 time, 2 minutes each
70% ethanol	1 time, 2 minutes each
50% ethanol	1 time, 2 minutes each
H_2O	2 times, 2 minutes each

The sections were then acid treated to denature RNA at room temperature by the following way:

0.2 M HCl	15 minutes
H_2O	rinse

PBS	3 times, 1 minute each

The sections were then treated with proteinase K to permeabilize the cells as follows:

(20 µg/ml proteinase K,	6-8 minutes

50 Mm Tris pH 7.5, 5 mM EDTA)

H_2O	1 time, 5 minutes

The sections were then post fixed at room temperature with 4% paraformaldehyde PBS for 15 minutes followed by 2 washes in PBS for 2 minutes and finally rinsed with water once for 2 minutes. The slides were then acetylated twice with a mixture of 0.1 M triethanolamine and acetic anhydride. The sections were washed twice in H_2O and air dried for 30 minutes before the hybridization step.

For hybridization, a humidified box at 50° C by using 50% formamide to soak tissue paper and kept tightly closed for 30-60 minutes. The hybridization mixture was prepared by adding 7 µl of DEPC- H_2O, 50 µl of formamide, 10 µl of 10x salts, 2µl of tRNA, 1 µl of 1M DTT, 5µl of probe and 25 µl of dextran sulfate. This made the final probe concentration 5×10^4 cpm/µl. Both sense and anti-sense probes were made. The hybridization mixture was heated at 95° C for 10 minutes and then spun down evaporated solution and incubated on ice for 2 minutes. 80 µl of probe mixture was put on the glass slide, and spread well over the sections with a tip. The section was carefully covered with a coverslip avoiding making air bubbles. The slides were incubated in the prepared humidified chamber at 50° C overnight.

On Day 2, the coverslips were removed by immersing the slides one by one in 5x SSC solution at in a 60° C water bath. The slides were washed in FSM in a 60 degree C waterbath for 30 minutes and washed twice in STE at 37° C for 10 minutes. The slides were then incubated in STE containing 20 µg/ml RNase A at 37° C for 30 minutes and then the slides were incubated in STE containing 20 mM β-Me at 37° C for 10 minutes. The slides were washed in FSM at 60° C for 30 minutes. Next, the slides were washed in 2x SSC at 37° C and then in 0.1x SSC at room temperature for 5 minutes. Finally the slides were washed twice in distilled H_2O and air dried for 3 hours. The slides were exposed to the x-ray film over night and developed the following day.

Castration and administration of DHT:

Mice were castrated and two weeks later were administered with DHT. The prostates lobes AP, DP, VP and LP were harvested from the uncastrated control and the castrated mice at various time points. The tissues were fixed overnight in RNA later and subsequently RNA was isolated.

Tissue recombination and kidney capsule grafting:

Pregnant rats were obtained and rat UGM was prepared from 18-day embryonic fetuses (plug date denoted as day 0). Urogenital sinuses were dissected from fetuses and separated into epithelial and mesenchymal components by tryptic digestion, as described previously. UGM was then additionally reduced to single cells by a 90-min digestion at

37° C with 187 U/ml collagenase (Life Technologies Inc., Grand Island, NY, USA). After digestion the mesenchymal cells were washed extensively with RPMI 1640 tissue culture medium. Viable cells were then counted using a hemacytometer, with viability determined by Trypan blue exclusion.

PC3-EV or PC3-Tbx2 DN cells were released from tissue culture plastic with trypsin, washed in growth medium containing 20% FBS, and viable cells were counted using Trypan blue exclusion and a hemacytometer. Cell recombinants were prepared by mixing 100,000 epithelial (PC3-EV or PC3-Tbx2 DN) cells with 300,000 mesenchymal cells in suspension. Cells were pelleted and resuspended in 50 µl of neutralized type 1 rat tail collagen prepared. 100,000 PC3-EV or PC3-Tbx2 DN epithelial cells without rUGM were also pelleted and resuspended in 50 µl collagen. The recombinants were allowed to set at 37° C for 15 min and were then covered with growth medium (RPMI 1640+5% FBS), and cultured overnight. Recombinants were then grafted beneath the renal capsule of adult male outbred athymic mice. All of the animals were housed in Vanderbilt University laboratory animal resource center with food and drinking water under controlled conditions (12 h light, 12 h dark, and 20±2°C).

Hosts were killed at 4 weeks by anesthetic overdose followed by cervical dislocation. Kidneys were excised, and grafts were dissected free of the host kidney and then processed for histology and immunohistochemistry. The castrated mice were killed at 2 days or 2 weeks after castration. At 2 h prior to death, 5-bromo-2'-deoxyuridine (BrdU) (10 mg/kg body wt) was injected i.p. for *in vivo* labeling of proliferating cells.

Micro–computed tomography, X-ray, and histomorphometric analyses:

For gross analysis of trabecular bone volume (BV), formalin-fixed tibias were scanned at an isotropic voxel size of 12 μm using a microCT40 (SCANCO Medical). The tissue volume (TV) was derived from generating a contour around the metaphyseal trabecular bone that excluded the cortices. The area of measurement began at least 0.2 mm below the growth plate and was extended by 0.12 mm. BV included all bone tissue that had a material density of >438.7 mgHA/cm^3. These analyses allowed for the calculation of the BV/TV ratio. The same threshold setting for bone tissue was used for all samples. Radiographic images (Faxitron X-ray Corp.) were obtained using an energy of 35 kV and an exposure time of 8 s. The tumor volume (TuV) was calculated as a function of the total TV of the tibial medullary canal using Metamorph software (Molecular Devices). For histomorphometry, three nonserial sections of tumor-bearing limbs were H&E stained to assess the BV/TV ratio or with TRAcP to assess osteoclast number per millimeter of bone at the tumor-bone interface using Metamorph.

HEPSIN COPERATES WITH MYC IN THE PROGRESSION OF ADENOCARCINOMA IN A PROSTATE CANCER MOUSE MODEL

Introduction:

Following the development of prostatic intraepithelial neoplasia (PIN), the natural course of progression in human prostate cancer typically involves the development of adenocarcinoma with local invasion, and the final development of distal metastases. Transgenic mouse models provide an excellent opportunity to identify genes that contribute to the development of prostate adenocarcinoma, and to elucidate the molecular basis of prostate cancer progression *in vivo*. However, several transgenic mouse models develop androgen independent neuroendocrine cancer, and neuroendocrine pathophysiology does not reflect the predominant androgen dependent adenocarcinoma phenotype observed in human prostate cancer (Klezovitch et al., 2004; Masumori et al., 2001; Perez-Stable et al., 1997). Thus, there is a need to develop and characterize novel transgenic models that better mimic prostate adenocarcinoma in humans.

Proteolytic activity associated with both secreted and cell surface proteases are thought to play a critical role in progression of cancer to an advanced stage (Noel et al., 1997; Woodward et al., 2007). Cell surface proteases have been hypothesized to play a role in the cleavage of extracellular matrix proteins that are components of the basement

membrane, thus allowing tumor cells to invade and metastasize (Birkedal-Hansen, 1995). Several studies have shown that hepsin, a type II transmembrane serine protease (TTSP), is upregulated at both the mRNA and protein levels in more than 90% of human prostate cancers. For example, one study reported that hepsin is up-regulated by 34 fold in Gleason grades 4 and 5. (Landers et al., 2005; Stephan et al., 2004). Hepsin levels have been correlated positively with disease aggressiveness with highest hepsin expression levels present in tumors of Gleason grade 4/5 (Xuan et al., 2006). This suggests a role for hepsin in aggressive prostate cancers. A transgenic mouse model over-expressing hepsin in the prostate was created by using the prostate-specific probasin promoter (Klezovitch et al., 2004). Prostates in these mice showed normal cell proliferation and differentiation but the basement membrane showed disorganization (Klezovitch et al., 2004). Further, these hepsin transgenic mice when crossed with the LPB-Tag 12T-7f model showed significant tumor progression and metastases to the bone making it the only mouse model to develop bone metastases (Klezovitch et al., 2004). This study indicated that hepsin plays a key role in the progression of prostate cancer to a metastatic phenotype, consistent with the high levels of hepsin found in patients with advanced prostate cancer. However, these bigenic mice developed adenocarcinoma and neuroendocrine tumors at the primary site but the metastatic lesions are NE cancer, a rare type of human prostate cancer.

To determine the role of hepsin in the progression of adenocarcinoma of the prostate, we crossed the PB-hepsin mice with PB-Hi-myc mice, the probasin directed myc mouse model of prostate adenocarcinoma. The PB-Hi-myc model (hereafter referred as myc mice) expresses high levels of myc and develops adenocarcinoma by 6 months of

age (Ellwood-Yen et al., 2003). Herein we provide evidence that over-expression of hepsin in the myc tumors decreases the time required for development of adenocarcinoma from 6 months to 4.5 months. Further, with aging, the PB-hepsin/PB-Hi myc mice (hereafter referred to as hepsin/myc mice) developed a pathologically higher grade of tumor as compared to the tumors of the age-matched myc transgenic mice. In short, our data confirms that hepsin co-operates with myc in the progression of adenocarcinoma in a mouse model of prostate cancer and underscores the relevance of hepsin during prostate cancer progression indicating that enzymatic inhibition of hepsin activity may have therapeutic benefit.

Characterization of hepsin/myc bigenic mice:

Since both myc and hepsin genes are over-expressed in human prostate tumors (Chen et al., 2003; Dhanasekaran et al., 2001; Ernst et al., 2002; Halvorsen et al., 2005; Jenkins et al., 1997; Luo et al., 2001; Magee et al., 2001; Nesbit et al., 1999; Qian et al., 1997; Sato et al., 1999; Singh et al., 2002), it was essential that we specifically drove expression of these transgenes to the luminal epithelial cells of the prostate in a temporal manner. Immunohistochemical analyses revealed the presence of myc expression in the epithelial cells of the hepsin/myc and myc mice (**Fig. 4**, Panels A through F). Immunohistochemical analyses revealed that hepsin expression was low in the myc transgenic mice and, as expected, was higher in the hepsin/myc mice at all ages (**Fig. 4**, Panels G through L). Notably, the myc transgenic mice spontaneously developed a low level of endogenous hepsin that increased as the myc tumors progressed, consistent with

the elevated levels of hepsin found in advanced human prostate cancer (Landers et al., 2005; Stephan et al., 2004). Our results indicate that forced hepsin and myc transgene expression was specifically targeted to the epithelial compartment of bigenic mice and that as the transgenic myc mouse ages, hepsin is spontaneously expressed.

Histological examination of prostates from the myc and hepsin/myc mice showed progressive tumor development with age (**Figs. 5 and 6**; **Table 2**). The prostates were characterized by a pathologist in a blinded manner as either containing no histologic abnormality, low grade prostatic intraepithelial neoplasia (LGPIN), high grade prostatic intraepithelial neoplasia (HGPIN) or adenocarcinoma with various grades (**Figs. 5 and 6**; **Table 2**). A detailed mouse-by-mouse description of the histopathological findings has been provided in **Table 2**. LGPIN and HGPIN were described by crowding of epithelial cells within a gland but still bound by the basement membrane combined with cytologic abnormalities such as nuclear enlargement. HGPIN (**Fig 5**, Panel B) differed from LGPIN (**Fig 5**, Panels A & D) based on pronouncement of these features including nuclear atypia, increased number of heterochromatic nuclei and higher mitotic rates.. Adenocarcinoma was characterized by invasive lesions that lacked glandular prostate differentiation and absence of a clear basement membrane contour (**Fig 5**, Panels C, E &F; **Fig 6**, Panels A through F; **Table 2**). This data indicates that hepsin/myc bigenic mice develop histo-pathological hallmarks associated with adenocarcinoma.
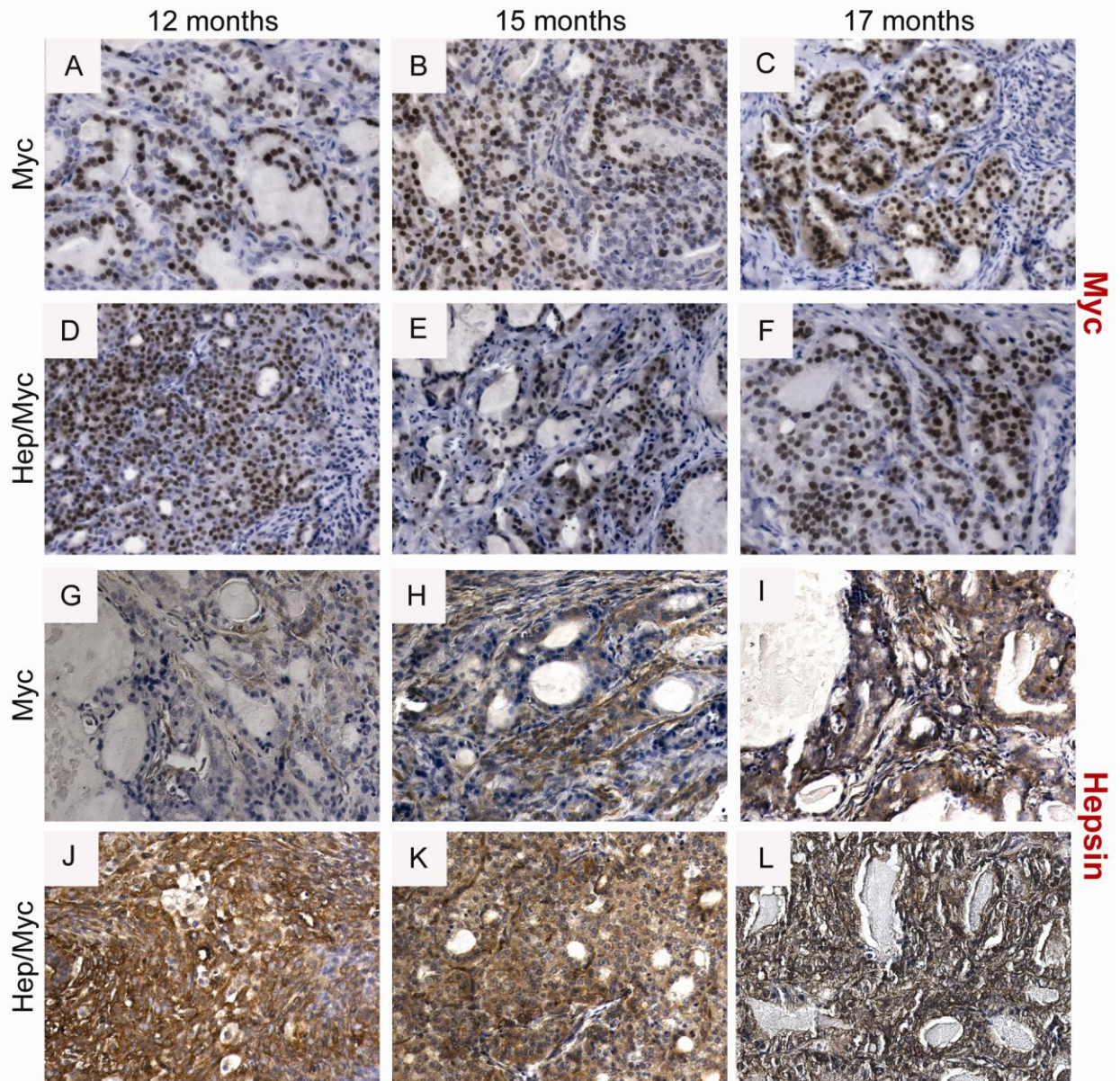
Figure 4: Immunohistochemical staining of myc and hepsin in the transgenic animals showing progression from 12 to 17 months. (Panels A & G) Myc staining and Hepsin staining respectively of 12 month old myc mice; (Panels D & J) Myc staining and Hepsin staining respectively of 12 month old hepsin/myc mice; (Panels B & H) Myc staining and Hepsin staining respectively of 15 month old myc mice; (Panels E & K) Myc staining and Hepsin staining respectively of 15 month old hepsin/myc mice; (Panels C & I) Myc staining and Hepsin staining respectively of 17 month old myc mice ; (Panels F & L) Myc staining and Hepsin staining respectively of 17 month old hepsin/myc mice
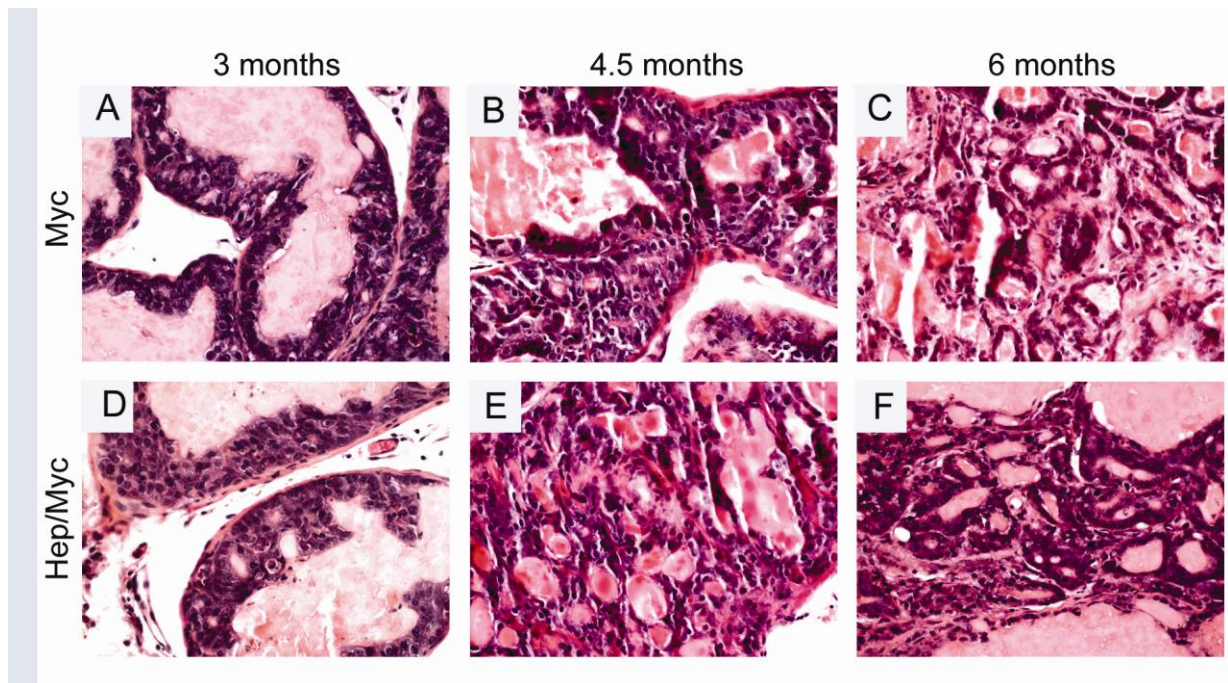
Figure 5: Histopathology (H&E) of transgenic animals showing progression from 3 to 6 months. Panels A & D showing LGPIN in 3 month old myc and hepsin/myc mice respectively; Panel B showing HGPIN & Panel E showing adenocarcinoma in 4.5 month old myc and hepsin/myc mice respectively; Panel C & F showing adenocarcinoma in 6 month old myc and hepsin/myc mice respectively.

Fig. 6: Histopathology (H&E) of transgenic animals showing progression of adenocarcinoma from 12 to 17 months. (Panels A & D) H&E of 12 month old myc and hepsin/myc mice respectively; (Panels B & E) H&E of 15 month old myc and hepsin/myc mice respectively; (Panels C & F) H&E of 17 month old myc and hepsin/myc mice respectively.
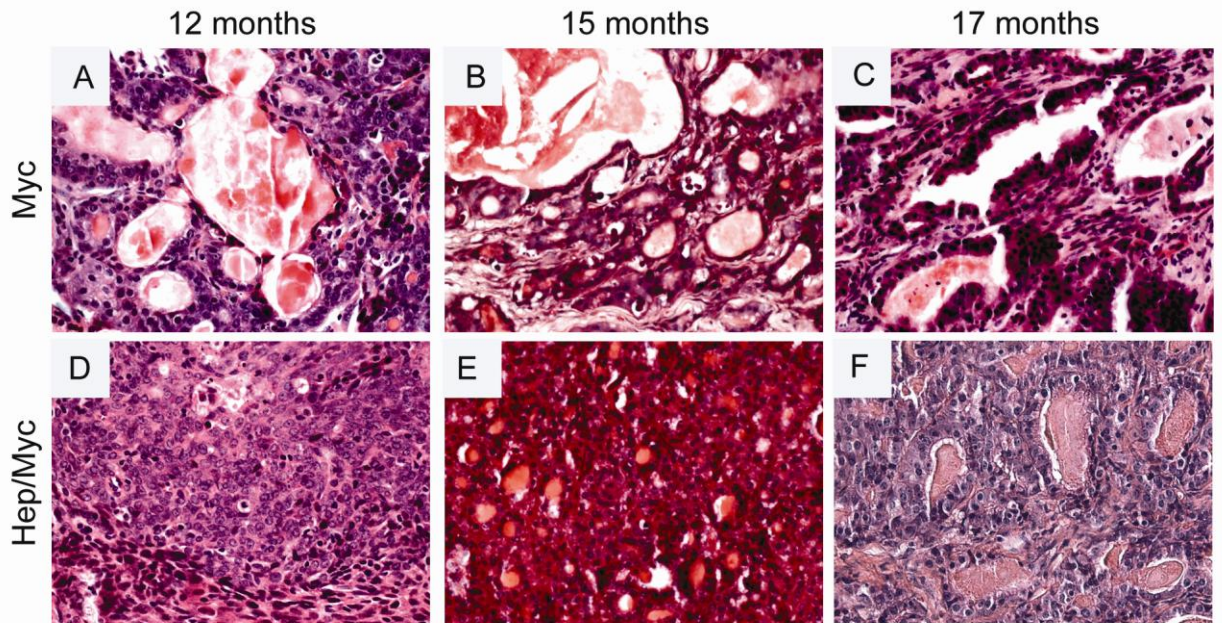
Hepsin/myc bigenic mice display accelerated tumor progression:

The PB-hepsin transgenic mice when crossed with the LPB-Tag mice has been shown to display significant progression from HGPIN to adenocarcinoma and NE cancers (Klezovitch et al., 2004). Further, these NE cancers metastasized to the liver, lungs, and bone (Klezovitch et al., 2004). Our model tested if the overexpression of hepsin causes progression of adenocarcinoma in the myc model. Since adenocarcinoma develops first in the dorsolateral prostate of the myc mouse, the histology of these lobes was carefully examined in the hepsin/myc bigenic mice. We found that at 3 months, both myc and hepsin/myc mice displayed PIN lesions (**Fig. 5**, Panels A & D; **Table 2**). But notably, in contrast to the myc mice, the hepsin/myc mice displayed adenocarcinoma at 4.5 months (5 out of 6 mice) since all the PIN lesions had advanced to adenocarcinoma (**Fig 5**, Panel E; **Table 1**; **Table 2**) whereas none of the myc mice displayed adenocarcinoma (0 out of 6 mice) but instead developed HGPIN (**Fig. 5**, Panel B; **Table 1**; **Table2**; p=0.015). At 6 months, both hepsin/myc and myc mice displayed invasive adenocarcinoma (**Fig. 5**, Panels C & F; **Table1**). Since Foxa1 is an established marker to detect prostate luminal epithelial cells, invasion of the tumor cells into the surrounding stroma can be visualized by Foxa1 staining. (**Fig. 7**, Panels A through F; **Fig. 8**, Panels A through F). It has been previously shown that hepsin causes significant progression of prostate cancer in the LPB-Tag model including metastases to the bone (Klezovitch et al., 2004). These tumors were shown to express neuroendocrine markers including synaptophysin (Klezovitch et al., 2004). In our model of the hepsin/myc mouse, neuroendocrine differentiation, as detected by synaptophysin staining was negative (**Fig. 10**). Further, to check the status of the androgen receptor in the tumors, we performed

immunohistochemistry with androgen receptor (**Fig. 7**, Panels G through L; **Fig. 8**, Panels G through L). Both myc and hepsin/myc tumors at all ages stained positive for the androgen receptor. This data indicates that when compared to myc transgenic mice, bigenic hepsin/myc mice develop adenocarcinoma at an accelerated rate and that both myc and hepsin/myc tumors are adenocarcinomas devoid of any neuroendocrine (NE) differentiation.
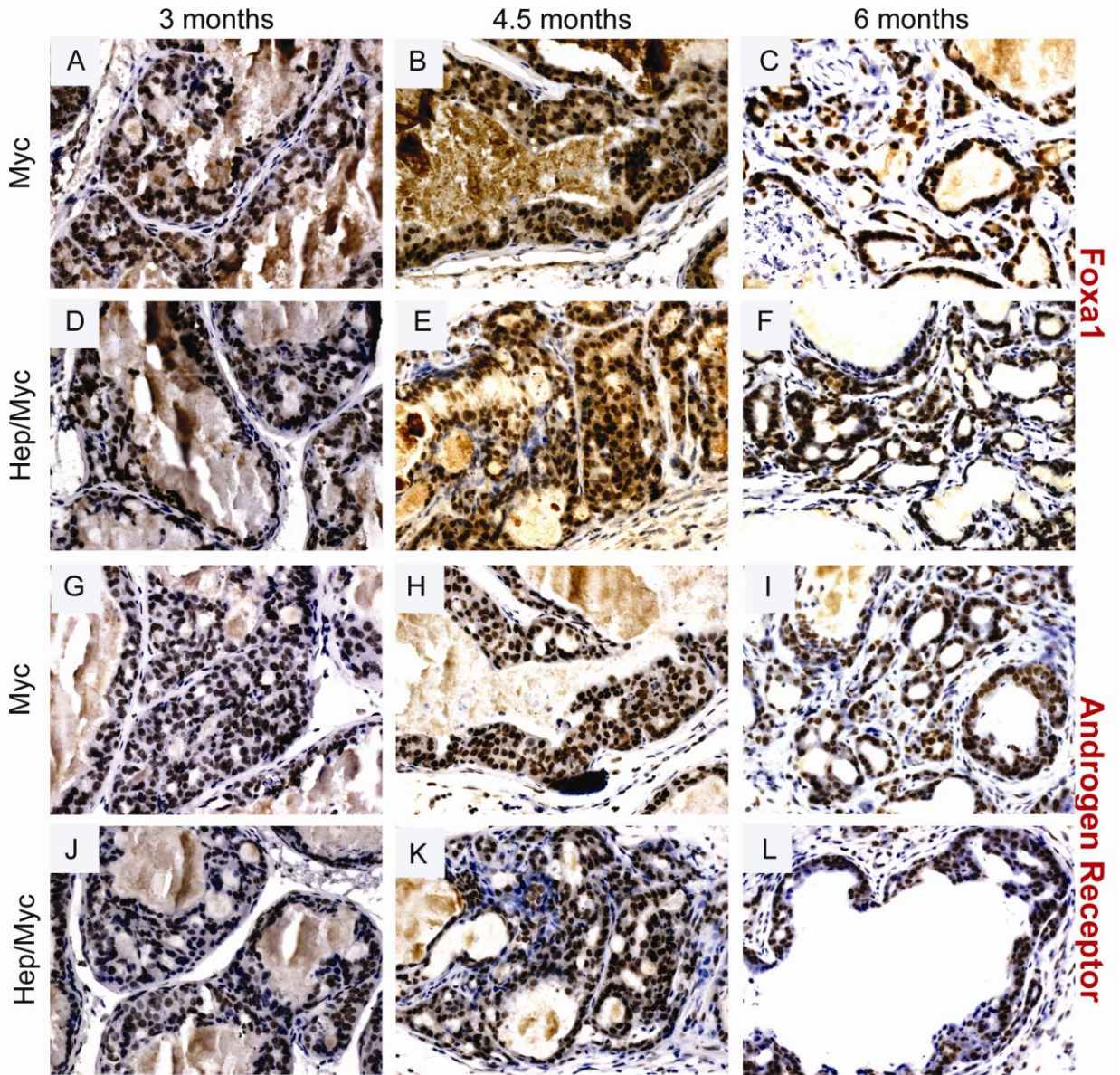
Figure 7: Immunohistochemical staining of Foxa1 and AR in the transgenic animals showing progression from 3 to 6 months. (Panels A & G) Foxa1 and AR staining respectively of 3 month old myc mice; (Panels D & J) Foxa1 and AR staining respectively of 3 month old hepsin/myc mice; (Panels B & H) Foxa1 and AR staining respectively of 4.5 month old myc mice; (Panels E & K) Foxa1 and AR staining respectively of 4.5 month old hepsin/myc mice; (Panels C & I) Foxa1 and AR staining respectively of 6 month old myc mice; (Panels F & L) Foxa1 and AR staining respectively of 6 month old hepsin/myc mice.
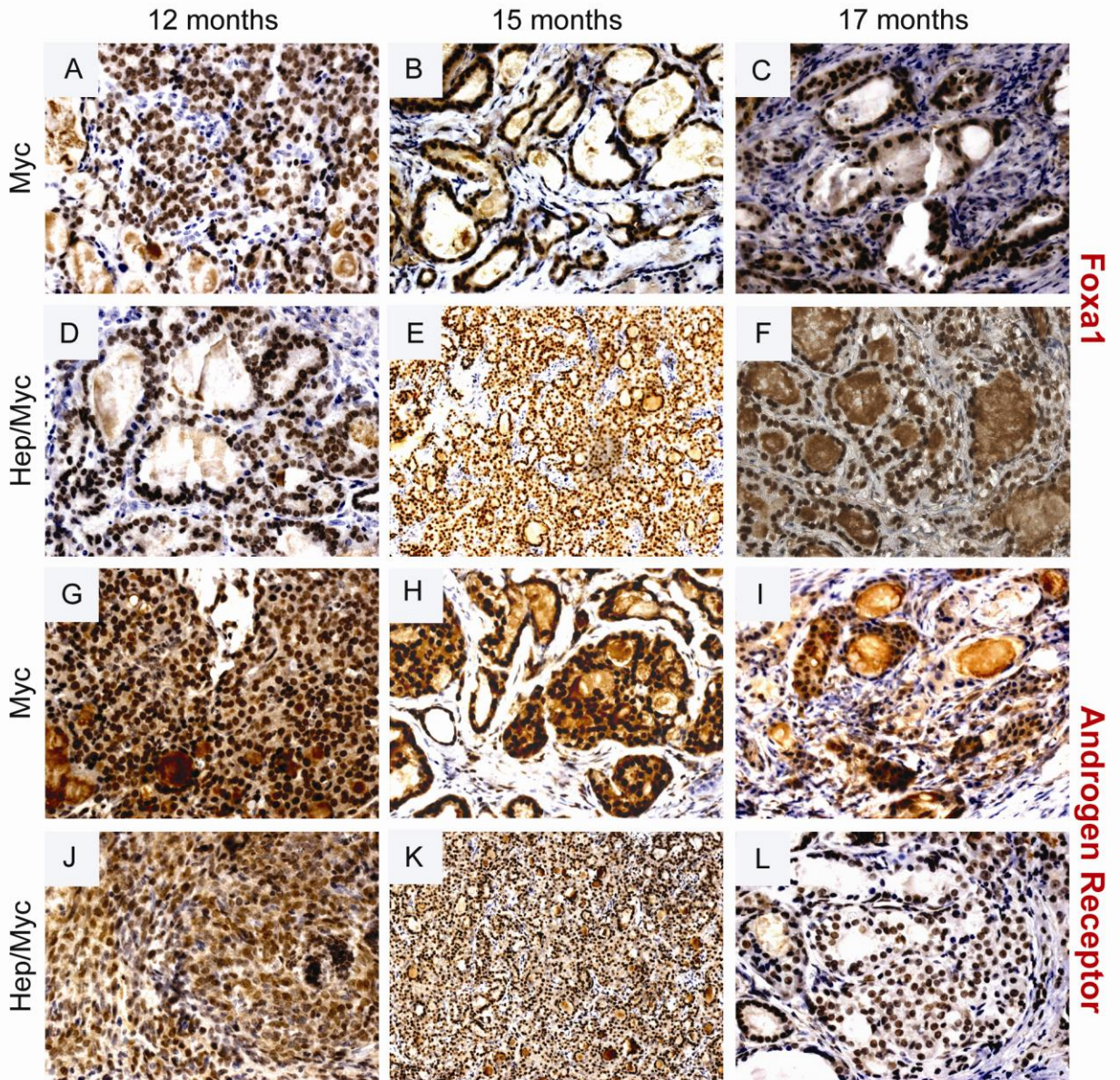
Figure 8: Immunohistochemical staining of Foxa1 and AR in the transgenic animals showing progression from 12 to 17 months. (Panels A & G) Foxa1 and AR staining respectively of 12 month old myc mice; (Panels D & J) Foxa1 and AR staining respectively of 12 month old hepsin/myc mice; (Panels B & H) Foxa1 and AR staining respectively of 15 month old myc mice; (Panels E & K) Foxa1 and AR staining respectively of 15 month old hepsin/myc mice; (Panels C & I) Foxa1 and AR staining respectively of 17 month old myc mice; (Panels F & L) Foxa1 and AR staining respectively of 17 month old hepsin/myc mice.

Prostate tumors from aged hepsin/myc mice exhibit a higher grade of adenocarcinoma compared with myc mice:

In an effort to determine if increased hepsin expression in the tumors would lead to further progression, mice were aged up to 17 months. Staining with the GFP antibody [since the mouse PB-hepsin construct is tagged with GFP (Klezovitch et al., 2004)] was used to detect potential metastasis in the lymph nodes, femur and jaw bones, kidney, lung, liver etc. No metastases were detected. Notably, hepsin/myc tumors (12-17 months) exhibited a higher grade adenocarcinoma as compared with the myc tumors (4 out of 6 mice) (**Fig. 6**; **Table 1**; **Table 2**). (A detailed mouse-by-mouse description of the histopathological findings along with the grades of the respective tumors has been provided in **Table 2**.) The tumor size was not significantly different between hepsin/myc and myc mice. As expected, hepsin levels were significantly higher ($p<0.05$) in the tumors of hepsin/myc mice compared with age matched myc tumors, as measured by quantitative real-time, qRT-PCR (**Fig. 9**) and immunohistochemistry (**Fig. 4**, Panels G through L). Notably, hepsin/myc tumors displayed less stroma as compared with the myc alone tumors. To determine if tumors in the myc mice reflected the pathobiology of human adenocarcinoma, we analyzed hepsin expression of myc tumors during progression from PIN to higher grade cancer. Notably, with aging, the prostates of the myc mice begin to spontaneously express hepsin. Further, hepsin expression in the myc tumors increased significantly ($p<0.05$) in the 12, 15 and 17 month time points compared to 6 month prostate tumor from myc mice (**Fig. 9**). This change in hepsin expression also was detected by immunohistochemistry (**Fig. 4**, Panels G through I). This data indicates that hepsin expression in the hepsin/myc tumors causes the tumors to progress to a higher

grade and that endogenous hepsin expression in the myc tumors increases with age progression.
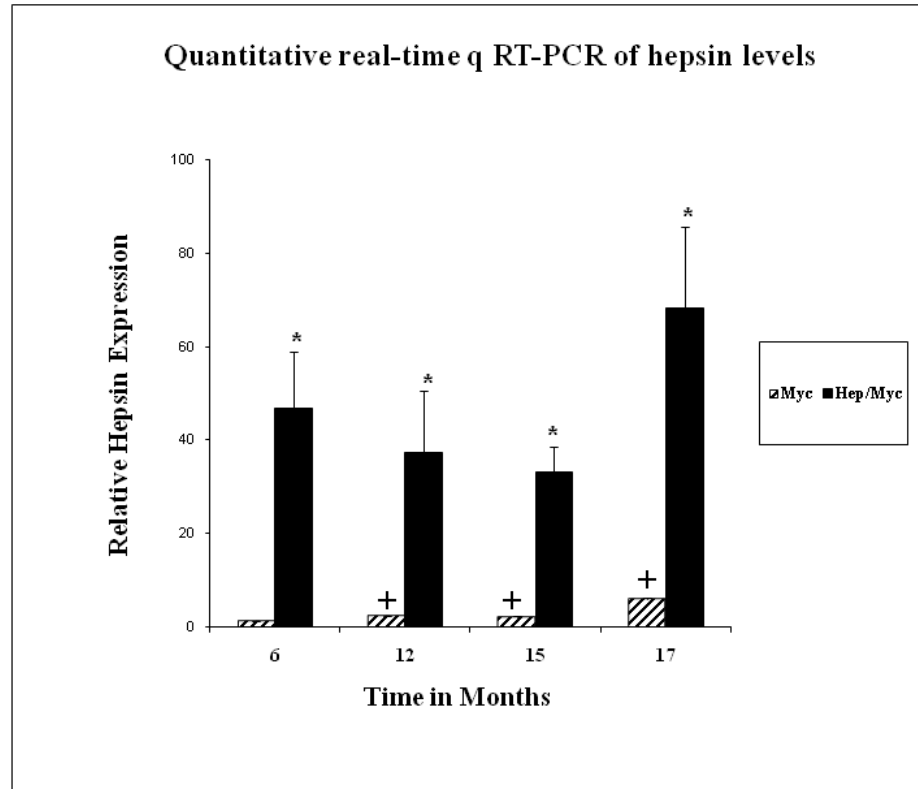
Figure 9: Quantitative real-time q RT-PCR of hepsin expression in hep/myc and myc mice: Hepsin expression in 6, 12, 15 and 17 month hep/myc and myc mice. (*) represents significant difference ($p<0.05$) in hepsin expression between myc and hep/myc mice. (+) represents significant difference ($p<0.05$) in hepsin expression between 6 month old myc mice as compared with 12, 15 and 17 month old myc mice respectively.

Table 1:

Table 1: Incidence of PIN / adenocarcinoma in Hep/Myc
and Myc mice with age progression

Age (months)	No. of mice		PIN / Adenocarcinoma /	Higher grade (if applicable)
4.5	Myc	6	PIN in all 6 mice	
	Hep/Myc	6	PIN in 1, Adenocarcinoma in 5 mice	
6-10	Myc	2	Adenocarcinoma in both mice	
	Hep/Myc	2	Adenocarcinoma in both mice	
12-17	Myc	6	Adenocarcinoma in all 6 mice	
	Hep/Myc	6	Adenocarc. in all 6 mice,	Higher grade in 4/6 mice compared with Myc alone

Figure 10: Negative synaptophysin staining in myc and hep/myc transgenic mice. Myc (panel B) and hep/myc (panel C) tumors are negative for synaptophysin, a marker of neuroendocrine differentiation

Table 2:

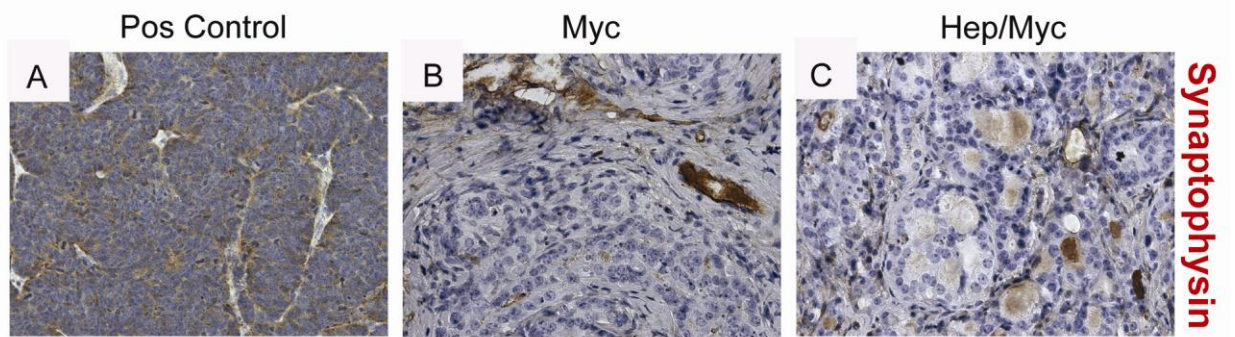| Mouse Strain / Age / Number	Description of Pathology
Myc / 3 mos / A8906	**PIN lesions**
Hep Myc / 3 mos / A8905	**PIN lesions**
Myc / 4.5 mos / A8914	**High Grade PIN**
Hep Myc / 4.5 mos / A8913	Adenocarcinoma, nuclear enlargement, focal hyperchromatin, rare nucleoli, focal areas of glandular infiltration, single area of infiltrative glandular loss **Grade 2+**
Myc / 4.5 mos / A9171	**PIN lesions**
Hep Myc / 4.5 mos / A9185	Adenocarcinoma, minute area of infiltrative glands with mild nuclear enlargement, rare nucleoli, stipled chromatin, loss of cell borders **Grade 1+**
Myc / 4.5 mos / A9166	**PIN lesions**
Hepsin Myc / 4.5 mos / A9186	Adenocarcinoma, nuclear enlargement, hyperchromatia, infiltrative glands **Grade 2+**
Myc / 4.5 mos / B310	**High Grade PIN**
Hepsin Myc / 4.5 mos / A9187	Adenocarcinoma, primarily gland forming with infiltrative focal areas of gland formation, nuclear enlargement, stipled chromatin, prominent nucleoli **Grade 2+**
Myc / 4.5 mos / A9163	**PIN lesions**
Hepsin Myc / 4.5 mos / B307	**PIN lesions**
Myc / 4.5 mos / B301	**PIN lesions**
Hepsin Myc / 4.5 mos / B302	Adenocarcinoma, mild nuclear enlargement, single minute foci of infiltrative gland **Grade 1+**
Myc / 6 mos / A8912	Adenocarcinoma, infiltrative glands, nuclear enlargement, stipled chromatin **Grade 2**
Hepsin Myc / 6 mos / A8921	Adenocarcinoma, areas of glandular infiltration, nuclear enlargement, stipled chromatin **Grade 2**
Myc / 12 mos / A9935	Adenocarcinoma with gland formation and loss of gland formation, no definable single cells, nuclei hyperchromatic, vesiculated; prominent nucleoli, stipled chromatin and granulated cytoplasm **Grade 2**
Hepsin Myc / 12 mos / A9952	Adenocarcinoma with very little gland formation, nuclear enlargement, stipled chromatin, prominent nucleoli, loss of cell borders with cells streaming and in sheets, rare rudimentary gland formation **Grade 3+**
Myc / 12 mos / A9946	Adenocarcinoma with gland formation and loss of gland

	formation, nuclear enlargement, stipled chromatin, macronucleoli, focal loss of cell borders, cells are in cohesive bundles **Grade 2**
Hepsin Myc / 12 mos / A9936	Adenocarcinoma, nuclear enlargement, stipled chromatin, prominent nucleoli, focal macronucleoli, primarily loss of glandular formation with focal glandular formation with focal single cells, reactive stroma **Grade 2+**
Myc / 12 mos / A8912	Adenocarcinoma with gland formation and loss of gland formation, nuclear enlargement, hyperchromatic, focal macronucleoli, loss of cell borders, high apoptotic rate **Grade 2**
Hepsin Myc / 12 mos / A9930	Adenocarcinoma with complex gland formation, nuclear enlargement, prominent nuclei with abundant macronucleoli, some loss of cell borders, scattered apoptosis **Grade 2+**
Myc / 15 mos / A9190	Adenocarcinoma with gland formation, mild nuclear enlargement, stipled chromatin, scattered prominent nucleoli **Grade 1+**
Hepsin Myc / 15 mos / A9180	Adenocarcinoma with tightly packed glands with focal loss of gland formation, sea of cells, stipled chromatin, no nuclear enlargement, rare prominent nucleoli, granular cytoplasm with loss of borders **Grade 3+**
Myc / 17 mos / A9162	Adenocarcinoma with complex gland formation, focal loss of gland formation, nuclear enlargement, prominent macronucleoli, granular cytoplasm with loss of cell borders **Grade 3+**
Hep Myc / 17 mos / A9181	Adenocarcinoma, primarily gland forming with focal loss of gland formation, prominent nucleoli with focal macronucleoli, hyperchromatin, nuclear enlargement, stipled chromatin **Grade 2+**
Myc / 17 mos / A9174	Adenocarcinoma, stipled chromatin, prominent nucleoli with areas of macronucleoli, gland formation with areas of glandular loss, small areas of infiltrating individual cells, focal stromal response **Grade 2+**
Hepsin Myc / 17 mos / A9173	Adenocarcinoma, stipled chromatin, prominent nucleoli, scattered macronucleoli, glandular formation with some areas of glandular loss **Grade 2+**

CHAPTER IV

BLOCKING ENDOGENOUS TBX2 IN PC3 HUMAN PROSTATE CANCER CELLS DECREASES THE OSTEOLYTIC BURDEN WHEN GRAFTED IN THE BONE MICROENVIRONMENT

Introduction:

Bone metastasis is a leading cause of mortality and morbidity in human prostate cancer patients with up to 90% of advanced hormone refractory disease cases have clinical evidence of bone metastases. After homing in the bone, prostate cancer cells adapt themselves to the new environment of the bone, a process termed as "osteomimicry" by secreting growth factors that are abundant in the bone milieu (Koeneman et al., 1999). This interaction between prostate cancer cells and the bone creates a vicious cycle of bone formation and bone destruction thereby destabilizing the inherently delicate homeostasis within the bone. In prostate cancer, this process leads to metastatic lesions that are predominantly osteoblastic. However within the background of bone formation, several groups have reported that bone resorption is an integral part of prostate cancer bone lesions.

Tbx2 belongs to the T-box family of transcription repressors that play important roles in tissue development. Tbx2 is known to repress the senescence mechanism and

thereby promote immortalization by negatively regulating p21 and p19 arf genes (reference). Tbx2 has been reported to be upregulated in breast, pancreatic and melanoma cancer cell lines. The gene lies in the 17q23 amplicon that has been reported to be frequently amplified in 46% of late stage hormone refractory adenocarcinoma and 31% of metastases. Further, Tbx2 has been reported to regulate Shh and BMP2 genes in a feedback and feedforward mechanism and both the Shh pathway and BMP2 have been reported to be dysregulated in human prostate cancer. We have found in this study that Tbx2 is over-expressed in the more aggressive human prostate cancer cell lines as compared to the benign ones and this expression correlates with BMP2 expression in the same cell lines. Further, BMP2 induces Tbx2 expression in human prostate cancer cells in a time dependent manner. Further, using an intra-tibial model of tumor grafting, we have found that blocking endogenous Tbx2 in PC3 human prostate cancer cell line reduces tumor burden and the osteolytic activity when compared to the control cells. Since blocking BMP2 pathway has been postulated to be a clinical approach to reducing the osteogenic burden in human prostate cancer bone lesions, manipulating Tbx2 could be a potential approach for such a therapy in the future.

Tbx2 is over-expressed in aggressive prostate cancer cell lines that express high levels of BMP2:

We examined Tbx2 expression by quantitative real time PCR in human prostate cancer cell lines **(Fig 11a)**. Tbx2 is expressed in low levels in the less aggressive human prostate cancer cell lines RWPE1, LNCaP and C42-B whereas Tbx2 is over-expressed in the more aggressive PC3, DU145 and LAPC4 cell lines. RWPE1 and LNCaP are androgen dependent cell lines, while C42-B is a derivative of LNCaP cell line that is androgen independent. All three cell lines are relatively benign prostate cell lines while PC3, DU145 and LAPC4 are aggressive human prostate cancer cell lines that have been reported to form aggressive invasive tumor xenografts in mouse models. Interestingly, the human prostate cancer cell lines that we examined to have high levels of Tbx2 also express high levels of BMP2 **(Fig 11b)**. We also looked at Tbx2 expression in mouse prostate by *in-situ* hybridization technique and Tbx2 expression appears to be epithelial in nature **(Fig 12)**.
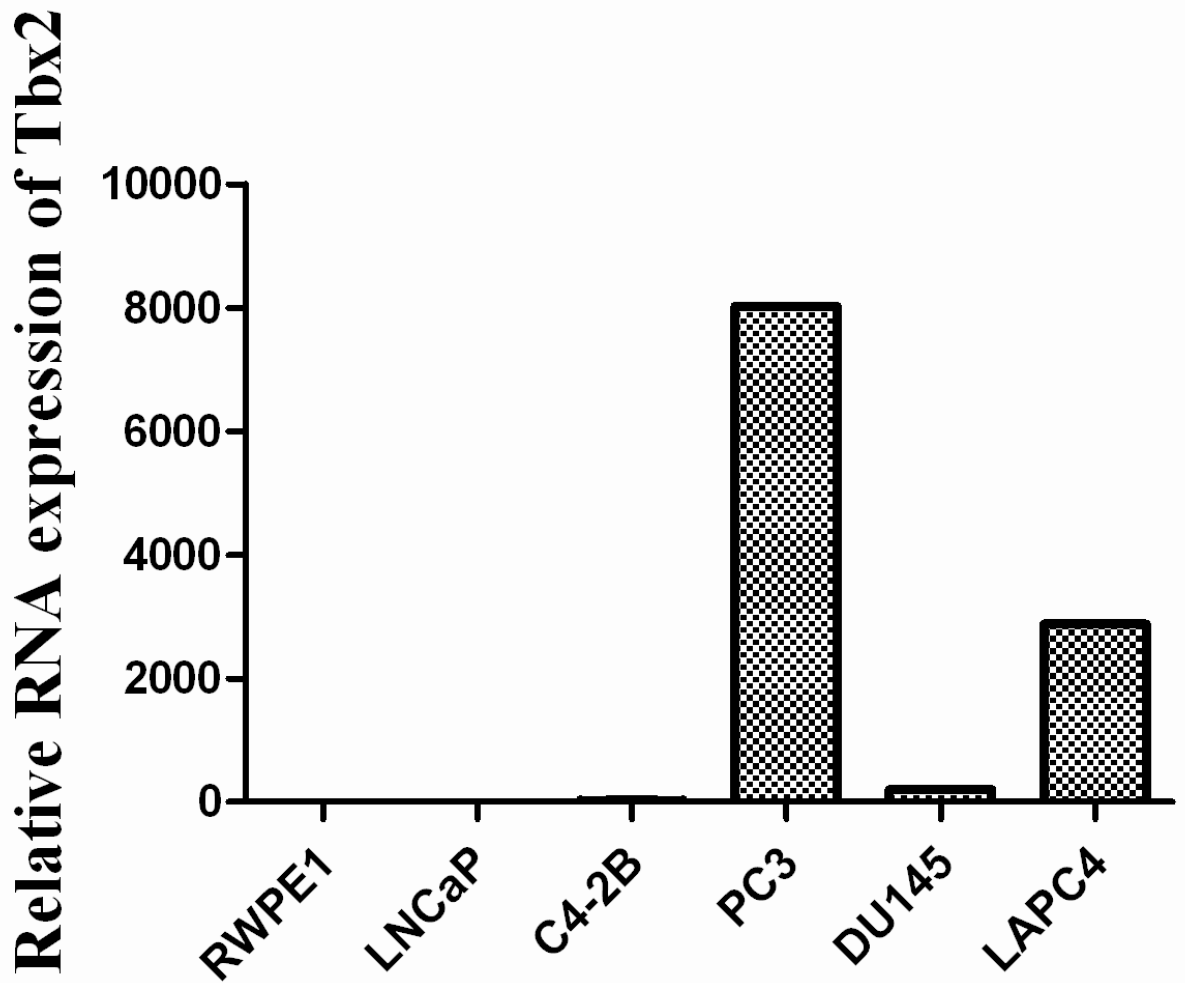
Figure 11a: Quantitative real-time PCR showing relative mRNA expression of Tbx2 in prostate cancer cell lines. Tbx2 is expressed in low levels in the benign human prostate cancer cell lines RWPE1, LNCaP and C4-2B but is expressed in very high levels in the aggressive cell lines including PC3, DU145 and LAPC4.
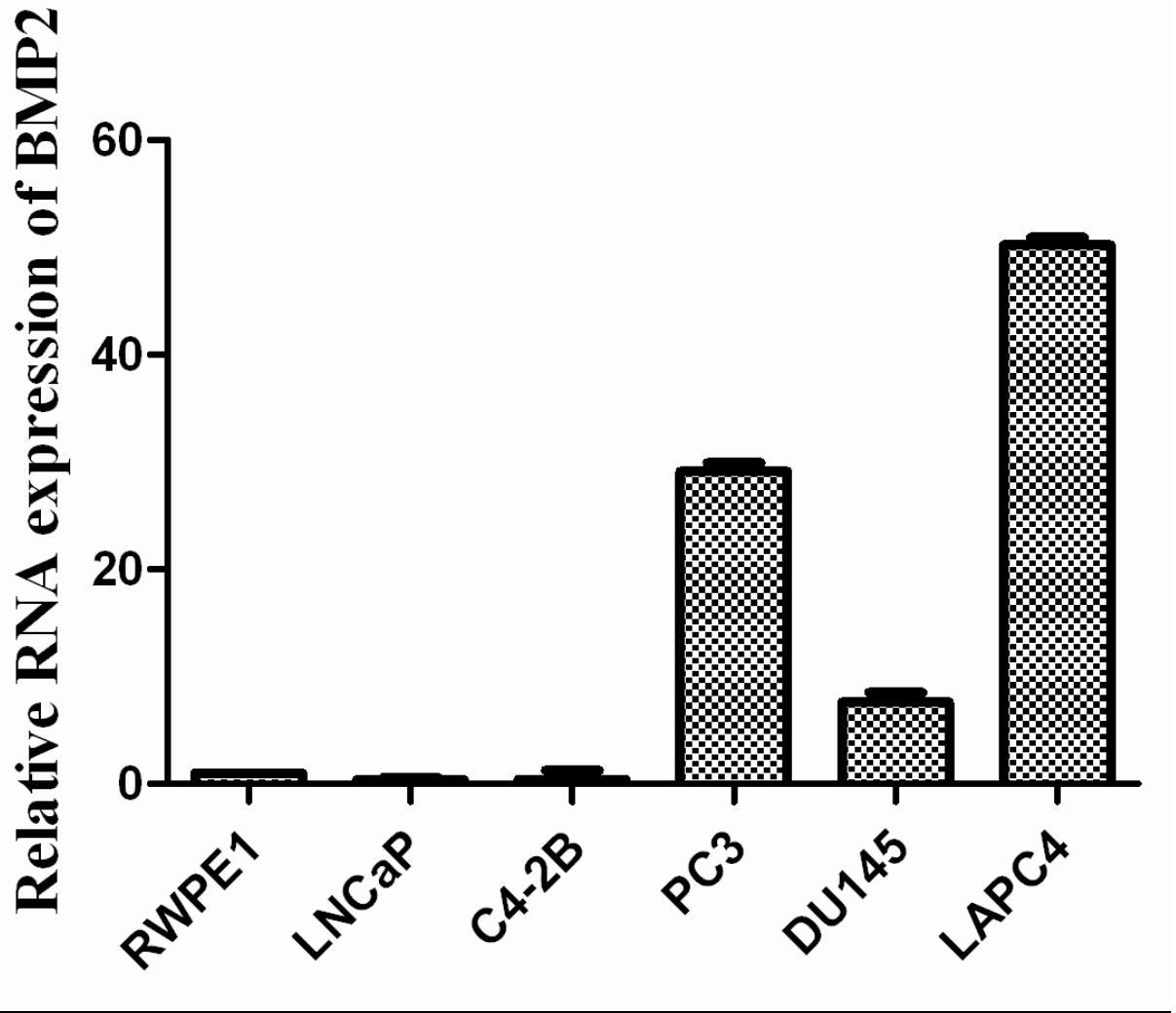
Figure 11b: Quantitative real-time PCR showing relative mRNA expression of BMP2 in prostate cancer cell lines. BMP2 is expressed in low levels in the benign human prostate cancer cell lines RWPE1, LNCaP and C4-2B but is expressed in very high levels in the aggressive cell lines including PC3, DU145 and LAPC4.
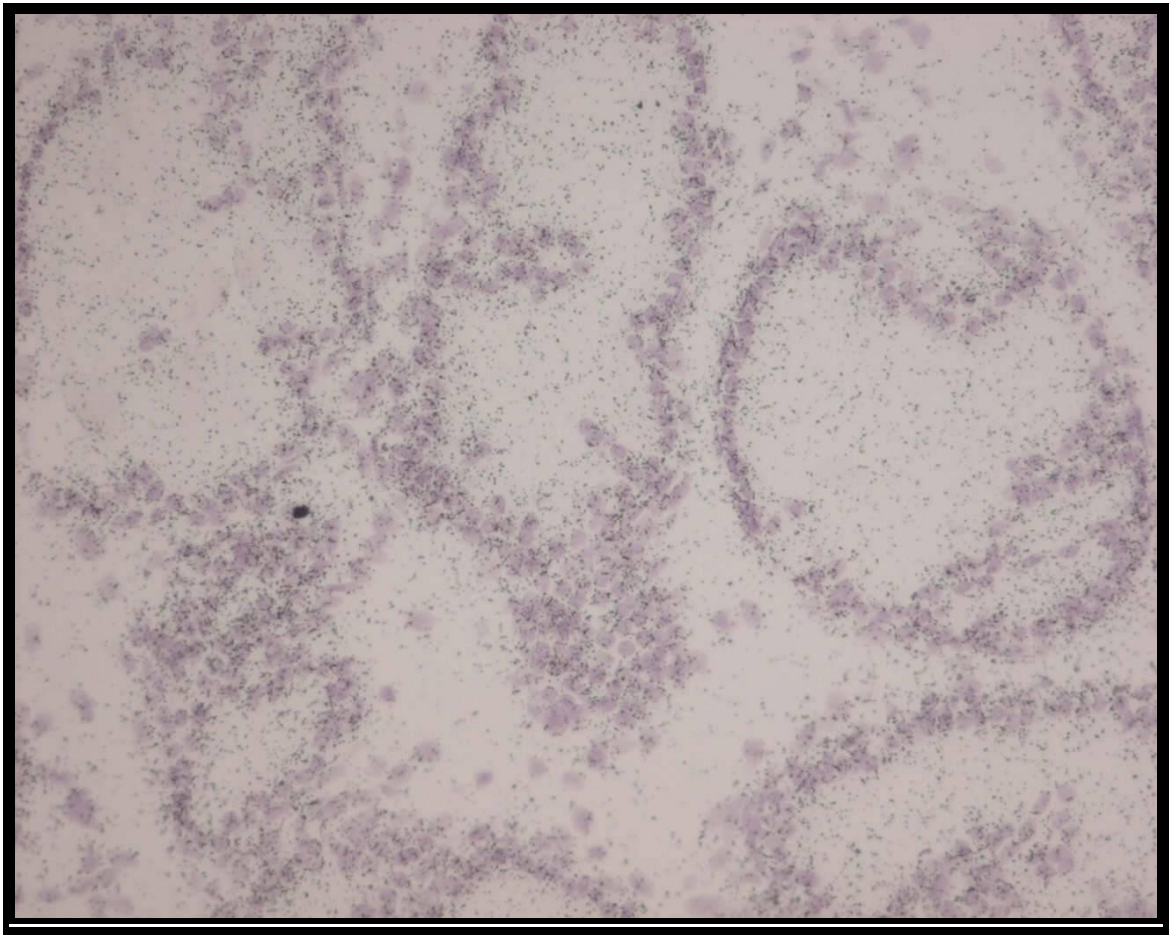
Figure 12: *In situ* **hybridization showing Tbx2 expression in 10 week dorsal lobe of normal mouse prostate.** Tbx2 appears to be expressed in the epithelial cells of the mouse prostate.

Tbx2 expression is androgen regulated:

We looked at the effect of androgens on Tbx2 expression by treating LNCaP cells with either androgen DHT or ethanol as control **(Fig. 13)**. LNCaP cells have very low levels of endogenous Tbx2. Upon DHT administration, Tbx2 expression was induced after 2 hours and continued to be induced until 12 hours post DHT treatment. PSA expression was used as a positive control. The maximum induction was seen after 12 hours of treatment. Following this *in vitro* study, we check Tbx2 expression in castrated mice that are administered with DHT. Seven week old mice were castrated for 2 weeks and administered with androgen (DHT) or ethanol for various time points. Consistent with the results observed in LNCaP cells, we saw a slight induction of Tbx2 as early as 15 minutes after DHT treatment in the anterior (AP) and ventral (VP) prostate lobes of the mouse prostate suggesting that Tbx2 is directly regulated by the androgens. This induction is clearly seen 48 after DHT treatment **(Fig 14)**. A transcription factor search of the human Tbx2 promoter has revealed a consensus glucocorticoid response element (GRE), a DNA sequence that has routinely been used to mimic an androgen response element (ARE).

To test the possibility if the androgen receptor (AR) binds and regulates Tbx2 expression, we utilized a 960 base pair Tbx2 promoter-luciferase construct, transfected in LNCaP cells and performed a luciferase assay. Since BMP2 and retinoic acid are also known to regulate Tbx2 expression, we included BMP2 and retinoic acid treatments in addition to androgens (DHT). Following serum starvation, we treated LNCaP cells with either DHT, BMP2, retinoic acid or in combinations **(Fig. 15).** Neither individual

treatments nor combinations of the three produced any appreciable luciferase activity. In contrast, the positive control for the luciferase experiment, the ARR2PB luciferase construct gave a robust activity with the addition of DHT. It is possible that the GRE / ARE sequence in the 960 bp Tbx2 promoter is not the correct hormone response element or that it functions in a cooperative manner with additional AREs that are further upstream of the 960 bp promoter.
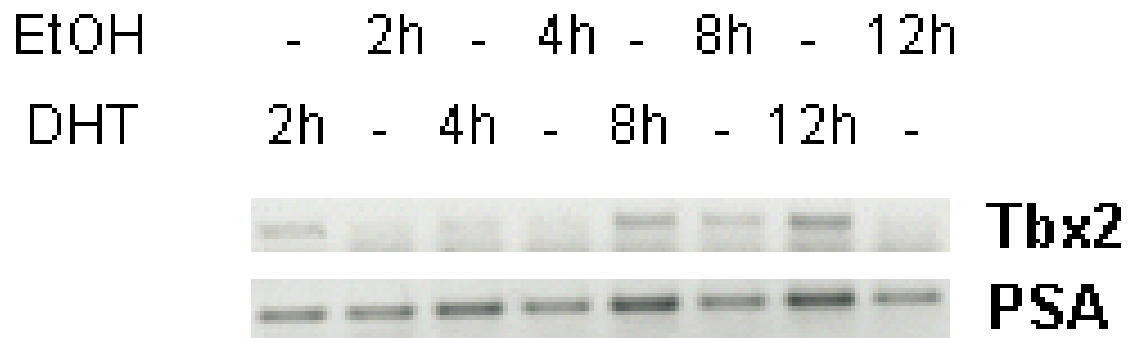
Figure 13: RT-PCR analysis showing induction of Tbx2 in LNCaP cells after DHT treatment. Induction of Tbx2 mRNA after 2,4,8 and 12 hours of DHT treatment. Induction of PSA is used as control in the lower panel.
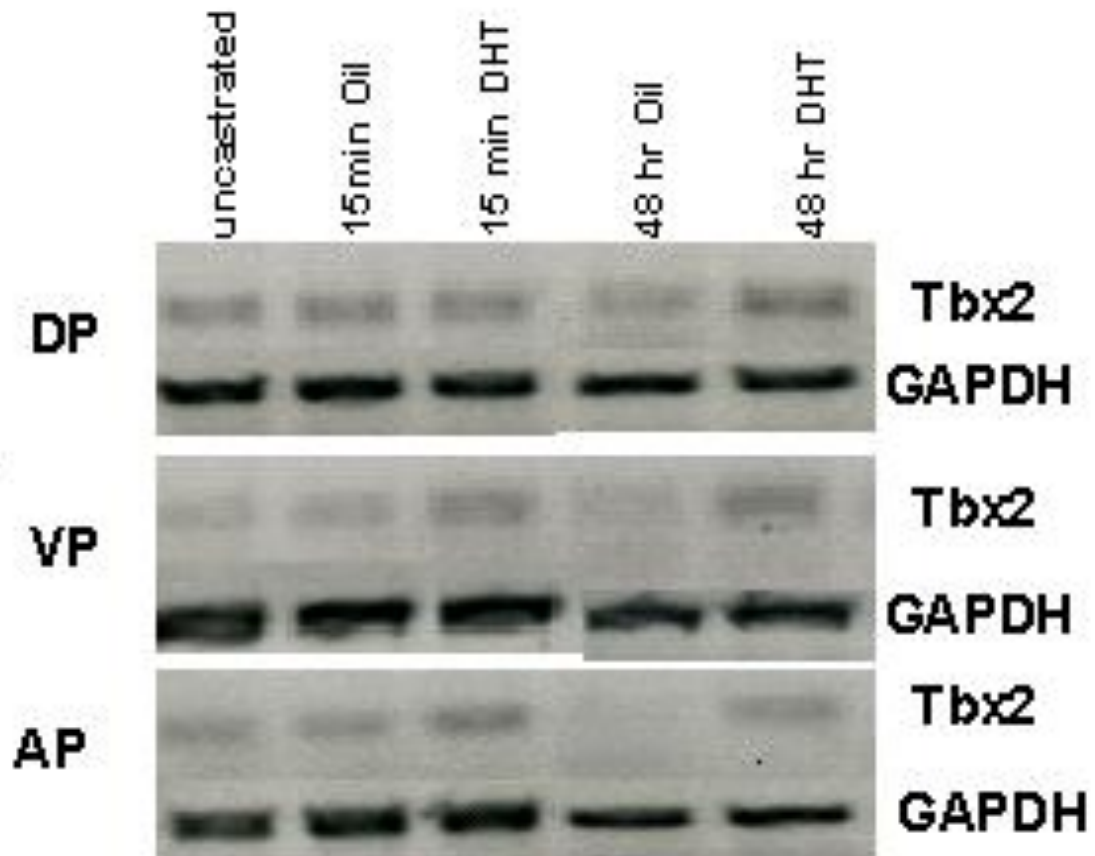
Figure 14: RT-PCR analysis showing induction of Tbx2 in the mouse prostate tissue after various times of DHT administration following 2 weeks of castration. Induction of Tbx2 mRNA in the anterior prostate (AP), ventral prostate (VP) and dorsal prostate (DP) after 15 minutes and 48 hours of DHT administration to male mice subsequent to 2-week castration. Lower panels show GAPDH as control.
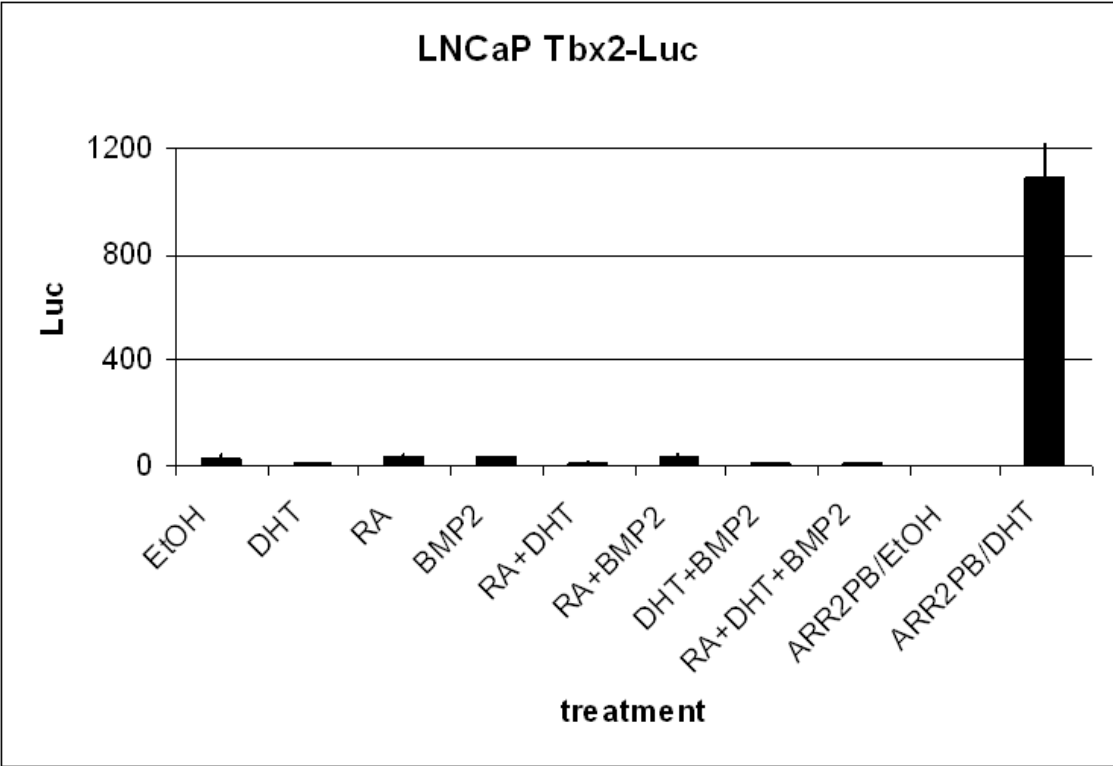
Figure 15: Luciferase assay showing that the 960 base pair Tbx2 promoter does not respond to DHT, RA, BMP2 or in combinations.

BMP2 induces Tbx2 and Wnt 3a expression:

Since it is previously known that BMP2 induces Tbx2 expression in other developmental model systems, we wanted to test if BMP2 can stimulate Tbx2 expression in prostate cancer cells. Following serum starvation for 48 hours, we treated LAPC4 cells, an androgen dependent human prostate cancer cell line with BMP2 at a concentration of 50 ng/ml. BMP2 induced Tbx2 expression robustly after 24 hours of treatment and remained induced in the 48 and 72 hour time points. **(Fig. 16)** Tbx2 is known to inhibit p16 arf expression and we observed inhibited p16 arf expression at 24 and 48 hour time points. **(Fig. 16)** The increased p16 arf expression at the 72 hour time point is not clear at this time. Though Tbx2 is also known to inhibit p21 expression, we observed that p21 expression is also induced after 24 hours. **(Fig. 16)** Since BMP2 is known to signal through Wnts, we checked the expression of Wnt genes following BMP2 addition to LAPC4 cells. Of all the canonical and non-canonical Wnts we examined by RT-PCR, we observed that Wnt 3a, a canonical Wnt, is induced after 24 hours following the addition of BMP2. **(Fig. 16)** The induction of Tbx2 and Wnt 3a following BMP2 addition has interesting implications from the bone metastasis point of view.
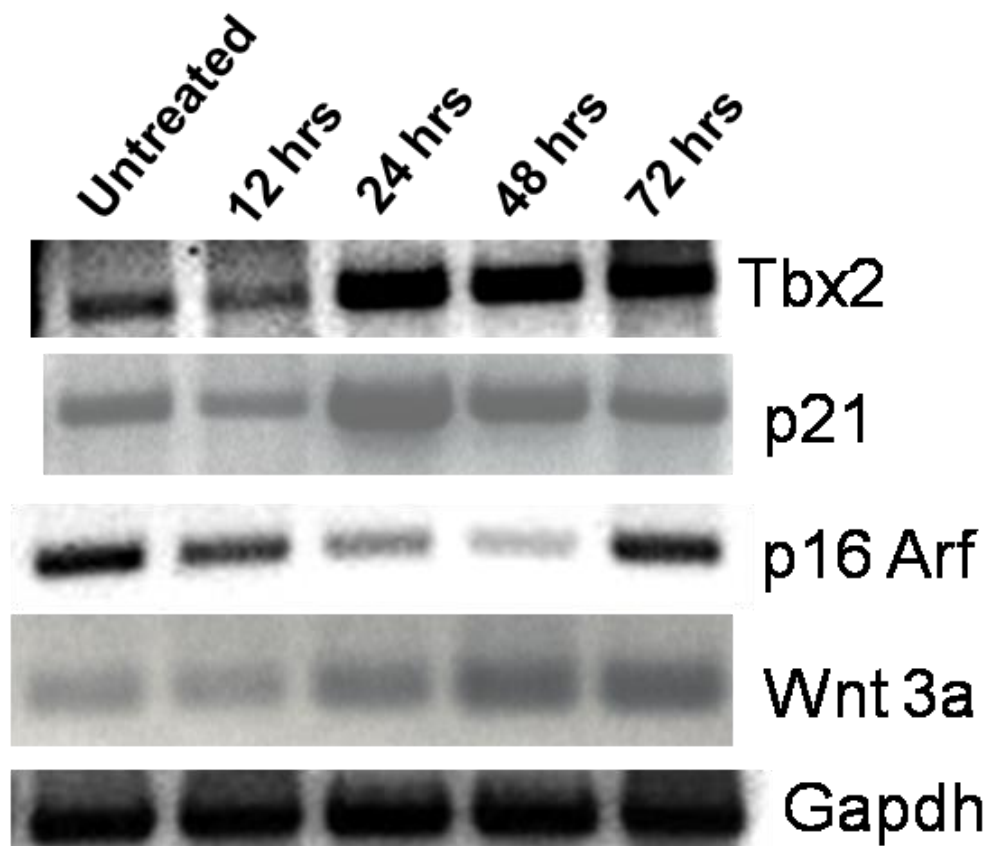
Figure 16: RT-PCR analysis showing change in mRNA expression of Tbx2, p21, p16 Arf and Wnt 3a in LAPC4 cells with BMP2 treatment. Tbx2 mRNA is induced after 24 hours of BMP2 treatment in LAPC4 cells. p21 levels increase with BMP2 treatment while p16 levels decrease. Wnt 3a levels increase after 24 hours.

Characterization of prostate cancer cell lines stably infected with Tbx2 DN vector:

We chose two androgen independent human prostate cancer cell lines DU145 and PC3 to block endogenous Tbx2 expression with the help of a Tbx2 dominant negative construct. We also chose the NeoTag-2 cells (a cell line generated from the LPB Tag 12T-7 mouse model of prostate adenocarcinoma) to block Tbx2 expression. The NeoTag-2 cells are androgen dependent. In addition, we used the LAPC4 cells to introduce the dominant negative construct. The NeoTag-2 cells when recombined with rat UGM (to induce prostate development) and placed in the kidney form foci of adenocarcinoma. Therefore it is interesting to see what effect knocking down of Tbx2 has on the adenocarcinoma morphology formed by Neotag-2 cells recombined with UGM. We characterized all the four prostate cancer cell lines stably infected with the Tbx2 dominant negative construct for HA tag (the Tbx2 DN construct contains an HA tag), p21 or p19 arf expression. As expected, all four cell lines having dominant negative vector showed the expression of HA Tag **(Fig. 17).** All the three human cell lines LAPC4, PC3 and DU145 showed enhanced expression of p21 expression as expected **(Fig. 17).**
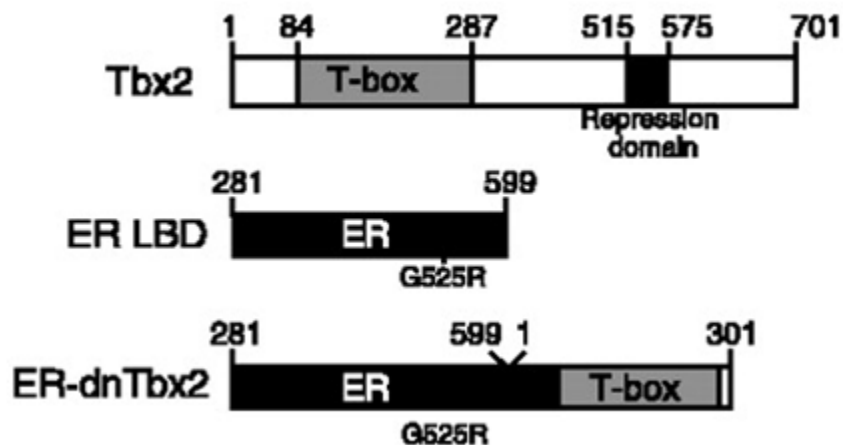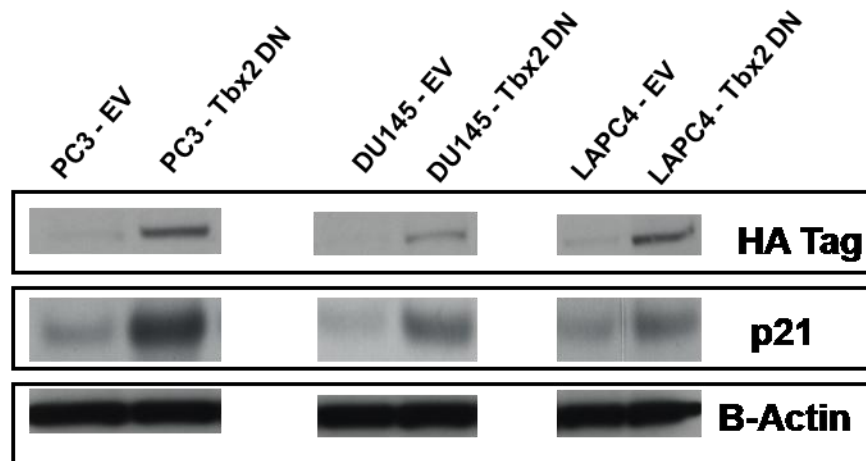
Figure 17: Western blot analysis showing characterization of human prostate cancer cells stably infected with Tbx2 DN vector as compared to control cells Presence of HA tag and increase in p21 levels in human prostate cancer cell lines stably infected with Tbx2DN vector as compared to the respective empty vector (EV) infected control cells. Lower panel shows the cartoon depicting the construction of the inducible Tbx2 dominant negative vector.

Tbx2 DN vector decreases proliferation of prostate cancer cells *in vitro:*

Cell proliferation assays shoed that prostate cancer cells stably infected with the Tbx2 DN vector showed decreased proliferation *in vitro* as compared with the respective cells infected with the empty vector (EV). This was seen in three human prostate cancer cell lines PC3, DU145, LAPC4 **(Fig 18).**
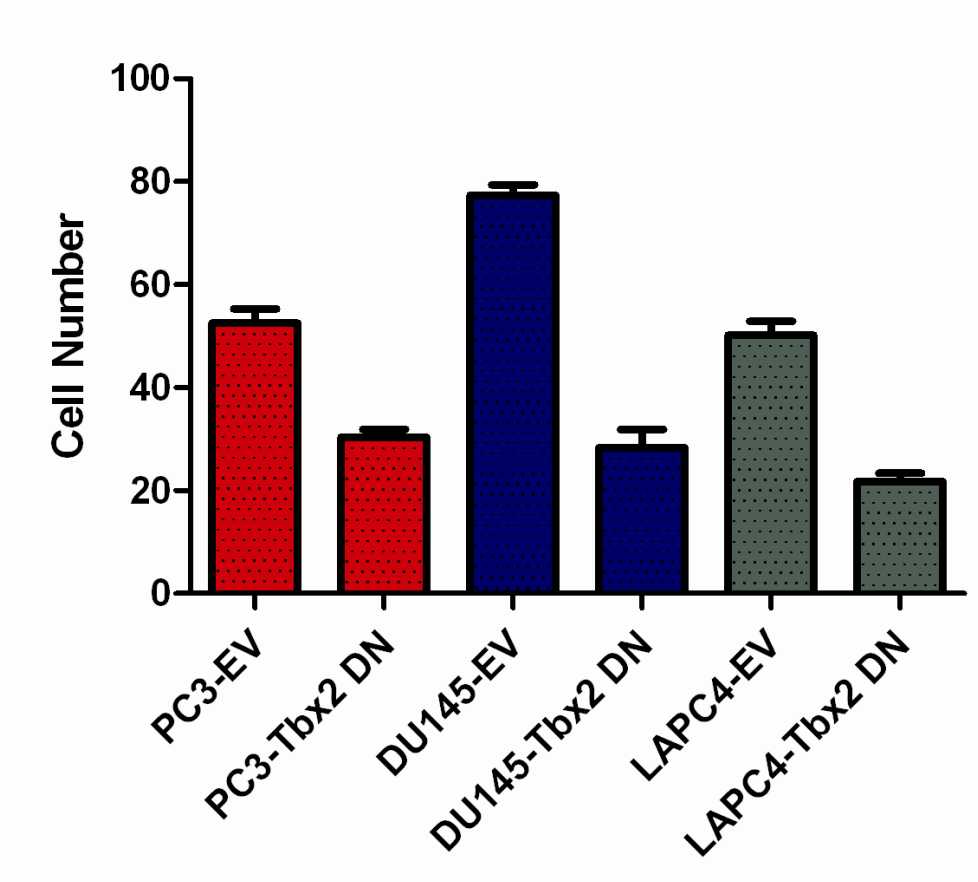
Figure 18: *In vitro* Cell proliferation assay showing reduced proliferation in human prostate cancer cells stably infected with Tbx2 DN vector.

Kidney capsule grafts of PC3-Tbx2 DN vector show no difference in size of grafts compared with PC3-EV grafts:

In order to find the *in vivo* effect of blocking endogenous Tbx2, we utilized the technique of tissue recombination and grafted PC3-Tbx2 DN and PC3-EV after recombining the cells with urogenital mesenchyme (UGM). Tissue recombination is a technique that makes use of epithelial-stromal interactions and this technique can be utilized to simulate and examine disease progression in the prostate by genetically modifying either the epithelial or the stromal cells. Contrary to expectations, we did not observe a statistical difference in the size of the grafts in PC3-Tbx2 DN and PC3-EV cells. Morphologically, PC3-EV grafts looked loose while PC3-Tbx2 DN grafts looked more compact **(Fig. 19).**
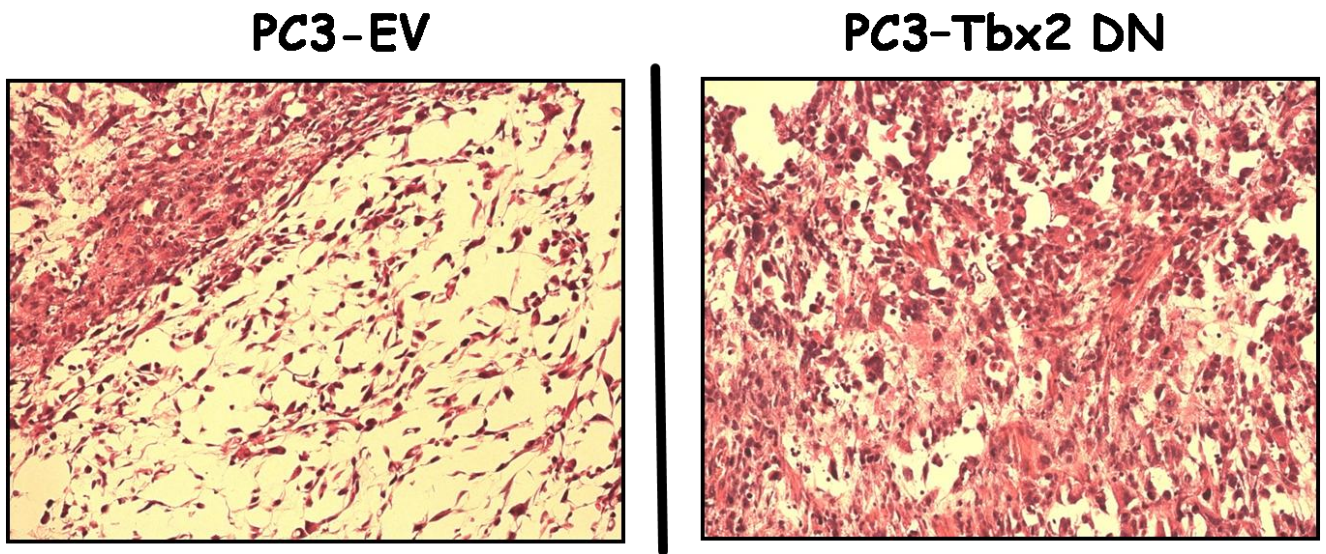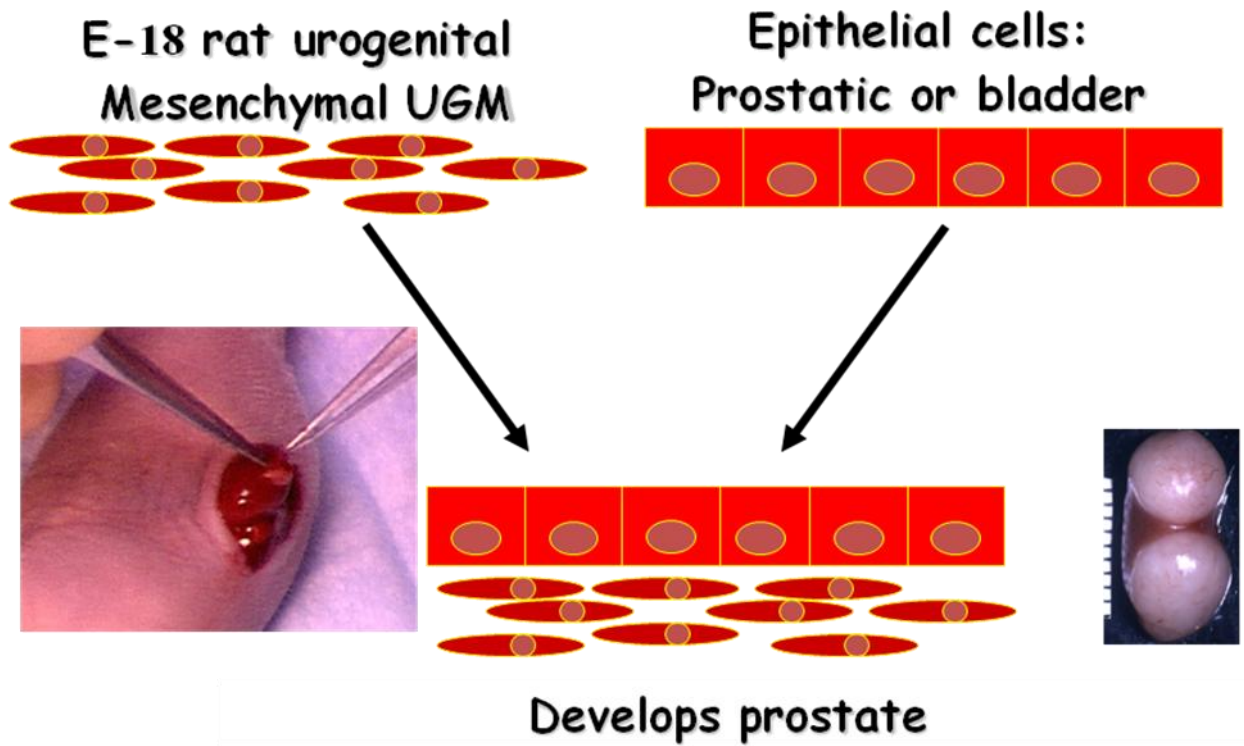
Figure 19: Tissue recombination scheme and H&E staining of tissue recombination grafts of PC-EV and PC3-Tbx2 DN cells.

Tbx2 DN cells grafted in the bone produce grafts that are less osteolytic as compared with PC3-EV grafts:

In order to test the role played by Tbx2 in the growth of prostate cancer cells in bone microenvironment, we inoculated (2×10^5 cells in 10ul PBS) of either PC3-EV or PC3-Tbx2 DN cells utlizing the technique of intra-tibial inoculation in the tibia of nude mice. As a control, the contra-lateral tibia of the mouse was injected with 10 ul PBS. Intra-tibial inoculation (**Fig. 20,** Upper Panel) is a technique which allows us to study the growth and effect of tumor cells on the bone microenvironment. In this technique, tumor cells are injected into the tibia of mice, the injected cells form lesions in the bone and the nature of these lesions, whether osteoblastic (bone forming) or osteolytic (bone depleting) is monitored and analyzed by weekly X-rays and the size of lesions is quantitated by using micro CT analyses.

PC3 cells when injected in the tibia are known to be osteolytic in nature. As analyzed by x-ray analysis after 4 weeks of inoculation, we found that PC3-Tbx2 DN cells were reduced in their ability to elicit an osteolytic response in the bone as compared to PC3-EV cells (**Fig. 20**, Lower Panel). Also, the size of PC3-Tbx2 DN lesions was smaller as compared to PC3-EV cell lesions as seen on X-ray as well as by H&E analyses (**Fig. 21**) of bone tibial sections performed after fixation of harvested tibiae. Micro CT analysis revealed that the bone lesions formed by PC3-Tbx2 DN cells were more osteolytic as compared with bone grafts of PC3-EV cells (**Fig 22,** Upper Panel)**.** The bone loss was quantitated and plotted in a graph (**Fig. 22,** Lower Panel).
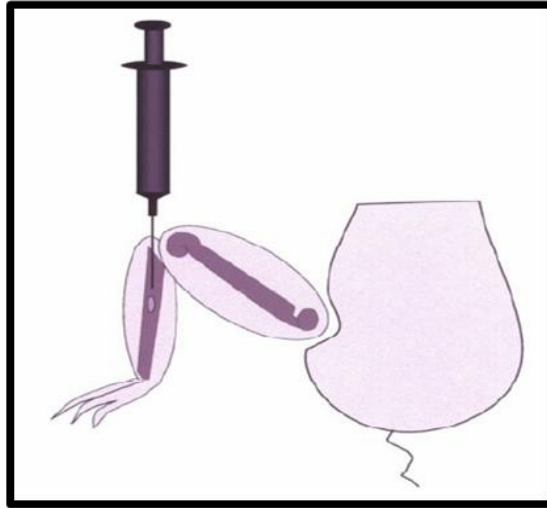
PC3-EV　　　　　　　　　　**PC3-Tbx2 DN**

Figure 20: Cartoon of intra-tibial inoculation model and x-ray pictures of mouse tibia injected with PC3-EV and PC3-Tbx2DN cells respectively. Upper panel shows cartoon depicting the intra-tibial inoculation model. Lower panel shows x-ray pictures of mouse tibia injected with PC3-EV and PC3-Tbx2DN cells respectively.
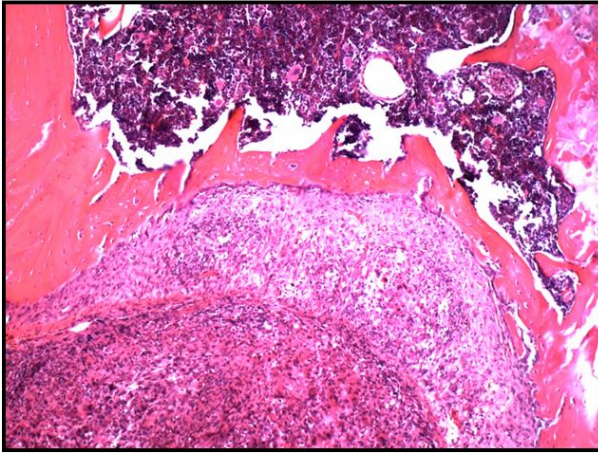
PC3-EV **PC3-Tbx2 DN**
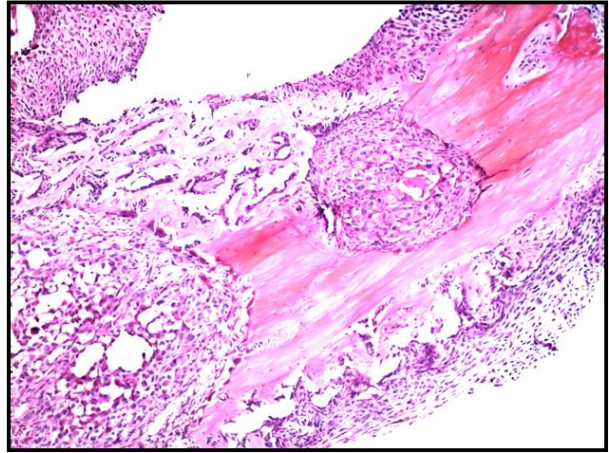
Figure 21: H&E analysis showing tumor lesions in PC3-EV and PC3-Tbx2DN injected tibiae respectively. Bone lesions of PC3 human prostate cancer cells infected with Tbx2 DN vector show reduced size of lesion compared to empty vector (EV) infected PC3 cells.
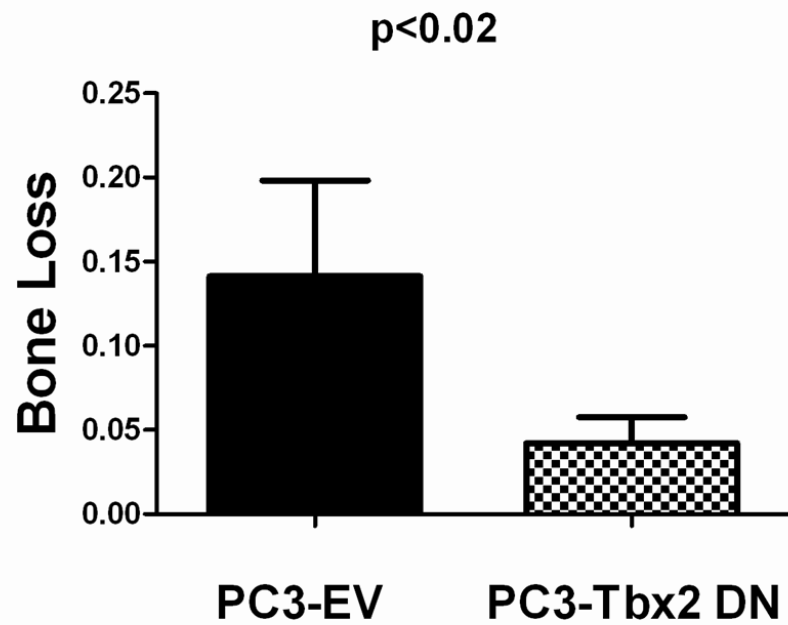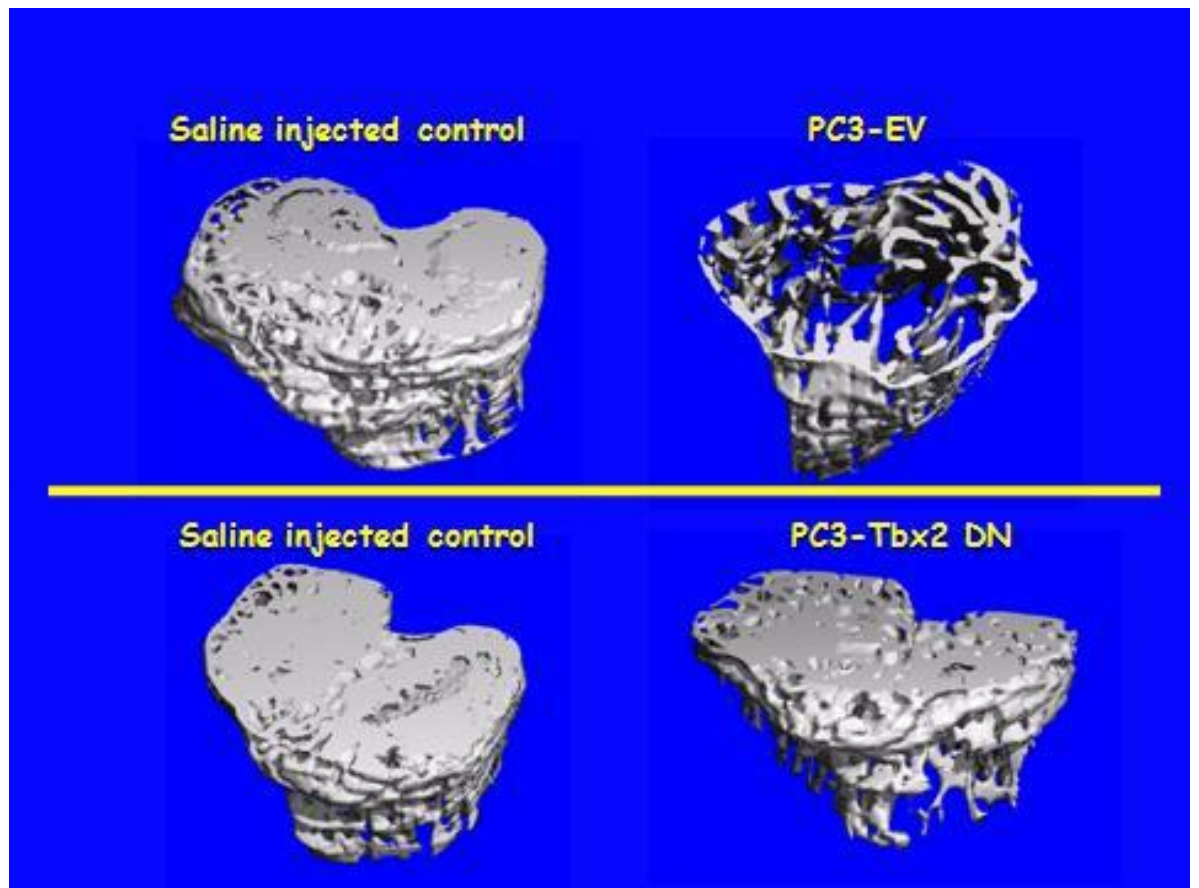
Figure 22: Micro CT analysis showing osteolysis in PC3-EV and PC3-Tbx2 DN injected cells in the tibiae. Lower panel shows the quantitation of bone loss.

PC3-Tbx2 DN cells show reduced levels of Wnt 3a, Gli2 and PTHrP as compared with PC3-EV cells:

Since we found that BMP2 treatment induces Wnt 3a in LAPC4 prostate cancer cells, we looked at Wnt 3a in Pc3-Tbx2 DN cells. Interestingly, PC3-Tbx2 DN cells in vitro showed a reduction in Wnt 3a levels as compared to PC3-EV cells by real-time quantitative PCR analysis **(Fig. 23).** We also looked at Gli2 and PTHrP since Wnt 3a has been reported to regulate Gli2 and Gli2 has been reported to regulate PTHrP. Interestingly, we found that both Gli2 and PTHrP were reduced in PC3-Tbx2 DN cells as compared with PC-EV cells by real-time quantitative PCR analysis **(Fig. 23).**

Figure 23: Quantitative RT-PCR analysis showing change in expression of Wnt3a, Gli2 and PTHrP in PC3-EV and PC3-Tbx2DN cells.

**PC3-Tbx2 DN cells show a reduction in nuclear phospho SMAD 1,5,8 levels *in vitro:*

Since BMP2 is known to signal through downstream SMAD 1,5,8, we looked at SMAD 1,5,8 levels in PC3-Tbx2 DN cells. *In vitro*, PC3-Tbx2 DN cells showed reduced nuclear levels of SMAD 1,5,8 as compared with PC3-EV cells **(Fig 24).**
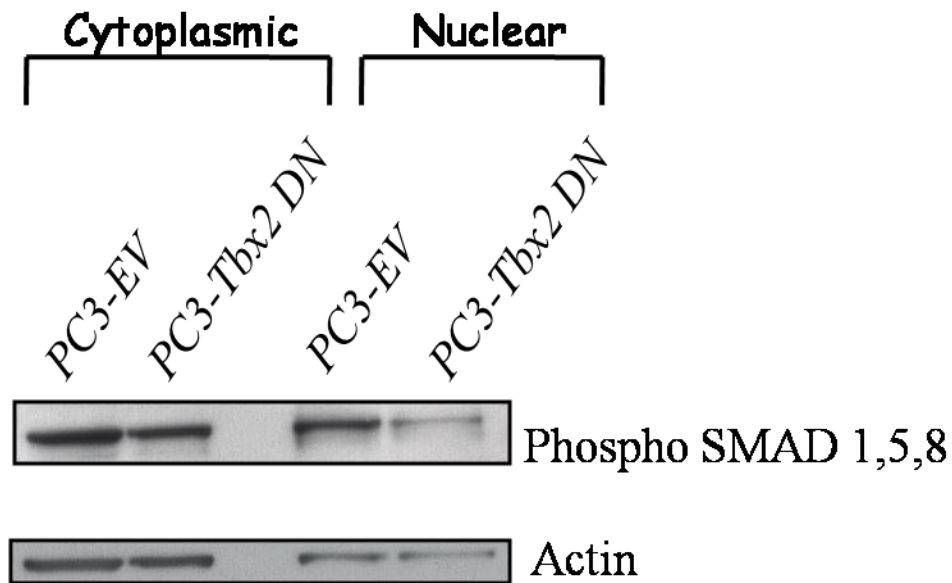
Figure 24: Western blot analysis of cytoplasmic and nuclear fractions showing change in SMAD 1,5,8 levels in PC3-EV and PC3-Tbx2 DN cells respectively. PC3 human prostate cells stably infected with Tbx2 DN vector show reduced levels of nuclear phosphor SMAD 1,5,8 as compared to empty vector (EV) infected PC3 cells.

CHAPTER IV

DISCUSSION AND FUTURE DIRECTIONS

Metastasis to the bone occurs in up to 70% of patients with advanced prostate or breast cancer and these two cancer types account for a staggering 80% of the total cases with metastatic bone involvement (Coleman, 1997; Coleman, 2001; Roodman, 2004). Most of the patients who suffer from prostate cancer do not die due to the tumor at the primary site but rather due to complications when the tumor has spread to the bone. It is estimated that each year, about 350,000 people die of bone metastasis in the United States. The causative tumor becomes incurable once the bone has been invaded and only 25% of prostate cancer patients are able to live 5 years subsequent to their diagnosis of bone metastasis (Roodman, 2004). Bone metastasis phenotype in prostate cancer patients results in significant morbidity and mortality due to extreme pain, pathologic fractures and other skeletal related complications including spinal cord compression. These patients have a mean survival period of 9 months to one year (Cheville et al., 2002) and currently, there is no available therapy to treat the bone metastases. In the coming years, due to the increase in the average life expectancy, it is expected that the incidence and mortality of prostate cancer will continue to increase.

The metastatic process consists of a number of sequential steps including loss of polarity, epithelial structure disorganization, disruption of the basement membrane

leading to degradation of extracellular matrix, invasion of blood and lymph vessels, escape of the tumor cells into blood and lymph vessels or extravasation, establishment of secondary foci by the escaped tumor cells and angiogenesis.

Creating and characterizing mouse models that better mimic the progression in human prostate cancer is a powerful tool to study and delineate the various steps in tumor progression. Most of the currently available mouse models of prostate cancer successfully recapitulate the early steps of tumor progression in the primary site but fail to metastasize to other organs especially to the bone. Amongst the existing ones, transgenic models that are created by dysregulating a gene that is widely known to be altered in human prostate cancer are considered to be more reflective of the human disease. This is in contrast to transgenic mouse models that overexpress the small t and large T antigens that despite the phenotype they produce, are considered to have little physiological significance.

Hepsin is consistently up-regulated in more than 90% of human prostate tumors, including one report which provided evidence of increases of 34-fold when compared to non-tumor controls (Landers et al., 2005; Stephan et al., 2004). Additionally, hepsin expression levels have been shown to positively correlate with disease progression in human prostate cancer (Chen et al., 2003; Stamey et al., 2001; Xuan et al., 2006). A number of well characterized models for mouse prostate adenocarcinoma exist; however, in most of these models hepsin levels are low or nonexistent (Hu et al., 2002; Wu and Parry, 2007). Transgenic mice expressing hepsin under the control of the prostate specific probasin promoter do not display changes in cell proliferation or differentiation but do show a disorganization of the basement membrane (Klezovitch et al., 2004). Further,

when PB-hepsin transgenic mice are crossed with a transgenic line expressing the SV40 Large-T antigen in the prostate (LPB-Tag 12-7f line), the resulting bigenic offspring displayed dramatic acceleration in tumor progression and metastasis to the bone making it the only transgenic prostate cancer mouse model displaying reproducible bone metastasis (Klezovitch et al., 2004). These studies indicated that hepsin plays a key role in prostate cancer progression, as opposed to the initiation of prostate tumorigenesis. However, previously developed LPB-Tag/PB-hepsin mice develop invasive adenocarcinoma as well as neuroendocrine cancer in the primary tumor. Further, the metastatic lesions in these LPB-Tag/PB-hepsin mice were neuroendocrine in nature. In human prostate cancer, the vast majority of primary tumors are adenocarcinomas (Grignon, 2004). However, in several human prostate tumors, following androgen deprivation therapy, the adenocarcinoma progresses to more aggressive androgen independent tumors that develop varying degrees of neuroendocrine differentiation. Primary human prostate tumors that are neuroendocrine in nature are extremely rare and akin to NE cancers in other tissues are highly aggressive (Azumi et al., 1984; Capella et al., 1995; Capella et al., 1981; Cohen et al., 1990; di Sant'Agnese and de Mesy Jensen, 1984; Ghali and Garcia, 1984; Trias et al., 2001). Therefore, a more desirable mouse model for prostate cancer would incorporate the predominant features of human prostate cancer including reliable and faster progression to invasive adenocarcinoma, absence of neuroendocrine differentiation, and development of adenocarcinoma metastases to the bone. In order to directly test the role of increased hepsin expression in prostate cancer progression, we introduced high levels of hepsin expression into the prostate of the Hi-myc mouse model of prostate adenocarcinoma. This resulting hepsin/myc bigenic mouse

98

model showed that the increased expression of hepsin results in earlier development of prostate adenocarcinoma, and eventually a higher grade tumor when compared to tumors derived from the myc mice.

The myc protooncogene has been shown to cause increased cell proliferation in multiple studies. Several reports have demonstrated increased myc copy number in up to 30% of human prostate tumors (Fleming et al., 1986; Jenkins et al., 1997; Nesbit et al., 1999; Qian et al., 1997; Sato et al., 1999). The myc transgenic mouse model utilizing the prostate specific probasin promoter displays a reliable penetrance to HGPIN lesions and progression to invasive adenocarcinoma in 6 months (Ellwood-Yen et al., 2003). The myc transgenic mice develop PIN with progression to an adenocarcinoma that is devoid of any neuroendocrine differentiation. However, the myc model of prostate cancer spontaneously expresses low hepsin levels suggesting that progression of the cancer in this model is paralleling events that occur in human prostate cancer. However, these low levels of hepsin expression may not accurately reflect the physiological consequences that the widespread over-expression of hepsin causes in human prostate tumors.

To investigate the effect of hepsin over-expression in a mouse model of prostate adenocarcinoma, we generated the hepsin/myc bigenic mouse. Hepsin up-regulation in the myc model accelerates the incidence of adenocarcinoma from 6 months to 4.5 months. As mice were aged up to 17 months, the prostate tumors of hepsin/myc mice displayed a higher pathological grade of cancer when compared to age matched mice expressing myc alone in the prostate. This finding further supports an important role for increased hepsin expression and activity during progression of adenocarcinoma. Also, the

tumors in our bigenic mice did not develop features of neuroendocrine differentiation and were negative for synaptophysin, a neuroendocrine marker. Further, we found that endogenous hepsin levels, although low when compared to the probasin targeted hepsin, were present in the myc mice and increased significantly ($p < 0.05$) as the myc tumors progressed to 12, 15 and 17 months when compared with the 6 month myc tumor. This finding demonstrates that expression of hepsin in the myc tumors occurs spontaneously and reflects similar events seen during the progression of human prostate cancer.

Another important step that has been documented in the progression of human prostate cancer is loss of Laminin-332, a component of the basement membrane (Calaluce et al., 2001; Davis et al., 2001; Hao et al., 2001; Nagle, 2004). We therefore wanted to investigate if the increased aggressiveness in hepsin/myc tumors is associated with the loss of Laminin-332. Interestingly, we found that compared with age matched myc alone tumor, the 12 month hepsin/myc tumor tissue displayed increased degradation of Laminin-332. Our data is consistent with a recent report that shows that hepsin proteolytically cleaves the beta 3 chain of Laminin-332 *in vitro* and that there is enhanced *in vitro* migration of prostate cancer cells due to this cleavage event (Tripathi et al., 2008). Although only a few other substrates for hepsin including blood clotting factors, pro-urokinase and pro-hepatocyte growth factor have been identified, hepsin targets must play an important role in the progression of prostate cancer (Kazama et al., 1995; Kirchhofer et al., 2005; Moran et al., 2006). We suggest that the cleavage of Laminin-332 is an important step during progression to higher grade cancer. Since the degradation of Laminin-332 occurs as human prostate cancer progresses, our data would suggest that the

elevated levels of hepsin is responsible for the loss of Laminin-332 during progression of human prostate cancer.

The data showing that disorganization of the basement membrane in transgenic mice over-expressing hepsin combined with data showing that hepsin cleaves Laminin-332 strongly indicates that hepsin may be directly involved in the disruption of the basement membrane through degradation of the extracellular matrix proteins (Tripathi et al., 2008). Further, interestingly, since hepsin expression is decreased in metastatic lesions (Dhanasekaran et al., 2001) suggests that there is no positive selection for the expression of hepsin at the stage when tumor cells are trying to re-establish themselves at distant sites. A plausible meachanism of action of hepsin is that while its expression and proteolytic activity is necessary during the initial stages of tumorigenesis to disrupt the basement membrane and initiate invasion, this activity is counter-productive when the cells are trying to establish themselves at distant sites since the cells at this stage are attempting to adhere to the extracellular matrix. In agreement, metastasis derived prostate cancer cell lines do not express hepsin and overexpression of hepsin in these cells results in retardation of cell growth and increase in apoptosis (Srikantan et al., 2002). It is possible to hypothesize that hepsin along with other proteloytic enzymes may play different roles at the different steps of progression of cancer and metastasis. In contrast to artificial systems of tissue culture or in systems where tumor cells are injected into immunocompromised mice, transgenic model systems represent a more holistic approach of looking at the tumor progression from normal tissue to PIN to adenocarcinoma to metastasis. Such an approach helps dissect the entire sequence of events leading to metastasis.

The changes in the role of hepsin during the progression of prostate cancer suggest that different treatments are required to target the different stages in the progression of prostate cancer. Further, it would suggest that the approach of targeting a particular protein for at an early step of adenocarcinoma such as the initial invasion and escape of cells, may not be a suitable approach while targeting the late stage when the cancer cells that form metastatic lesions at distant organs. In other words, drugs that target the initial stages of the tumor would need to be discontinued and other drugs that target the more advanced tumors would need to be administered. Otherwise the drug of the former type may actually promote the establishment of the tumor cells in distant organs. In the future, strategies to treat cancer may include the precisely monitoring of the tumor stage and administering treatment depending on that stage. In keeping with the data on hepsin, the potential use of the inhibitors of hepsin may be particularly suited during watchful waiting which is often clinically chosen for patients who have low grade prostate cancer. If the potential use of hepsin inhibitor can slow down the progression of prostate cancer in its early stage, it may hypothetically be able to push the onset of advance prostate cancer and extend the average life span, thus eliminating prostate cancer as a cause of disease and death in men.

However, unlike the LPB-Tag/PB-hepsin mice, no metastasis was detected in either myc alone or hepsin/myc bigenic mice. It has been argued that while hepsin may play an important role in the primary tumors by degrading basement membrane molecules, the low levels of hepsin in the metastatic lesions and metastasis-derived human prostate cell lines indicates a paradoxical nature of hepsin as a metastasis promoting gene. It is plausible to hypothesize that hepsin may play varying roles

depending on the prostate tumor type (adenocarcinoma or neuroendocrine tumor) and also depending on its expression at specific time points in the tumor progression cascade. We speculate that the absence of metastasis in this model is linked to the relatively less aggressive adenocarcinoma that occurs in the myc mice as compared to the LPB-Tag/PB-hepsin mice that develop aggressive neuroendocrine cancers. This data suggests that hepsin expression in the tumor is not sufficient to induce metastasis from the slowly developing adenocarcinoma of the myc mouse prostate; however, hepsin expression does cause adenocarcinoma to appear earlier and tumor grade to increase at a faster rate than when myc alone is expressed in the mouse prostate.

Our hepsin/myc model develops cancer as early as 4.5 months **(Fig 25)** and only the knock out (KO) of Pten in the prostate and the TRAMP models develop cancer at such an early age (Greenberg et al., 1995; Wang et al., 2003). However, TRAMP mice develop neuroendocrine cancer rather than adenocarcinoma (Chiaverotti et al., 2008). Both the hepsin/myc and Pten models develop primary tumors that are adenocarcinoma. However, prostates of Pten KO mice have limited adenocarcinoma cells that show neuroendocrine differentiation that further increased in castrated mice (Liao et al., 2007). In our hepsin/myc model, no neuroendocrine differentiation occurs in either intact or castrated mice.

In summary, our hepsin/myc model shows rapid progression (**Fig 25**) to prostate adenocarcinoma and mimics multiple features of human prostate cancer progression by the over-expression of hepsin as well as myc and the loss of Laminin-332. The use of this new bigenic model will aid in the identification of novel hepsin substrates that contribute

to prostate adenocarcinoma progression and more importantly aid in the testing of compounds that inhibit hepsin activity, thus identifying compounds for prostate cancer therapy in humans.
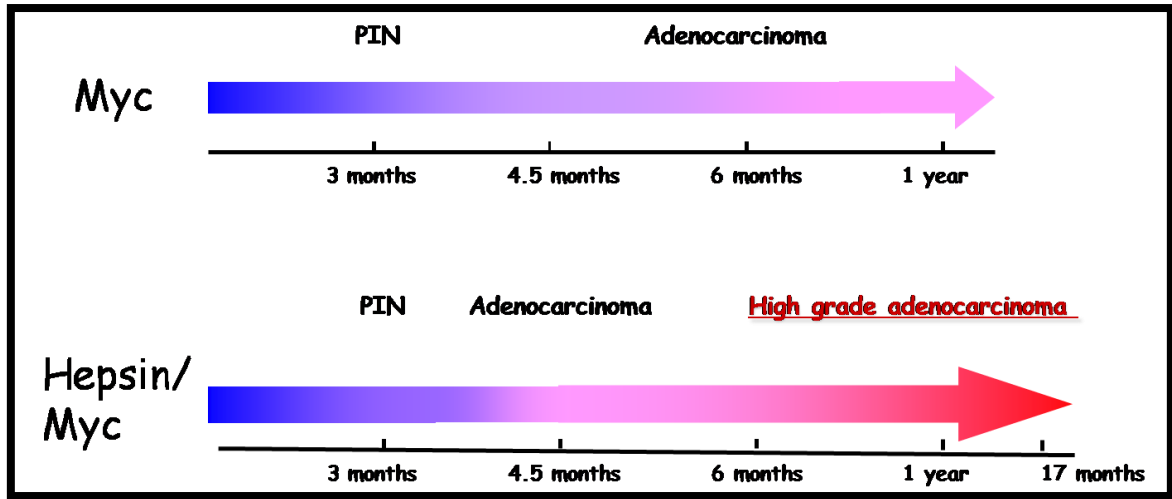
Figure 25: **Cartoon depicting the progression of adenocarcinoma in the myc and the hepsin/myc mice.**

The myc mice develop PIN at 3 months and adenocarcinoma by 6 months. In contrast, the hepsin/myc bigenic mice develop PIN lesions at 3 months but progress to the adenocarcinoma step at 4.5 months. Further, the hepsin/myc mice develop a higher grade of adenocarcinoma at higher ages compared with the myc mice.

The final step in the metastatic cascade is the colonization and growth of the tumor cells in the bone and the various physiological complications associated with it in cancer patients. Since the establishment of bone metastases is dependent on the bone microenvironment, understanding the cellular interaction between prostate carcinoma cells and the bone microenvironment may provide a critical insight about the origin and maintenance of prostate cancer bone lesions. It has been proposed that the homing of prostate cancer cells in the bone is a non-random process that involves multiple steps. Further, it is now known that a vicious cycle is created between prostate cancer cells and the bone microenvironment that is mediated by factors secreted by the tumor cells and that the bone plays an important role in supporting and sustaining these bone metastases. Although, human prostate cancer produces bone lesions that are predominantly osteoblastic in nature, but osteoclastic resorption has been shown to be an integral part of skeletal metastases in this cancer (Basaria et al., 2002; Clarke et al., 1992). It has been shown that prostate cancer patients with bone metastases have higher levels of bone resorption markers as compared to patients without bone metastases (Maeda et al., 1997).

Further, recent clinical trials have indicated that treatment strategies that block osteoclastic bone resorption decrease the skeletal related complications in prostate cancer patients (Oades et al., 2002). But intriguingly, the inhibition of osteoclast activity in a murine model did not lead to a decrease in the development of osteoblastic metastasis (Lee et al., 2002). It is therefore not clear whether bone destruction takes place before the development of osteoblastic metastases or if it is caused by increased bone formation. Interestingly, Yi et al working with an animal model of osteoblastic bone metastasis have reported that increased bone formation is preceded by an initial phase of bone resorption,

thereby suggesting that the activation of osteoclasts may play an important role in the development of osteoblastic metastases (Yi et al., 2002). The established cell lines of human prostate cancer when injected in bone microenvironment of immunocompromised mice produce both osteoblastic and osteolytic phenotypes (Corey et al., 2002; Zhau et al., 1996).

One important area of prostate cancer research that needs particular attention is the development of relevant animal models that reflect or mimic the final step in human prostate cancer progression, i.e. the manifestation of skeletal metastases. Such an understanding of the interactions between prostate cancer cells and the bone microenvironment will lead to novel approaches towards the discovery of selective therapeutic targets for the treatment of the skeletal metastases. A large number of transgenic mouse models that mimic prostate cancer have been created; although all these models have contributed greatly to our understanding of the multistep nature of prostate cancer, however, spontaneous bone metastases from these models are rare. In order to recapitulate human prostate cancer metastasis, the tumor cells in a transgenic mouse model must be able to disseminate from the primary tumor, metastasize to bone and produce an osteoblastic reaction in the bone. Intriguingly, very few of the experimental mouse models for mouse prostate cancer mimic the bone metastasis step that is so widespread in human prostate cancer. Experimental models of bone metastasis therefore consist of injecting cancer cells or tissue orthotopically, intracardially, intravenously (via the tail vein) or directly intraosseously into immunocompromised mice. While the intrafemoral/intratibial injection of cancer cells is not considered an appropriate technique to study the early rate-limiting steps of the metastatic cascade, the technique

however provides a powerful tool to model the interactions between the cancer cells and the bone microenvironment.

A number of factors are known to drive the vicious cycle between prostate carcinoma cells and bone cells. Cancer cells interact and participate with the bone cells to induce osteoclasts or osteoblasts, thereby creating a metabolic imbalance between the number of osteoblasts and osteoclasts. This imbalance may push the bone equilibrium towards an osteoblastic process as in human prostate cancer bone metastases. It has been proposed that cancer cells undergo phenotypic changes that allow them to form bone and this phenomenon has been referred to as "osteomimicry" (Koeneman et al., 1999). This process allows cancer cells to survive and proliferate in the bone microenvironment by utilizing the abundance of growth factors and extracellular matrix molecules found in the bone, thereby creating a vicious cycle. Prostate cancer cells that have successfully colonized the bone frequently secrete osteoblast promoting factors including BMPs, Wnt-family ligands, endothelin-1 (ET-1) and PDGF. Guise proposed that this vicious cycle also involves transforming growth factor β that is produced by the bone cells, that promotes the tumor cells to produce parathyroid hormone-related protein (PTHrP), which in turn promotes bone turnover by fostering osteolysis of the bone (Guise, 2000).Therefore, a vicious cycle of bone turnover and tumor cell-promoted osteolytic response is set forth since rapid production of bone stimulates the release of TGF-β that in turn promotes the release of PTHrP by tumor cells. It is known that this vicious cycle between TGF-β and PTHrP plays a role in the osteolytic metastases of breast carcinoma and it is possible that the same mechanism may be operative in some prostate carcinoma cells. In addition to TGF-β and PTHrP, a number of other molecules may play a role in

the vicious cycle between tumor cells and bone microenvironment. There is evidence that endothelin-1 (ET-1), a prominent cytokine produced by tumor cells may play a role in the osteoblastic reaction produced by prostate cancer cells that get lodged in the bone (Nelson and Carducci, 2000). It has been reported that ET-1 and its receptor ET-A may play a role in the osteoblastic phenotype by increased production of interleukin 1β (IL-1β), TGF-β and TNF-α. Further, it is known that increased synthesis of TGF-β, endothelial growth factor and IL-1α in turn up regulates ET-1, thus causing the imbalance of growth factors and cytokines in the bone microenvironment. It is believed that such mechanisms that cause increase in the production of growth factors and cytokines may play a role in the survival and growth of prostate cancer cells in the bone (Granchi et al., 2001; Le Brun et al., 1999).

Bone morphogenic proteins (BMPs) are a family of growth factors that belong to the TGF-β superfamily and are known to play a role in the stimulation of bone synthesis by prostate cancer cells (Hogan, 1996). The BMPs initiate downstream signaling through 2 two types of serine/threonine transmembrane receptor kinases, type I and type II. BMPs bind the type II receptor which in turn activates the type I receptor. The type I receptor activates members of the SMAD family of proteins, particularly SMAD 1,5 and 8; these SMADS interact with SMAD 4 that translocates to the nucleus and leads to the activation of the target genes. BMP-2, -3, -4 and -6 have been reported in normal and cancerous prostate tissue (Autzen et al., 1998; Harris et al., 1994b) and BMP-4, -6 and -7 were detected in prostate skeletal metastases (Autzen et al., 1998; Thomas and Hamdy, 2000). Further, BMP receptors have been reported to be expressed in prostate tissue and cell lines (Brubaker et al., 2004; Ide et al., 1997; Kim et al., 2000). These studies suggest that

BMPs expressed by prostate tumor and bone may play a direct effect on prostate cancer cells. It has been shown that BMP2 inhibits LNCaP cell growth by increased levels of p21 and causes further downstream inactivation of Rb protein (Brubaker et al., 2004). In PC3 cells, BMP2 treatment increased p21 levels although proliferation was not affected. Further, it was also reported that in PC3 cells, BMP2 treatment increased the level of OPG which is a decoy receptor for the receptor activator for NF-κB, a molecule that stimulates osteolysis(Brubaker et al., 2004). However, since PC3 cells are strongly osteolytic, the remodeling pathways involving OPG in PC3 cells may well be masked by factors that stimulate bone resorption such as matrix metalloproteases (Nemeth et al., 2002), urokinase plasminogen activator (Yoshida et al., 1994), RANKL (Brown et al., 2001) and PTHrP (Iwamura et al., 1994) that are expressed by PC3 cells.

Since our hepsin/myc transgenic model did not develop bone metastases, we took the approach of studying the effect of Tbx2, a T-box transcription repressor to model the interactions between the bone and prostate tumor cells. We initially stumbled on Tbx2 in a screen for androgen regulated genes. Interestingly, Tbx2 expression was up regulated in LNCaP human prostate cancer cells with androgen treatment. To study the androgen regulation in an *in vivo* setting, we castrated male mice, administered androgens two weeks following castration and looked at Tbx2 expression. Consistent with the *in vitro* data, Tbx2 levels increased following androgen treatment in all the lobes of the rodent prostate as compared to the oil control. Further, Tbx2 is very highly expressed in all the aggressive human prostate cancer cell lines including PC3, DU145, and LAPC4 cells and very low in the relatively benign cell lines including RWPE1 and LNCaP cells. This

intrigued us since it has been reported that Tbx2 is highly expressed in human melanoma, pancreatic and breast cancer cell lines.

Further, BMP2, a member of the bone morphogenic protein family that belongs to the TGF-beta superfamily, is also very highly expressed in the more aggressive prostate cancer cells. This correlation further intrigued us since BMP2 has been reported to be dysregulated during human prostate cancer progression and interestingly it has been shown previously that during development, there is a feedback and feed forward signaling between BMP2 and Tbx2. Further, Tbx2 has also been reported to have a similar feedback and feed forward regulation with sonic hedgehog signaling, a pathway that has also been reported to be dysregulated in human prostate cancer.

We found that BMP2 when added in the culture medium induces Tbx2 expression in LAPC4 cells that are known to have the BMP2 receptor. Further, addition of BMP2 induced Wnt 3a. This was of interest to us since the Wnt family of proteins has been reported to be involved in bone formation. We next took the approach of repressing endogenous Tbx2 in human prostate cancer cells by utilizing a dominant negative construct which we stably infected into human prostate cancer cell lines LAPC4, PC3 and DU145. *In vitro* cell proliferation was decreased in all three cell lines. Since BMP2 has been reported to mediate osteogenic effects and Tbx2 is downstream of BMP2, we were interested in looking at the effect of manipulating Tbx2 on the interactions between prostate cancer cells and the bone microenvironment. When inoculated into the intra-tibial model, PC3 cells infected with the Tbx2 DN construct produced smaller lesions that were significantly less osteolytic when compared to the lesions produced by the control

110

PC3 cells. This decrease in osteolysis was seen by x-ray analysis which is semi-quantitative technique for estimating the change in bone density. Therefore, the decrease in osteolytic effect was further confirmed by micro CT analysis which provides a quantitative measure of the change in bone density. Since BMP2 is known to signal downstream through the phosphorylation of SMAD 1,5,8, we looked at this SMAD and found that nuclear levels of phospho SMAD 1,5,8 is decreased in PC3 cells with dominant negative Tbx2. Further, *in vitro*, Tbx2 dominant negative construct decreases Wnt3a, Gli2 and PTHRP signaling in PC3 cells.

In summary, we have found that blocking endogenous Tbx2 levels reduces tumor and osteolytic burden in PC3 human prostate cancer cells. Since research in recent years has indicated that one of the ways to reduce the osteogenic burden of prostate tumors is through reducing the osteolytic activity that occurs in the background of the overall osteoblastic effect, blocking Tbx2 may be used as a therapeutic target in the future.

Future Directions:

Since orthotopic grafts are widely considered to have a greater physiological relevance to the study of tumor progression as compared with kidney capsule or subcutaneous grafts, an alternative approach to test the effect of Tbx2 DN construct in PC3 cells would be to graft these cells in the anterior prostatic lobe of nude mice. PC3 cells when grafted orthotopically into the NOD-SCID mice have been reported to display metastases to a variety of soft tissues but bone metastases have not been reported.

Interestingly however, when fragments from a subcutaneous xenograft were used for an orthotopic graft in the prostate of nude mice, the primary prostatic tumor resulted in extensive skeletal metastases as well as soft tissue metastases (Yang et al., 1999).

Also, although tibial inoculation of tumor cells allows us to study the tumor cell–bone microenvironment interactions, it is not a good model for the study of metastasis. Therefore, in order to study the metastatic ability of cells, an elegant alternative is the intracardiac injection of cells in nude mice. Following intracardiac injection, luciferase tagged PC3 cells have been shown to colonize the lumbar spine, teeth and hind limbs and this progression was shown in a quantitative fashion facilitated by the presence of the luciferase in the cells (Kalikin et al., 2003).

An alternate method of testing the genetic manipulation of Tbx2 in prostate cancer cells would be to over-express Tbx2 in human prostate cancer cells that express low Tbx2 levels. LNCaP cells are relatively benign human prostate cancer cells that do not form aggressive grafts when placed under the kidney capsule and express low levels of endogenous Tbx2. Further, LNCaP cells when grafted into mouse tibia do not show significant growth. Therefore a good approach of testing the effects of Tbx2 would be to stably overexpress Tbx2 in LNCaP cells and perform under the kidney capsule, subcutaneously, orthotopic, tibial inoculation and by intracardiac injection experiments of LNCaP cells over-expressing Tbx2 compared to control LNCaP cells. The presence of GFP in the cells would enable imaging the tumor at the sites of the grafts, at potential metastatic sites, and by in the tumor sections by immunohistochemical analyses. Based upon my data, it would be expected that overexpression of Tbx2 in LNCaP cells would

make these cells more aggressive when placed under the kidney capsule, subcutaneously, orthotopic, tibial inoculation and by intracardiac injection experiments. The kidney capsule grafts are a good model to study invasion at the interface of the tumor and the kidney surface while the other grafting site would test the ability to grow in specific microenvironments. Intracardiac injection would test the role of Tbx2 to cause a tumor to colonize other tissues. Further, my data would suggest that the overexpression of Tbx2 would make LNCaP cells form osteoblastic lesions when placed in the bone microenvironment or to spread to that site when injected intracardially in mice.

Following the studies with LNCaP cells overexpressing Tbx2, an elegant idea would be the creation of a transgenic mouse model overexpressing Tbx2 in the mouse prostate. Tbx2 expression can be targeted specifically to the prostatic epithelial cells utilizing the prostate specific probasin promoter. It would be expected that overexpression of Tbx2 in the prostatic cells would lead to neoplastic transformation of the cells resulting in adenocarcinoma. Further, the Tbx2 transgenic mouse could be crossed with another mouse model that develops prostate cancer like the Pten conditional KO mouse or the PB-Hi-Myc mouse to look for further progression and even metastasis to the bone.

This research supports a fundamental role for Tbx2 during the progression of prostate cancer to metastatic sites. Further studies on the pathways that Tbx2 controls during the metastatic process can result in the identification of new targets genes for therapeutic intervention.

REFERENCES:

Abate-Shen, C., and Shen, M. M. (2000). Molecular genetics of prostate cancer. Genes Dev *14*, 2410-2434.

Achbarou, A., Kaiser, S., Tremblay, G., Ste-Marie, L. G., Brodt, P., Goltzman, D., and Rabbani, S. A. (1994). Urokinase overproduction results in increased skeletal metastasis by prostate cancer cells in vivo. Cancer Res *54*, 2372-2377.

Adell, T., Grebenjuk, V. A., Wiens, M., and Muller, W. E. (2003). Isolation and characterization of two T-box genes from sponges, the phylogenetically oldest metazoan taxon. Dev Genes Evol *213*, 421-434.

Agulnik, S. I., Garvey, N., Hancock, S., Ruvinsky, I., Chapman, D. L., Agulnik, I., Bollag, R., Papaioannou, V., and Silver, L. M. (1996). Evolution of mouse T-box genes by tandem duplication and cluster dispersion. Genetics *144*, 249-254.

Ahmed, N. N., Grimes, H. L., Bellacosa, A., Chan, T. O., and Tsichlis, P. N. (1997). Transduction of interleukin-2 antiapoptotic and proliferative signals via Akt protein kinase. Proc Natl Acad Sci U S A *94*, 3627-3632.

Andersen, C. L., Monni, O., Wagner, U., Kononen, J., Barlund, M., Bucher, C., Haas, P., Nocito, A., Bissig, H., Sauter, G., and Kallioniemi, A. (2002). High-throughput copy number analysis of 17q23 in 3520 tissue specimens by fluorescence in situ hybridization to tissue microarrays. Am J Pathol *161*, 73-79.

114

Aparicio, A., Gardner, A., Tu, Y., Savage, A., Berenson, J., and Lichtenstein, A. (1998). In vitro cytoreductive effects on multiple myeloma cells induced by bisphosphonates. Leukemia *12*, 220-229.

Asamoto, M., Hokaiwado, N., Cho, Y. M., and Shirai, T. (2002). Effects of genetic background on prostate and taste bud carcinogenesis due to SV40 T antigen expression under probasin gene promoter control. Carcinogenesis *23*, 463-467.

Aumailley, M., Bruckner-Tuderman, L., Carter, W. G., Deutzmann, R., Edgar, D., Ekblom, P., Engel, J., Engvall, E., Hohenester, E., Jones, J. C.*, et al.* (2005). A simplified laminin nomenclature. Matrix Biol *24*, 326-332.

Autzen, P., Robson, C. N., Bjartell, A., Malcolm, A. J., Johnson, M. I., Neal, D. E., and Hamdy, F. C. (1998). Bone morphogenetic protein 6 in skeletal metastases from prostate cancer and other common human malignancies. Br J Cancer *78*, 1219-1223.

Azumi, N., Shibuya, H., and Ishikura, M. (1984). Primary prostatic carcinoid tumor with intracytoplasmic prostatic acid phosphatase and prostate-specific antigen. Am J Surg Pathol *8*, 545-550.

Barlund, M., Monni, O., Kononen, J., Cornelison, R., Torhorst, J., Sauter, G., Kallioniemi, O.-P., and Kallioniemi, A. (2000). Multiple genes at 17q23 undergo amplification and overexpression in breast cancer. Cancer Res *60*, 5340-5344.

Basaria, S., Lieb, J., 2nd, Tang, A. M., DeWeese, T., Carducci, M., Eisenberger, M., and Dobs, A. S. (2002). Long-term effects of androgen deprivation therapy in prostate cancer patients. Clin Endocrinol (Oxf) *56*, 779-786.

Beato, M. (1989). Gene regulation by steroid hormones. Cell *56*, 335-344.

Bekker, P. J., Holloway, D. L., Rasmussen, A. S., Murphy, R., Martin, S. W., Leese, P. T., Holmes, G. B., Dunstan, C. R., and DePaoli, A. M. (2004). A single-dose placebo-controlled study of AMG 162, a fully human monoclonal antibody to RANKL, in postmenopausal women. J Bone Miner Res *19*, 1059-1066.

Bendjennat, M., Boulaire, J., Jascur, T., Brickner, H., Barbier, V., Sarasin, A., Fotedar, A., and Fotedar, R. (2003). UV irradiation triggers ubiquitin-dependent degradation of p21(WAF1) to promote DNA repair. Cell *114*, 599-610.

Bentley, H., Hamdy, F. C., Hart, K. A., Seid, J. M., Williams, J. L., Johnstone, D., and Russell, R. G. (1992). Expression of bone morphogenetic proteins in human prostatic adenocarcinoma and benign prostatic hyperplasia. Br J Cancer *66*, 1159-1163.

Berruti, A., Tucci, M., Mosca, A., Tarabuzzi, R., Gorzegno, G., Terrone, C., Vana, F., Lamanna, G., Tampellini, M., Porpiglia, F*., et al.* (2005). Predictive factors for skeletal complications in hormone-refractory prostate cancer patients with metastatic bone disease. Br J Cancer *93*, 633-638.

Bertelli, G., Heouaine, A., Arena, G., Botto, A., Garrone, O., Colantonio, I., Occelli, M., Fea, E., Giubergia, S., and Merlano, M. (2006). Weekly docetaxel and zoledronic acid

every 4 weeks in hormone-refractory prostate cancer patients. Cancer Chemother Pharmacol *57*, 46-51.

Birkedal-Hansen, H. (1995). Proteolytic remodeling of extracellular matrix. Curr Opin Cell Biol *7*, 728-735.

Bobinac, D., Maric, I., Zoricic, S., Spanjol, J., Dordevic, G., Mustac, E., and Fuckar, Z. (2005). Expression of bone morphogenetic proteins in human metastatic prostate and breast cancer. Croat Med J *46*, 389-396.

Bonkhoff, H. (1998). Analytical molecular pathology of epithelial-stromal interactions in the normal and neoplastic prostate. Anal Quant Cytol Histol *20*, 437-442.

Bookstein, R., Rio, P., Madreperla, S. A., Hong, F., Allred, C., Grizzle, W. E., and Lee, W. H. (1990). Promoter deletion and loss of retinoblastoma gene expression in human prostate carcinoma. Proc Natl Acad Sci U S A *87*, 7762-7766.

Bowen, C., Bubendorf, L., Voeller, H. J., Slack, R., Willi, N., Sauter, G., Gasser, T. C., Koivisto, P., Lack, E. E., Kononen, J*., et al.* (2000). Loss of NKX3.1 expression in human prostate cancers correlates with tumor progression. Cancer Res *60*, 6111-6115.

Brown, J. E., Cook, R. J., Major, P., Lipton, A., Saad, F., Smith, M., Lee, K. A., Zheng, M., Hei, Y. J., and Coleman, R. E. (2005). Bone turnover markers as predictors of skeletal complications in prostate cancer, lung cancer, and other solid tumors. J Natl Cancer Inst *97*, 59-69.

Brown, J. E., Neville-Webbe, H., and Coleman, R. E. (2004). The role of bisphosphonates in breast and prostate cancers. Endocr Relat Cancer *11*, 207-224.

Brown, J. M., Corey, E., Lee, Z. D., True, L. D., Yun, T. J., Tondravi, M., and Vessella, R. L. (2001). Osteoprotegerin and rank ligand expression in prostate cancer. Urology *57*, 611-616.

Brubaker, K. D., Corey, E., Brown, L. G., and Vessella, R. L. (2004). Bone morphogenetic protein signaling in prostate cancer cell lines. J Cell Biochem *91*, 151-160.

Bubendorf, L., Schopfer, A., Wagner, U., Sauter, G., Moch, H., Willi, N., Gasser, T. C., and Mihatsch, M. J. (2000). Metastatic patterns of prostate cancer: an autopsy study of 1,589 patients. Hum Pathol *31*, 578-583.

Cairns, P., Okami, K., Halachmi, S., Halachmi, N., Esteller, M., Herman, J. G., Jen, J., Isaacs, W. B., Bova, G. S., and Sidransky, D. (1997). Frequent inactivation of PTEN/MMAC1 in primary prostate cancer. Cancer Res *57*, 4997-5000.

Calaluce, R., Kunkel, M. W., Watts, G. S., Schmelz, M., Hao, J., Barrera, J., Gleason-Guzman, M., Isett, R., Fitchmun, M., Bowden, G. T.*, et al.* (2001). Laminin-5-mediated gene expression in human prostate carcinoma cells. Mol Carcinog *30*, 119-129.

Canalis, E., Centrella, M., and McCarthy, T. (1988). Effects of basic fibroblast growth factor on bone formation in vitro. J Clin Invest *81*, 1572-1577.

Canalis, E., Lorenzo, J., Burgess, W. H., and Maciag, T. (1987). Effects of endothelial cell growth factor on bone remodelling in vitro. J Clin Invest *79*, 52-58.

Capella, C., Heitz, P. U., Hofler, H., Solcia, E., and Kloppel, G. (1995). Revised classification of neuroendocrine tumours of the lung, pancreas and gut. Virchows Arch *425*, 547-560.

Capella, C., Usellini, L., Buffa, R., Frigerio, B., and Solcia, E. (1981). The endocrine component of prostatic carcinomas, mixed adenocarcinoma-carcinoid tumours and non-tumour prostate. Histochemical and ultrastructural identification of the endocrine cells. Histopathology *5*, 175-192.

Carducci, M. A., Nelson, J. B., Bowling, M. K., Rogers, T., Eisenberger, M. A., Sinibaldi, V., Donehower, R., Leahy, T. L., Carr, R. A., Isaacson, J. D.*, et al.* (2002). Atrasentan, an endothelin-receptor antagonist for refractory adenocarcinomas: safety and pharmacokinetics. J Clin Oncol *20*, 2171-2180.

Carducci, M. A., Padley, R. J., Breul, J., Vogelzang, N. J., Zonnenberg, B. A., Daliani, D. D., Schulman, C. C., Nabulsi, A. A., Humerickhouse, R. A., Weinberg, M. A.*, et al.* (2003). Effect of endothelin-A receptor blockade with atrasentan on tumor progression in men with hormone-refractory prostate cancer: a randomized, phase II, placebo-controlled trial. J Clin Oncol *21*, 679-689.

Carreira, S., Dexter, T. J., Yavuzer, U., Easty, D. J., and Goding, C. R. (1998). Brachyury-related transcription factor Tbx2 and repression of the melanocyte-specific TRP-1 promoter. Mol Cell Biol *18*, 5099-5108.

Chackal-Roy, M., Niemeyer, C., Moore, M., and Zetter, B. R. (1989). Stimulation of human prostatic carcinoma cell growth by factors present in human bone marrow. J Clin Invest *84*, 43-50.

Chang, B. D., Swift, M. E., Shen, M., Fang, J., Broude, E. V., and Roninson, I. B. (2002). Molecular determinants of terminal growth arrest induced in tumor cells by a chemotherapeutic agent. Proc Natl Acad Sci U S A *99*, 389-394.

Chapman, D. L., and Papaioannou, V. E. (1998). Three neural tubes in mouse embryos with mutations in the T-box gene Tbx6. Nature *391*, 695-697.

Chen, Z., Fan, Z., McNeal, J. E., Nolley, R., Caldwell, M. C., Mahadevappa, M., Zhang, Z., Warrington, J. A., and Stamey, T. A. (2003). Hepsin and maspin are inversely expressed in laser capture microdissected prostate cancer. J Urol *169*, 1316-1319.

Cheville, J. C., Tindall, D., Boelter, C., Jenkins, R., Lohse, C. M., Pankratz, V. S., Sebo, T. J., Davis, B., and Blute, M. L. (2002). Metastatic prostate carcinoma to bone: clinical and pathologic features associated with cancer-specific survival. Cancer *95*, 1028-1036.

Chiaverotti, T., Couto, S. S., Donjacour, A., Mao, J. H., Nagase, H., Cardiff, R. D., Cunha, G. R., and Balmain, A. (2008). Dissociation of epithelial and neuroendocrine carcinoma lineages in the transgenic adenocarcinoma of mouse prostate model of prostate cancer. Am J Pathol *172*, 236-246.

Cho, Y. M., Takahashi, S., Asamoto, M., Suzuki, S., Inaguma, S., Hokaiwado, N., and Shirai, T. (2003). Age-dependent histopathological findings in the prostate of

probasin/SV40 T antigen transgenic rats: lack of influence of carcinogen or testosterone treatment. Cancer Sci *94*, 153-157.

Clarke, N. W., McClure, J., and George, N. J. (1992). Disodium pamidronate identifies differential osteoclastic bone resorption in metastatic prostate cancer. Br J Urol *69*, 64-70.

Clarke, N. W., McClure, J., and George, N. J. (1993). Osteoblast function and osteomalacia in metastatic prostate cancer. Eur Urol *24*, 286-290.

Clines, G. A., and Guise, T. A. (2005). Hypercalcaemia of malignancy and basic research on mechanisms responsible for osteolytic and osteoblastic metastasis to bone. Endocr Relat Cancer *12*, 549-583.

Cohen, R. J., Glezerson, G., Haffejee, Z., and Afrika, D. (1990). Prostatic carcinoma: histological and immunohistological factors affecting prognosis. Br J Urol *66*, 405-410.

Coleman, R. E. (1997). Skeletal complications of malignancy. Cancer *80*, 1588-1594.

Coleman, R. E. (2001). Metastatic bone disease: clinical features, pathophysiology and treatment strategies. Cancer Treat Rev *27*, 165-176.

Corey, E., Brown, L. G., Kiefer, J. A., Quinn, J. E., Pitts, T. E., Blair, J. M., and Vessella, R. L. (2005). Osteoprotegerin in prostate cancer bone metastasis. Cancer Res *65*, 1710-1718.

Corey, E., Brown, L. G., Quinn, J. E., Poot, M., Roudier, M. P., Higano, C. S., and Vessella, R. L. (2003). Zoledronic acid exhibits inhibitory effects on osteoblastic and osteolytic metastases of prostate cancer. Clin Cancer Res *9*, 295-306.

Corey, E., Quinn, J. E., Bladou, F., Brown, L. G., Roudier, M. P., Brown, J. M., Buhler, K. R., and Vessella, R. L. (2002). Establishment and characterization of osseous prostate cancer models: intra-tibial injection of human prostate cancer cells. Prostate *52*, 20-33.

Cramer, S. D., Chen, Z., and Peehl, D. M. (1996). Prostate specific antigen cleaves parathyroid hormone-related protein in the PTH-like domain: inactivation of PTHrP-stimulated cAMP accumulation in mouse osteoblasts. J Urol *156*, 526-531.

Cunha, G. R. (1994). Role of mesenchymal-epithelial interactions in normal and abnormal development of the mammary gland and prostate. Cancer *74*, 1030-1044.

Cunha, G. R., Donjacour, A. A., Cooke, P. S., Mee, S., Bigsby, R. M., Higgins, S. J., and Sugimura, Y. (1987). The endocrinology and developmental biology of the prostate. Endocr Rev *8*, 338-362.

Dai, J., Keller, J., Zhang, J., Lu, Y., Yao, Z., and Keller, E. T. (2005). Bone morphogenetic protein-6 promotes osteoblastic prostate cancer bone metastases through a dual mechanism. Cancer Res *65*, 8274-8285.

Dallas, S. L., Miyazono, K., Skerry, T. M., Mundy, G. R., and Bonewald, L. F. (1995). Dual role for the latent transforming growth factor-beta binding protein in storage of

latent TGF-beta in the extracellular matrix and as a structural matrix protein. J Cell Biol *131*, 539-549.

Dallas, S. L., Park-Snyder, S., Miyazono, K., Twardzik, D., Mundy, G. R., and Bonewald, L. F. (1994). Characterization and autoregulation of latent transforming growth factor beta (TGF beta) complexes in osteoblast-like cell lines. Production of a latent complex lacking the latent TGF beta-binding protein. J Biol Chem *269*, 6815-6821.

Davis, T. L., Cress, A. E., Dalkin, B. L., and Nagle, R. B. (2001). Unique expression pattern of the alpha6beta4 integrin and laminin-5 in human prostate carcinoma. Prostate *46*, 240-248.

De Marzo, A. M., DeWeese, T. L., Platz, E. A., Meeker, A. K., Nakayama, M., Epstein, J. I., Isaacs, W. B., and Nelson, W. G. (2004). Pathological and molecular mechanisms of prostate carcinogenesis: implications for diagnosis, detection, prevention, and treatment. J Cell Biochem *91*, 459-477.

De Schepper, S., Bruwiere, H., Verhulst, T., Steller, U., Andries, L., Wouters, W., Janicot, M., Arts, J., and Van Heusden, J. (2003). Inhibition of histone deacetylases by chlamydocin induces apoptosis and proteasome-mediated degradation of survivin. J Pharmacol Exp Ther *304*, 881-888.

DeCaprio, J. A., Ludlow, J. W., Figge, J., Shew, J. Y., Huang, C. M., Lee, W. H., Marsilio, E., Paucha, E., and Livingston, D. M. (1988). SV40 large tumor antigen forms a specific complex with the product of the retinoblastoma susceptibility gene. Cell *54*, 275-283.

Dhanasekaran, S. M., Barrette, T. R., Ghosh, D., Shah, R., Varambally, S., Kurachi, K., Pienta, K. J., Rubin, M. A., and Chinnaiyan, A. M. (2001). Delineation of prognostic biomarkers in prostate cancer. Nature *412*, 822-826.

di Sant'Agnese, P. A., and Cockett, A. T. (1996). Neuroendocrine differentiation in prostatic malignancy. Cancer *78*, 357-361.

di Sant'Agnese, P. A., and de Mesy Jensen, K. L. (1984). Somatostatin and/or somatostatin-like immunoreactive endocrine-paracrine cells in the human prostate gland. Arch Pathol Lab Med *108*, 693-696.

Dong, J. T., Lamb, P. W., Rinker-Schaeffer, C. W., Vukanovic, J., Ichikawa, T., Isaacs, J. T., and Barrett, J. C. (1995). KAI1, a metastasis suppressor gene for prostate cancer on human chromosome 11p11.2. Science *268*, 884-886.

Dunstan, C. R., Boyce, R., Boyce, B. F., Garrett, I. R., Izbicka, E., Burgess, W. H., and Mundy, G. R. (1999). Systemic administration of acidic fibroblast growth factor (FGF-1) prevents bone loss and increases new bone formation in ovariectomized rats. J Bone Miner Res *14*, 953-959.

Eastell, R. (1998). Treatment of postmenopausal osteoporosis. N Engl J Med *338*, 736-746.

Efstathiou, E., Bozas, G., Kostakopoulos, A., Kastritis, E., Deliveliotis, C., Antoniou, N., Skarlos, D., Papadimitriou, C., Dimopoulos, M. A., and Bamias, A. (2005). Combination of docetaxel, estramustine phosphate, and zoledronic acid in androgen-independent

metastatic prostate cancer: efficacy, safety, and clinical benefit assessment. Urology *65*, 126-130.

el-Deiry, W. S., Harper, J. W., O'Connor, P. M., Velculescu, V. E., Canman, C. E., Jackman, J., Pietenpol, J. A., Burrell, M., Hill, D. E., Wang, Y., and et al. (1994). WAF1/CIP1 is induced in p53-mediated G1 arrest and apoptosis. Cancer Res *54*, 1169-1174.

Ellwood-Yen, K., Graeber, T. G., Wongvipat, J., Iruela-Arispe, M. L., Zhang, J., Matusik, R., Thomas, G. V., and Sawyers, C. L. (2003). Myc-driven murine prostate cancer shares molecular features with human prostate tumors. Cancer Cell *4*, 223-238.

Elo, J. P., and Visakorpi, T. (2001). Molecular genetics of prostate cancer. Ann Med *33*, 130-141.

Ernst, D. S., Tannock, I. F., Winquist, E. W., Venner, P. M., Reyno, L., Moore, M. J., Chi, K., Ding, K., Elliott, C., and Parulekar, W. (2003). Randomized, double-blind, controlled trial of mitoxantrone/prednisone and clodronate versus mitoxantrone/prednisone and placebo in patients with hormone-refractory prostate cancer and pain. J Clin Oncol *21*, 3335-3342.

Ernst, T., Hergenhahn, M., Kenzelmann, M., Cohen, C. D., Bonrouhi, M., Weninger, A., Klaren, R., Grone, E. F., Wiesel, M., Gudemann, C*., et al.* (2002). Decrease and gain of gene expression are equally discriminatory markers for prostate carcinoma: a gene expression analysis on total and microdissected prostate tissue. Am J Pathol *160*, 2169-2180.

Evans, R. M. (1988). The steroid and thyroid hormone receptor superfamily. Science *240*, 889-895.

Fan, L., Pepicelli, C. V., Dibble, C. C., Catbagan, W., Zarycki, J. L., Laciak, R., Gipp, J., Shaw, A., Lamm, M. L., Munoz, A.*, et al.* (2004). Hedgehog signaling promotes prostate xenograft tumor growth. Endocrinology *145*, 3961-3970.

Feeley, B. T., Gamradt, S. C., Hsu, W. K., Liu, N., Krenek, L., Robbins, P., Huard, J., and Lieberman, J. R. (2005). Influence of BMPs on the formation of osteoblastic lesions in metastatic prostate cancer. J Bone Miner Res *20*, 2189-2199.

Feeley, B. T., Krenek, L., Liu, N., Hsu, W. K., Gamradt, S. C., Schwarz, E. M., Huard, J., and Lieberman, J. R. (2006). Overexpression of noggin inhibits BMP-mediated growth of osteolytic prostate cancer lesions. Bone *38*, 154-166.

Fidler, I. J. (1978). Tumor heterogeneity and the biology of cancer invasion and metastasis. Cancer Res *38*, 2651-2660.

Fidler, I. J. (2003). The pathogenesis of cancer metastasis: the 'seed and soil' hypothesis revisited. Nat Rev Cancer *3*, 453-458.

Fizazi, K., Yang, J., Peleg, S., Sikes, C. R., Kreimann, E. L., Daliani, D., Olive, M., Raymond, K. A., Janus, T. J., Logothetis, C. J.*, et al.* (2003). Prostate cancer cells-osteoblast interaction shifts expression of growth/survival-related genes in prostate cancer and reduces expression of osteoprotegerin in osteoblasts. Clin Cancer Res *9*, 2587-2597.

Fleming, W. H., Hamel, A., MacDonald, R., Ramsey, E., Pettigrew, N. M., Johnston, B., Dodd, J. G., and Matusik, R. J. (1986). Expression of the c-myc protooncogene in human prostatic carcinoma and benign prostatic hyperplasia. Cancer Res *46*, 1535-1538.

Fukumitsu, N., Uchiyama, M., Mori, Y., Kishimoto, K., and Nakada, J. (2003). A comparative study of prostate specific antigen (PSA), C-terminal propeptide of blood type I procollagen (PICP) and urine type I collagen-crosslinked N telopeptide (NTx) levels using bone scintigraphy in prostate cancer patients. Ann Nucl Med *17*, 297-303.

Gabril, M. Y., Onita, T., Ji, P. G., Sakai, H., Chan, F. L., Koropatnick, J., Chin, J. L., Moussa, M., and Xuan, J. W. (2002). Prostate targeting: PSP94 gene promoter/enhancer region directed prostate tissue-specific expression in a transgenic mouse prostate cancer model. Gene Ther *9*, 1589-1599.

Gao, A. C., Lou, W., Dong, J. T., and Isaacs, J. T. (1997). CD44 is a metastasis suppressor gene for prostatic cancer located on human chromosome 11p13. Cancer Res *57*, 846-849.

Gartel, A. L., Serfas, M. S., and Tyner, A. L. (1996). p21--negative regulator of the cell cycle. Proc Soc Exp Biol Med *213*, 138-149.

Ghali, V. S., and Garcia, R. L. (1984). Prostatic adenocarcinoma with carcinoidal features producing adrenocorticotropic syndrome. Immunohistochemical study and review of the literature. Cancer *54*, 1043-1048.

Giannelli, G., Falk-Marzillier, J., Schiraldi, O., Stetler-Stevenson, W. G., and Quaranta, V. (1997). Induction of cell migration by matrix metalloprotease-2 cleavage of laminin-5. Science *277*, 225-228.

Gingrich, J. R., Barrios, R. J., Morton, R. A., Boyce, B. F., DeMayo, F. J., Finegold, M. J., Angelopoulou, R., Rosen, J. M., and Greenberg, N. M. (1996). Metastatic prostate cancer in a transgenic mouse. Cancer Res *56*, 4096-4102.

Gleave, M., Hsieh, J. T., Gao, C. A., von Eschenbach, A. C., and Chung, L. W. (1991). Acceleration of human prostate cancer growth in vivo by factors produced by prostate and bone fibroblasts. Cancer Res *51*, 3753-3761.

Granchi, S., Brocchi, S., Bonaccorsi, L., Baldi, E., Vinci, M. C., Forti, G., Serio, M., and Maggi, M. (2001). Endothelin-1 production by prostate cancer cell lines is up-regulated by factors involved in cancer progression and down-regulated by androgens. Prostate *49*, 267-277.

Green, J. R. (2005). Skeletal complications of prostate cancer: pathophysiology and therapeutic potential of bisphosphonates. Acta Oncol *44*, 282-292.

Greenberg, N. M., DeMayo, F., Finegold, M. J., Medina, D., Tilley, W. D., Aspinall, J. O., Cunha, G. R., Donjacour, A. A., Matusik, R. J., and Rosen, J. M. (1995). Prostate cancer in a transgenic mouse. Proc Natl Acad Sci U S A *92*, 3439-3443.

Grignon, D. J. (2004). Unusual subtypes of prostate cancer. Mod Pathol *17*, 316-327.

Guise, T. A. (2000). Molecular mechanisms of osteolytic bone metastases. Cancer *88*, 2892-2898.

Guise, T. A., and Mohammad, K. S. (2004). Endothelins in bone cancer metastases. Cancer Treat Res *118*, 197-212.

Gurel, B., Iwata, T., Koh, C. M., Jenkins, R. B., Lan, F., Van Dang, C., Hicks, J. L., Morgan, J., Cornish, T. C., Sutcliffe, S.*, et al.* (2008). Nuclear MYC protein overexpression is an early alteration in human prostate carcinogenesis. Mod Pathol *21*, 1156-1167.

Hall, C. L., Bafico, A., Dai, J., Aaronson, S. A., and Keller, E. T. (2005). Prostate cancer cells promote osteoblastic bone metastases through Wnts. Cancer Res *65*, 7554-7560.

Halvorsen, O. J., Oyan, A. M., Bo, T. H., Olsen, S., Rostad, K., Haukaas, S. A., Bakke, A. M., Marzolf, B., Dimitrov, K., Stordrange, L.*, et al.* (2005). Gene expression profiles in prostate cancer: association with patient subgroups and tumour differentiation. Int J Oncol *26*, 329-336.

Hao, J., Jackson, L., Calaluce, R., McDaniel, K., Dalkin, B. L., and Nagle, R. B. (2001). Investigation into the mechanism of the loss of laminin 5 (alpha3beta3gamma2) expression in prostate cancer. Am J Pathol *158*, 1129-1135.

Harris, S. E., Bonewald, L. F., Harris, M. A., Sabatini, M., Dallas, S., Feng, J. Q., Ghosh-Choudhury, N., Wozney, J., and Mundy, G. R. (1994a). Effects of transforming growth factor beta on bone nodule formation and expression of bone morphogenetic protein 2,

osteocalcin, osteopontin, alkaline phosphatase, and type I collagen mRNA in long-term cultures of fetal rat calvarial osteoblasts. J Bone Miner Res *9*, 855-863.

Harris, S. E., Harris, M. A., Mahy, P., Wozney, J., Feng, J. Q., and Mundy, G. R. (1994b). Expression of bone morphogenetic protein messenger RNAs by normal rat and human prostate and prostate cancer cells. Prostate *24*, 204-211.

Haudenschild, D. R., Palmer, S. M., Moseley, T. A., You, Z., and Reddi, A. H. (2004). Bone morphogenetic protein (BMP)-6 signaling and BMP antagonist noggin in prostate cancer. Cancer Res *64*, 8276-8284.

He, M., Wen, L., Campbell, C. E., Wu, J. Y., and Rao, Y. (1999). Transcription repression by Xenopus ET and its human ortholog TBX3, a gene involved in ulnar-mammary syndrome. Proc Natl Acad Sci U S A *96*, 10212-10217.

Higano, C., Shields, A., Wood, N., Brown, J., and Tangen, C. (2004). Bone mineral density in patients with prostate cancer without bone metastases treated with intermittent androgen suppression. Urology *64*, 1182-1186.

Higano, C. S. (2003). Bone loss and the evolving role of bisphosphonate therapy in prostate cancer. Urol Oncol *21*, 392-398.

Hiraga, T., Williams, P. J., Mundy, G. R., and Yoneda, T. (2001). The bisphosphonate ibandronate promotes apoptosis in MDA-MB-231 human breast cancer cells in bone metastases. Cancer Res *61*, 4418-4424.

Hogan, B. L. (1996). Bone morphogenetic proteins in development. Curr Opin Genet Dev *6*, 432-438.

Holen, I., Croucher, P. I., Hamdy, F. C., and Eaton, C. L. (2002). Osteoprotegerin (OPG) is a survival factor for human prostate cancer cells. Cancer Res *62*, 1619-1623.

Hu, Y., Ippolito, J. E., Garabedian, E. M., Humphrey, P. A., and Gordon, J. I. (2002). Molecular characterization of a metastatic neuroendocrine cell cancer arising in the prostates of transgenic mice. J Biol Chem *277*, 44462-44474.

Ide, H., Katoh, M., Sasaki, H., Yoshida, T., Aoki, K., Nawa, Y., Osada, Y., Sugimura, T., and Terada, M. (1997). Cloning of human bone morphogenetic protein type IB receptor (BMPR-IB) and its expression in prostate cancer in comparison with other BMPRs. Oncogene *14*, 1377-1382.

Iwamura, M., Abrahamsson, P. A., Foss, K. A., Wu, G., Cockett, A. T., and Deftos, L. J. (1994). Parathyroid hormone-related protein: a potential autocrine growth regulator in human prostate cancer cell lines. Urology *43*, 675-679.

Iwamura, M., Hellman, J., Cockett, A. T., Lilja, H., and Gershagen, S. (1996). Alteration of the hormonal bioactivity of parathyroid hormone-related protein (PTHrP) as a result of limited proteolysis by prostate-specific antigen. Urology *48*, 317-325.

Izbicka, E., Dunstan, C., Esparza, J., Jacobs, C., Sabatini, M., and Mundy, G. R. (1996). Human amniotic tumor that induces new bone formation in vivo produces growth-

regulatory activity in vitro for osteoblasts identified as an extended form of basic fibroblast growth factor. Cancer Res *56*, 633-636.

Jacob, K., Webber, M., Benayahu, D., and Kleinman, H. K. (1999). Osteonectin promotes prostate cancer cell migration and invasion: a possible mechanism for metastasis to bone. Cancer Res *59*, 4453-4457.

Jacobs, J. J., Keblusek, P., Robanus-Maandag, E., Kristel, P., Lingbeek, M., Nederlof, P. M., van Welsem, T., van de Vijver, M. J., Koh, E. Y., Daley, G. Q., and van Lohuizen, M. (2000). Senescence bypass screen identifies TBX2, which represses Cdkn2a (p19(ARF)) and is amplified in a subset of human breast cancers. Nat Genet *26*, 291-299.

Jarrard, D. F., Modder, J., Fadden, P., Fu, V., Sebree, L., Heisey, D., Schwarze, S. R., and Friedl, A. (2002). Alterations in the p16/pRb cell cycle checkpoint occur commonly in primary and metastatic human prostate cancer. Cancer Lett *185*, 191-199.

Jenkins, R. B., Qian, J., Lieber, M. M., and Bostwick, D. G. (1997). Detection of c-myc oncogene amplification and chromosomal anomalies in metastatic prostatic carcinoma by fluorescence in situ hybridization. Cancer Res *57*, 524-531.

Kalikin, L. M., Schneider, A., Thakur, M. A., Fridman, Y., Griffin, L. B., Dunn, R. L., Rosol, T. J., Shah, R. B., Rehemtulla, A., McCauley, L. K., and Pienta, K. J. (2003). In vivo visualization of metastatic prostate cancer and quantitation of disease progression in immunocompromised mice. Cancer Biol Ther *2*, 656-660.

Kaplan-Lefko, P. J., Chen, T. M., Ittmann, M. M., Barrios, R. J., Ayala, G. E., Huss, W. J., Maddison, L. A., Foster, B. A., and Greenberg, N. M. (2003). Pathobiology of autochthonous prostate cancer in a pre-clinical transgenic mouse model. Prostate *55*, 219-237.

Karhadkar, S. S., Bova, G. S., Abdallah, N., Dhara, S., Gardner, D., Maitra, A., Isaacs, J. T., Berman, D. M., and Beachy, P. A. (2004). Hedgehog signalling in prostate regeneration, neoplasia and metastasis. Nature *431*, 707-712.

Kasper, S., Rennie, P. S., Bruchovsky, N., Sheppard, P. C., Cheng, H., Lin, L., Shiu, R. P., Snoek, R., and Matusik, R. J. (1994). Cooperative binding of androgen receptors to two DNA sequences is required for androgen induction of the probasin gene. J Biol Chem *269*, 31763-31769.

Kasper, S., Sheppard, P. C., Yan, Y., Pettigrew, N., Borowsky, A. D., Prins, G. S., Dodd, J. G., Duckworth, M. L., and Matusik, R. J. (1998). Development, progression, and androgen-dependence of prostate tumors in probasin-large T antigen transgenic mice: a model for prostate cancer. Lab Invest *78*, i-xv.

Kawano, Y., and Kypta, R. (2003). Secreted antagonists of the Wnt signalling pathway. J Cell Sci *116*, 2627-2634.

Kazama, Y., Hamamoto, T., Foster, D. C., and Kisiel, W. (1995). Hepsin, a putative membrane-associated serine protease, activates human factor VII and initiates a pathway of blood coagulation on the cell surface leading to thrombin formation. J Biol Chem *270*, 66-72.

Keller, E. T., and Brown, J. (2004). Prostate cancer bone metastases promote both osteolytic and osteoblastic activity. J Cell Biochem *91*, 718-729.

Kiefer, J. A., Vessella, R. L., Quinn, J. E., Odman, A. M., Zhang, J., Keller, E. T., Kostenuik, P. J., Dunstan, C. R., and Corey, E. (2004). The effect of osteoprotegerin administration on the intra-tibial growth of the osteoblastic LuCaP 23.1 prostate cancer xenograft. Clin Exp Metastasis *21*, 381-387.

Kim, I. Y., Lee, D. H., Ahn, H. J., Tokunaga, H., Song, W., Devereaux, L. M., Jin, D., Sampath, T. K., and Morton, R. A. (2000). Expression of bone morphogenetic protein receptors type-IA, -IB and -II correlates with tumor grade in human prostate cancer tissues. Cancer Res *60*, 2840-2844.

Kim, M. J., Cardiff, R. D., Desai, N., Banach-Petrosky, W. A., Parsons, R., Shen, M. M., and Abate-Shen, C. (2002). Cooperativity of Nkx3.1 and Pten loss of function in a mouse model of prostate carcinogenesis. Proc Natl Acad Sci U S A *99*, 2884-2889.

Kirchhofer, D., Peek, M., Lipari, M. T., Billeci, K., Fan, B., and Moran, P. (2005). Hepsin activates pro-hepatocyte growth factor and is inhibited by hepatocyte growth factor activator inhibitor-1B (HAI-1B) and HAI-2. FEBS Lett *579*, 1945-1950.

Kispert, A., and Herrmann, B. G. (1993). The Brachyury gene encodes a novel DNA binding protein. Embo J *12*, 3211-3220.

Klezovitch, O., Chevillet, J., Mirosevich, J., Roberts, R. L., Matusik, R. J., and Vasioukhin, V. (2004). Hepsin promotes prostate cancer progression and metastasis. Cancer Cell *6*, 185-195.

Koeneman, K. S., Yeung, F., and Chung, L. W. (1999). Osteomimetic properties of prostate cancer cells: a hypothesis supporting the predilection of prostate cancer metastasis and growth in the bone environment. Prostate *39*, 246-261.

Koshikawa, N., Schenk, S., Moeckel, G., Sharabi, A., Miyazaki, K., Gardner, H., Zent, R., and Quaranta, V. (2004). Proteolytic processing of laminin-5 by MT1-MMP in tissues and its effects on epithelial cell morphology. Faseb J *18*, 364-366.

Landers, K. A., Burger, M. J., Tebay, M. A., Purdie, D. M., Scells, B., Samaratunga, H., Lavin, M. F., and Gardiner, R. A. (2005). Use of multiple biomarkers for a molecular diagnosis of prostate cancer. Int J Cancer *114*, 950-956.

Le Brun, G., Aubin, P., Soliman, H., Ropiquet, F., Villette, J. M., Berthon, P., Creminon, C., Cussenot, O., and Fiet, J. (1999). Upregulation of endothelin 1 and its precursor by IL-1beta, TNF-alpha, and TGF-beta in the PC3 human prostate cancer cell line. Cytokine *11*, 157-162.

Lee, M. V., Fong, E. M., Singer, F. R., and Guenette, R. S. (2001). Bisphosphonate treatment inhibits the growth of prostate cancer cells. Cancer Res *61*, 2602-2608.

Lee, Y. P., Schwarz, E. M., Davies, M., Jo, M., Gates, J., Zhang, X., Wu, J., and Lieberman, J. R. (2002). Use of zoledronate to treat osteoblastic versus osteolytic lesions in a severe-combined-immunodeficient mouse model. Cancer Res *62*, 5564-5570.

Li, Y., Zhang, H., Choi, S. C., Litingtung, Y., and Chiang, C. (2004). Sonic hedgehog signaling regulates Gli3 processing, mesenchymal proliferation, and differentiation during mouse lung organogenesis. Dev Biol *270*, 214-231.

Liao, C. P., Zhong, C., Saribekyan, G., Bading, J., Park, R., Conti, P. S., Moats, R., Berns, A., Shi, W., Zhou, Z*., et al.* (2007). Mouse models of prostate adenocarcinoma with the capacity to monitor spontaneous carcinogenesis by bioluminescence or fluorescence. Cancer Res *67*, 7525-7533.

Liotta, L. A., and Kohn, E. (1990). Cancer invasion and metastases. Jama *263*, 1123-1126.

Liotta, L. A., and Kohn, E. C. (2001). The microenvironment of the tumour-host interface. Nature *411*, 375-379.

Lipton, A., Costa, L., Ali, S., and Demers, L. (2001). Use of markers of bone turnover for monitoring bone metastases and the response to therapy. Semin Oncol *28*, 54-59.

Lowe, S. W., and Sherr, C. J. (2003). Tumor suppression by Ink4a-Arf: progress and puzzles. Curr Opin Genet Dev *13*, 77-83.

Luo, J., Duggan, D. J., Chen, Y., Sauvageot, J., Ewing, C. M., Bittner, M. L., Trent, J. M., and Isaacs, W. B. (2001). Human prostate cancer and benign prostatic hyperplasia: molecular dissection by gene expression profiling. Cancer Res *61*, 4683-4688.

Ma, L., Lu, M. F., Schwartz, R. J., and Martin, J. F. (2005). Bmp2 is essential for cardiac cushion epithelial-mesenchymal transition and myocardial patterning. Development *132*, 5601-5611.

Maddison, L. A., Sutherland, B. W., Barrios, R. J., and Greenberg, N. M. (2004). Conditional deletion of Rb causes early stage prostate cancer. Cancer Res *64*, 6018-6025.

Maeda, H., Koizumi, M., Yoshimura, K., Yamauchi, T., Kawai, T., and Ogata, E. (1997). Correlation between bone metabolic markers and bone scan in prostatic cancer. J Urol *157*, 539-543.

Magee, J. A., Araki, T., Patil, S., Ehrig, T., True, L., Humphrey, P. A., Catalona, W. J., Watson, M. A., and Milbrandt, J. (2001). Expression profiling reveals hepsin overexpression in prostate cancer. Cancer Res *61*, 5692-5696.

Mansson, P. E., Adams, P., Kan, M., and McKeehan, W. L. (1989). Heparin-binding growth factor gene expression and receptor characteristics in normal rat prostate and two transplantable rat prostate tumors. Cancer Res *49*, 2485-2494.

Marcelli, M., Tilley, W. D., Wilson, C. M., Wilson, J. D., Griffin, J. E., and McPhaul, M. J. (1990). A single nucleotide substitution introduces a premature termination codon into

the androgen receptor gene of a patient with receptor-negative androgen resistance. J Clin Invest *85*, 1522-1528.

Marinkovich, M. P. (2007). Tumour microenvironment: laminin 332 in squamous-cell carcinoma. Nat Rev Cancer *7*, 370-380.

Masumori, N., Thomas, T. Z., Chaurand, P., Case, T., Paul, M., Kasper, S., Caprioli, R. M., Tsukamoto, T., Shappell, S. B., and Matusik, R. J. (2001). A probasin-large T antigen transgenic mouse line develops prostate adenocarcinoma and neuroendocrine carcinoma with metastatic potential. Cancer Res *61*, 2239-2249.

Matuo, Y., Nishi, N., Matsui, S., Sandberg, A. A., Isaacs, J. T., and Wada, F. (1987). Heparin binding affinity of rat prostatic growth factor in normal and cancerous prostates: partial purification and characterization of rat prostatic growth factor in the Dunning tumor. Cancer Res *47*, 188-192.

Mayahara, H., Ito, T., Nagai, H., Miyajima, H., Tsukuda, R., Taketomi, S., Mizoguchi, J., and Kato, K. (1993). In vivo stimulation of endosteal bone formation by basic fibroblast growth factor in rats. Growth Factors *9*, 73-80.

McNeal, J. E. (1988). Normal histology of the prostate. Am J Surg Pathol *12*, 619-633.

Moran, P., Li, W., Fan, B., Vij, R., Eigenbrot, C., and Kirchhofer, D. (2006). Pro-urokinase-type plasminogen activator is a substrate for hepsin. J Biol Chem *281*, 30439-30446.

Nagle, R. B. (2004). Role of the extracellular matrix in prostate carcinogenesis. J Cell Biochem *91*, 36-40.

Nagle, R. B., Hao, J., Knox, J. D., Dalkin, B. L., Clark, V., and Cress, A. E. (1995). Expression of hemidesmosomal and extracellular matrix proteins by normal and malignant human prostate tissue. Am J Pathol *146*, 1498-1507.

Naiche, L. A., and Papaioannou, V. E. (2003). Loss of Tbx4 blocks hindlimb development and affects vascularization and fusion of the allantois. Development *130*, 2681-2693.

Narla, G., Heath, K. E., Reeves, H. L., Li, D., Giono, L. E., Kimmelman, A. C., Glucksman, M. J., Narla, J., Eng, F. J., Chan, A. M.*, et al.* (2001). KLF6, a candidate tumor suppressor gene mutated in prostate cancer. Science *294*, 2563-2566.

Nelson, J. B., and Carducci, M. A. (2000). The role of endothelin-1 and endothelin receptor antagonists in prostate cancer. BJU Int *85 Suppl 2*, 45-48.

Nelson, J. B., Hedican, S. P., George, D. J., Reddi, A. H., Piantadosi, S., Eisenberger, M. A., and Simons, J. W. (1995). Identification of endothelin-1 in the pathophysiology of metastatic adenocarcinoma of the prostate. Nat Med *1*, 944-949.

Nelson, J. B., Nabulsi, A. A., Vogelzang, N. J., Breul, J., Zonnenberg, B. A., Daliani, D. D., Schulman, C. C., and Carducci, M. A. (2003). Suppression of prostate cancer induced bone remodeling by the endothelin receptor A antagonist atrasentan. J Urol *169*, 1143-1149.

Nemeth, J. A., Yousif, R., Herzog, M., Che, M., Upadhyay, J., Shekarriz, B., Bhagat, S., Mullins, C., Fridman, R., and Cher, M. L. (2002). Matrix metalloproteinase activity, bone matrix turnover, and tumor cell proliferation in prostate cancer bone metastasis. J Natl Cancer Inst *94*, 17-25.

Nesbit, C. E., Tersak, J. M., and Prochownik, E. V. (1999). MYC oncogenes and human neoplastic disease. Oncogene *18*, 3004-3016.

Noel, A., Gilles, C., Bajou, K., Devy, L., Kebers, F., Lewalle, J. M., Maquoi, E., Munaut, C., Remacle, A., and Foidart, J. M. (1997). Emerging roles for proteinases in cancer. Invasion Metastasis *17*, 221-239.

Noguchi, M., Yahara, J., and Noda, S. (2003). Serum levels of bone turnover markers parallel the results of bone scintigraphy in monitoring bone activity of prostate cancer. Urology *61*, 993-998.

Oades, G. M., Coxon, J., and Colston, K. W. (2002). The potential role of bisphosphonates in prostate cancer. Prostate Cancer Prostatic Dis *5*, 264-272.

Oades, G. M., Senaratne, S. G., Clarke, I. A., Kirby, R. S., and Colston, K. W. (2003). Nitrogen containing bisphosphonates induce apoptosis and inhibit the mevalonate pathway, impairing Ras membrane localization in prostate cancer cells. J Urol *170*, 246-252.

Papaioannou, V. E. (2001). T-box genes in development: from hydra to humans. Int Rev Cytol *207*, 1-70.

Paxton, C., Zhao, H., Chin, Y., Langner, K., and Reecy, J. (2002). Murine Tbx2 contains domains that activate and repress gene transcription. Gene *283*, 117-124.

Pelengaris, S., Khan, M., and Evan, G. (2002a). c-MYC: more than just a matter of life and death. Nat Rev Cancer *2*, 764-776.

Pelengaris, S., Khan, M., and Evan, G. I. (2002b). Suppression of Myc-induced apoptosis in beta cells exposes multiple oncogenic properties of Myc and triggers carcinogenic progression. Cell *109*, 321-334.

Perez-Stable, C., Altman, N. H., Brown, J., Harbison, M., Cray, C., and Roos, B. A. (1996). Prostate, adrenocortical, and brown adipose tumors in fetal globin/T antigen transgenic mice. Lab Invest *74*, 363-373.

Perez-Stable, C., Altman, N. H., Mehta, P. P., Deftos, L. J., and Roos, B. A. (1997). Prostate cancer progression, metastasis, and gene expression in transgenic mice. Cancer Res *57*, 900-906.

Petrioli, R., Rossi, S., Caniggia, M., Pozzessere, D., Messinese, S., Sabatino, M., Marsili, S., Correale, P., Salvestrini, F., Manganelli, A., and Francini, G. (2004). Analysis of biochemical bone markers as prognostic factors for survival in patients with hormone-resistant prostate cancer and bone metastases. Urology *63*, 321-326.

Pinski, J., and Dorff, T. B. (2005). Prostate cancer metastases to bone: pathophysiology, pain management, and the promise of targeted therapy. Eur J Cancer *41*, 932-940.

Pipas, J. M., and Levine, A. J. (2001). Role of T antigen interactions with p53 in tumorigenesis. Semin Cancer Biol *11*, 23-30.

Pirila, E., Sharabi, A., Salo, T., Quaranta, V., Tu, H., Heljasvaara, R., Koshikawa, N., Sorsa, T., and Maisi, P. (2003). Matrix metalloproteinases process the laminin-5 gamma 2-chain and regulate epithelial cell migration. Biochem Biophys Res Commun *303*, 1012-1017.

Prendergast, G. C. (1999). Mechanisms of apoptosis by c-Myc. Oncogene *18*, 2967-2987.

Price, D. (1963). Comparative Aspects of Development and Structure in the Prostate. Natl Cancer Inst Monogr *12*, 1-27.

Prince, S., Carreira, S., Vance, K. W., Abrahams, A., and Goding, C. R. (2004). Tbx2 directly represses the expression of the p21(WAF1) cyclin-dependent kinase inhibitor. Cancer Res *64*, 1669-1674.

Qian, J., Jenkins, R. B., and Bostwick, D. G. (1997). Detection of chromosomal anomalies and c-myc gene amplification in the cribriform pattern of prostatic intraepithelial neoplasia and carcinoma by fluorescence in situ hybridization. Mod Pathol *10*, 1113-1119.

Qin, L. F., and Ng, I. O. (2001). Exogenous expression of p21(WAF1/CIP1) exerts cell growth inhibition and enhances sensitivity to cisplatin in hepatoma cells. Cancer Lett *172*, 7-15.

Quaranta, V., and Giannelli, G. (2003). Cancer invasion: watch your neighbourhood! Tumori *89*, 343-348.

Quinn, J. E., Brown, L. G., Zhang, J., Keller, E. T., Vessella, R. L., and Corey, E. (2005). Comparison of Fc-osteoprotegerin and zoledronic acid activities suggests that zoledronic acid inhibits prostate cancer in bone by indirect mechanisms. Prostate Cancer Prostatic Dis *8*, 253-259.

Rabbani, S. A., Mazar, A. P., Bernier, S. M., Haq, M., Bolivar, I., Henkin, J., and Goltzman, D. (1992). Structural requirements for the growth factor activity of the amino-terminal domain of urokinase. J Biol Chem *267*, 14151-14156.

Reddi, A. H. (1998). Role of morphogenetic proteins in skeletal tissue engineering and regeneration. Nat Biotechnol *16*, 247-252.

Rennie, P. S., Bruchovsky, N., Leco, K. J., Sheppard, P. C., McQueen, S. A., Cheng, H., Snoek, R., Hamel, A., Bock, M. E., MacDonald, B. S., and et al. (1993). Characterization of two cis-acting DNA elements involved in the androgen regulation of the probasin gene. Mol Endocrinol *7*, 23-36.

Riggs, B. L., Khosla, S., and Melton, L. J., 3rd (1998). A unitary model for involutional osteoporosis: estrogen deficiency causes both type I and type II osteoporosis in postmenopausal women and contributes to bone loss in aging men. J Bone Miner Res *13*, 763-773.

Rogers, M. J., Watts, D. J., and Russell, R. G. (1997). Overview of bisphosphonates. Cancer *80*, 1652-1660.

Roninson, I. B. (2002). Oncogenic functions of tumour suppressor p21(Waf1/Cip1/Sdi1): association with cell senescence and tumour-promoting activities of stromal fibroblasts. Cancer Lett *179*, 1-14.

Roodman, G. D. (2004). Mechanisms of bone metastasis. N Engl J Med *350*, 1655-1664.

Roudier, M. P., Vesselle, H., True, L. D., Higano, C. S., Ott, S. M., King, S. H., and Vessella, R. L. (2003). Bone histology at autopsy and matched bone scintigraphy findings in patients with hormone refractory prostate cancer: the effect of bisphosphonate therapy on bone scintigraphy results. Clin Exp Metastasis *20*, 171-180.

Rouillard, J. M., Erson, A. E., Kuick, R., Asakawa, J., Wimmer, K., Muleris, M., Petty, E. M., and Hanash, S. (2001). Virtual genome scan: a tool for restriction landmark-based scanning of the human genome. Genome Res *11*, 1453-1459.

Rousselle, P., Lunstrum, G. P., Keene, D. R., and Burgeson, R. E. (1991). Kalinin: an epithelium-specific basement membrane adhesion molecule that is a component of anchoring filaments. J Cell Biol *114*, 567-576.

Rowley, M., Grothey, E., and Couch, F. J. (2004). The role of Tbx2 and Tbx3 in mammary development and tumorigenesis. J Mammary Gland Biol Neoplasia *9*, 109-118.

Ryan, M. C., Christiano, A. M., Engvall, E., Wewer, U. M., Miner, J. H., Sanes, J. R., and Burgeson, R. E. (1996). The functions of laminins: lessons from in vivo studies. Matrix Biol *15*, 369-381.

Saad, F., Gleason, D. M., Murray, R., Tchekmedyian, S., Venner, P., Lacombe, L., Chin, J. L., Vinholes, J. J., Goas, J. A., and Chen, B. (2002). A randomized, placebo-controlled trial of zoledronic acid in patients with hormone-refractory metastatic prostate carcinoma. J Natl Cancer Inst *94*, 1458-1468.

Saitoh, H., Hida, M., Shimbo, T., Nakamura, K., Yamagata, J., and Satoh, T. (1984). Metastatic patterns of prostatic cancer. Correlation between sites and number of organs involved. Cancer *54*, 3078-3084.

Sato, K., Qian, J., Slezak, J. M., Lieber, M. M., Bostwick, D. G., Bergstralh, E. J., and Jenkins, R. B. (1999). Clinical significance of alterations of chromosome 8 in high-grade, advanced, nonmetastatic prostate carcinoma. J Natl Cancer Inst *91*, 1574-1580.

Schmitt, C. A. (2003). Senescence, apoptosis and therapy--cutting the lifelines of cancer. Nat Rev Cancer *3*, 286-295.

Shibata, M. A., Maroulakou, I. G., Jorcyk, C. L., Gold, L. G., Ward, J. M., and Green, J. E. (1996a). p53-independent apoptosis during mammary tumor progression in C3(1)/SV40 large T antigen transgenic mice: suppression of apoptosis during the transition from preneoplasia to carcinoma. Cancer Res *56*, 2998-3003.

Shibata, M. A., Ward, J. M., Devor, D. E., Liu, M. L., and Green, J. E. (1996b). Progression of prostatic intraepithelial neoplasia to invasive carcinoma in C3(1)/SV40 large T antigen transgenic mice: histopathological and molecular biological alterations. Cancer Res *56*, 4894-4903.

Shipman, C. M., and Croucher, P. I. (2003). Osteoprotegerin is a soluble decoy receptor for tumor necrosis factor-related apoptosis-inducing ligand/Apo2 ligand and can function as a paracrine survival factor for human myeloma cells. Cancer Res *63*, 912-916.

Shipman, C. M., Croucher, P. I., Russell, R. G., Helfrich, M. H., and Rogers, M. J. (1998). The bisphosphonate incadronate (YM175) causes apoptosis of human myeloma cells in vitro by inhibiting the mevalonate pathway. Cancer Res *58*, 5294-5297.

Showell, C., Binder, O., and Conlon, F. L. (2004). T-box genes in early embryogenesis. Dev Dyn *229*, 201-218.

Sinclair, C. S., Adem, C., Naderi, A., Soderberg, C. L., Johnson, M., Wu, K., Wadum, L., Couch, V. L., Sellers, T. A., Schaid, D.*, et al.* (2002). TBX2 is preferentially amplified in BRCA1- and BRCA2-related breast tumors. Cancer Res *62*, 3587-3591.

Singh, D., Febbo, P. G., Ross, K., Jackson, D. G., Manola, J., Ladd, C., Tamayo, P., Renshaw, A. A., D'Amico, A. V., Richie, J. P.*, et al.* (2002). Gene expression correlates of clinical prostate cancer behavior. Cancer Cell *1*, 203-209.

Skalnik, D. G., Dorfman, D. M., Williams, D. A., and Orkin, S. H. (1991). Restriction of neuroblastoma to the prostate gland in transgenic mice. Mol Cell Biol *11*, 4518-4527.

Small, E. J., Smith, M. R., Seaman, J. J., Petrone, S., and Kowalski, M. O. (2003). Combined analysis of two multicenter, randomized, placebo-controlled studies of pamidronate disodium for the palliation of bone pain in men with metastatic prostate cancer. J Clin Oncol *21*, 4277-4284.

Smith, M. R., Eastham, J., Gleason, D. M., Shasha, D., Tchekmedyian, S., and Zinner, N. (2003). Randomized controlled trial of zoledronic acid to prevent bone loss in men receiving androgen deprivation therapy for nonmetastatic prostate cancer. J Urol *169*, 2008-2012.

Smith, M. R., and Nelson, J. B. (2005). Future therapies in hormone-refractory prostate cancer. Urology *65*, 9-16; discussion 17.

Sordillo, E. M., and Pearse, R. N. (2003). RANK-Fc: a therapeutic antagonist for RANK-L in myeloma. Cancer *97*, 802-812.

Srikantan, V., Valladares, M., Rhim, J. S., Moul, J. W., and Srivastava, S. (2002). HEPSIN inhibits cell growth/invasion in prostate cancer cells. Cancer Res *62*, 6812-6816.

Stamey, T. A., Warrington, J. A., Caldwell, M. C., Chen, Z., Fan, Z., Mahadevappa, M., McNeal, J. E., Nolley, R., and Zhang, Z. (2001). Molecular genetic profiling of Gleason grade 4/5 prostate cancers compared to benign prostatic hyperplasia. J Urol *166*, 2171-2177.

Stege, R. (2000). Potential side-effects of endocrine treatment of long duration in prostate cancer. Prostate Suppl *10*, 38-42.

Stephan, C., Yousef, G. M., Scorilas, A., Jung, K., Jung, M., Kristiansen, G., Hauptmann, S., Kishi, T., Nakamura, T., Loening, S. A., and Diamandis, E. P. (2004). Hepsin is highly over expressed in and a new candidate for a prognostic indicator in prostate cancer. J Urol *171*, 187-191.

Suzuki, T., Takeuchi, J., Koshiba-Takeuchi, K., and Ogura, T. (2004). Tbx Genes Specify Posterior Digit Identity through Shh and BMP Signaling. Dev Cell *6*, 43-53.

Szentirmai, M., Constantinou, C., Rainey, J. M., and Loewenstein, J. E. (1995). Hypocalcemia due to avid calcium uptake by osteoblastic metastases of prostate cancer. West J Med *163*, 577-578.

Takuwa, Y., Ohue, Y., Takuwa, N., and Yamashita, K. (1989). Endothelin-1 activates phospholipase C and mobilizes Ca2+ from extra- and intracellular pools in osteoblastic cells. Am J Physiol *257*, E797-803.

Tassone, P., Tagliaferri, P., Viscomi, C., Palmieri, C., Caraglia, M., D'Alessandro, A., Galea, E., Goel, A., Abbruzzese, A., Boland, C. R., and Venuta, S. (2003). Zoledronic acid induces antiproliferative and apoptotic effects in human pancreatic cancer cells in vitro. Br J Cancer *88*, 1971-1978.

Teraishi, F., Kadowaki, Y., Tango, Y., Kawashima, T., Umeoka, T., Kagawa, S., Tanaka, N., and Fujiwara, T. (2003). Ectopic p21sdi1 gene transfer induces retinoic acid receptor beta expression and sensitizes human cancer cells to retinoid treatment. Int J Cancer *103*, 833-839.

Thomas, B. G., and Hamdy, F. C. (2000). Bone morphogenetic protein-6: potential mediator of osteoblastic metastases in prostate cancer. Prostate Cancer Prostatic Dis *3*, 283-285.

Trias, I., Algaba, F., Condom, E., Espanol, I., Segui, J., Orsola, I., Villavicencio, H., and Garcia Del Muro, X. (2001). Small cell carcinoma of the urinary bladder. Presentation of 23 cases and review of 134 published cases. Eur Urol *39*, 85-90.

Tripathi, M., Nandana, S., Yamashita, H., Ganesan, R., Kirchhofer, D., and Quaranta, V. (2008). Laminin-332 is a substrate for hepsin, a protease associated with prostate cancer progression. J Biol Chem *283*, 30576-30584.

Trotman, L. C., Niki, M., Dotan, Z. A., Koutcher, J. A., Di Cristofano, A., Xiao, A., Khoo, A. S., Roy-Burman, P., Greenberg, N. M., Van Dyke, T., *et al.* (2003). Pten dose dictates cancer progression in the prostate. PLoS Biol *1*, E59.

Tumpel, S., Sanz-Ezquerro, J. J., Isaac, A., Eblaghie, M. C., Dobson, J., and Tickle, C. (2002). Regulation of Tbx3 expression by anteroposterior signalling in vertebrate limb development. Dev Biol *250*, 251-262.

Umbas, R., Isaacs, W. B., Bringuier, P. P., Schaafsma, H. E., Karthaus, H. F., Oosterhof, G. O., Debruyne, F. M., and Schalken, J. A. (1994). Decreased E-cadherin expression is associated with poor prognosis in patients with prostate cancer. Cancer Res *54*, 3929-3933.

Varambally, S., Dhanasekaran, S. M., Zhou, M., Barrette, T. R., Kumar-Sinha, C., Sanda, M. G., Ghosh, D., Pienta, K. J., Sewalt, R. G., Otte, A. P.*, et al.* (2002). The polycomb group protein EZH2 is involved in progression of prostate cancer. Nature *419*, 624-629.

Vordos, D., Paule, B., Vacherot, F., Allory, Y., Salomon, L., Hoznek, A., Yiou, R., Chopin, D., Abbou, C. C., and de la Taille, A. (2004). Docetaxel and zoledronic acid in patients with metastatic hormone-refractory prostate cancer. BJU Int *94*, 524-527.

Wang, S., Gao, J., Lei, Q., Rozengurt, N., Pritchard, C., Jiao, J., Thomas, G. V., Li, G., Roy-Burman, P., Nelson, P. S.*, et al.* (2003). Prostate-specific deletion of the murine Pten tumor suppressor gene leads to metastatic prostate cancer. Cancer Cell *4*, 209-221.

Wang, S. I., Parsons, R., and Ittmann, M. (1998). Homozygous deletion of the PTEN tumor suppressor gene in a subset of prostate adenocarcinomas. Clin Cancer Res *4*, 811-815.

Welsh, J. B., Sapinoso, L. M., Su, A. I., Kern, S. G., Wang-Rodriguez, J., Moskaluk, C. A., Frierson, H. F., Jr., and Hampton, G. M. (2001). Analysis of gene expression identifies candidate markers and pharmacological targets in prostate cancer. Cancer Res *61*, 5974-5978.

Westendorf, J. J., Kahler, R. A., and Schroeder, T. M. (2004). Wnt signaling in osteoblasts and bone diseases. Gene *341*, 19-39.

Witters, L. M., Crispino, J., Fraterrigo, T., Green, J., and Lipton, A. (2003). Effect of the combination of docetaxel, zoledronic acid, and a COX-2 inhibitor on the growth of human breast cancer cell lines. Am J Clin Oncol *26*, S92-97.

Woodward, J. K., Holen, I., Coleman, R. E., and Buttle, D. J. (2007). The roles of proteolytic enzymes in the development of tumour-induced bone disease in breast and prostate cancer. Bone *41*, 912-927.

Wu, G., Sinclair, C., Hinson, S., Ingle, J. N., Roche, P. C., and Couch, F. J. (2001a). Structural analysis of the 17q22-23 amplicon identifies several independent targets of amplification in breast cancer cell lines and tumors. Cancer Res *61*, 4951-4955.

Wu, Q., and Parry, G. (2007). Hepsin and prostate cancer. Front Biosci *12*, 5052-5059.

Wu, X., Wu, J., Huang, J., Powell, W. C., Zhang, J., Matusik, R. J., Sangiorgi, F. O., Maxson, R. E., Sucov, H. M., and Roy-Burman, P. (2001b). Generation of a prostate epithelial cell-specific Cre transgenic mouse model for tissue-specific gene ablation. Mech Dev *101*, 61-69.

Xuan, J. A., Schneider, D., Toy, P., Lin, R., Newton, A., Zhu, Y., Finster, S., Vogel, D., Mintzer, B., Dinter, H., *et al.* (2006). Antibodies neutralizing hepsin protease activity do not impact cell growth but inhibit invasion of prostate and ovarian tumor cells in culture. Cancer Res *66*, 3611-3619.

Yan, Y., Sheppard, P. C., Kasper, S., Lin, L., Hoare, S., Kapoor, A., Dodd, J. G., Duckworth, M. L., and Matusik, R. J. (1997). Large fragment of the probasin promoter

targets high levels of transgene expression to the prostate of transgenic mice. Prostate *32*, 129-139.

Yanagisawa, M., Kurihara, H., Kimura, S., Tomobe, Y., Kobayashi, M., Mitsui, Y., Yazaki, Y., Goto, K., and Masaki, T. (1988). A novel potent vasoconstrictor peptide produced by vascular endothelial cells. Nature *332*, 411-415.

Yang, M., Jiang, P., Sun, F. X., Hasegawa, S., Baranov, E., Chishima, T., Shimada, H., Moossa, A. R., and Hoffman, R. M. (1999). A fluorescent orthotopic bone metastasis model of human prostate cancer. Cancer Res *59*, 781-786.

Yi, B., Williams, P. J., Niewolna, M., Wang, Y., and Yoneda, T. (2002). Tumor-derived platelet-derived growth factor-BB plays a critical role in osteosclerotic bone metastasis in an animal model of human breast cancer. Cancer Res *62*, 917-923.

Yin, J. J., Mohammad, K. S., Kakonen, S. M., Harris, S., Wu-Wong, J. R., Wessale, J. L., Padley, R. J., Garrett, I. R., Chirgwin, J. M., and Guise, T. A. (2003). A causal role for endothelin-1 in the pathogenesis of osteoblastic bone metastases. Proc Natl Acad Sci U S A *100*, 10954-10959.

Yonou, H., Kanomata, N., Goya, M., Kamijo, T., Yokose, T., Hasebe, T., Nagai, K., Hatano, T., Ogawa, Y., and Ochiai, A. (2003). Osteoprotegerin/osteoclastogenesis inhibitory factor decreases human prostate cancer burden in human adult bone implanted into nonobese diabetic/severe combined immunodeficient mice. Cancer Res *63*, 2096-2102.

Yoshida, E., Verrusio, E. N., Mihara, H., Oh, D., and Kwaan, H. C. (1994). Enhancement of the expression of urokinase-type plasminogen activator from PC-3 human prostate cancer cells by thrombin. Cancer Res *54*, 3300-3304.

Zetter, B. R. (1990). The cellular basis of site-specific tumor metastasis. N Engl J Med *322*, 605-612.

Zhang, J., Dai, J., Qi, Y., Lin, D. L., Smith, P., Strayhorn, C., Mizokami, A., Fu, Z., Westman, J., and Keller, E. T. (2001). Osteoprotegerin inhibits prostate cancer-induced osteoclastogenesis and prevents prostate tumor growth in the bone. J Clin Invest *107*, 1235-1244.

Zhang, J., Dai, J., Yao, Z., Lu, Y., Dougall, W., and Keller, E. T. (2003). Soluble receptor activator of nuclear factor kappaB Fc diminishes prostate cancer progression in bone. Cancer Res *63*, 7883-7890.

Zhang, J., Thomas, T. Z., Kasper, S., and Matusik, R. J. (2000). A small composite probasin promoter confers high levels of prostate-specific gene expression through regulation by androgens and glucocorticoids in vitro and in vivo. Endocrinology *141*, 4698-4710.

Zhau, H. Y., Chang, S. M., Chen, B. Q., Wang, Y., Zhang, H., Kao, C., Sang, Q. A., Pathak, S. J., and Chung, L. W. (1996). Androgen-repressed phenotype in human prostate cancer. Proc Natl Acad Sci U S A *93*, 15152-15157.

Zheng, X., Chou, P. M., Mirkin, B. L., and Rebbaa, A. (2004). Senescence-initiated reversal of drug resistance: specific role of cathepsin L. Cancer Res *64*, 1773-1780.

Zonnenberg, B. A., Groenewegen, G., Janus, T. J., Leahy, T. W., Humerickhouse, R. A., Isaacson, J. D., Carr, R. A., and Voest, E. (2003). Phase I dose-escalation study of the safety and pharmacokinetics of atrasentan: an endothelin receptor antagonist for refractory prostate cancer. Clin Cancer Res *9*, 2965-2972.